

SUMMARY

Aerodynamics: Typical Questions
MECA-Y402

Author:
Mischa MASSON

Professors:
Herman DECONINCK
Chris LACOR

Year 2016 - 2017

Appel à contribution

Synthèse Open Source



Ce document est grandement inspiré de l'excellent cours donné par Herman DECONINCK et Chris LACOR à l'EPB (École Polytechnique de Bruxelles), faculté de l'ULB (Université Libre de Bruxelles). Il est écrit par les auteurs susnommés avec l'aide de tous les autres étudiants et votre aide est la bienvenue ! En effet, il y a toujours moyen de l'améliorer surtout que si le cours change, la synthèse doit être changée en conséquence. On peut retrouver le code source à l'adresse suivante

<https://github.com/nenglebert/Syntheses>

Pour contribuer à cette synthèse, il vous suffira de créer un compte sur *Github.com*. De légères modifications (petites coquilles, orthographe, ...) peuvent directement être faites sur le site ! Vous avez vu une petite faute ? Si oui, la corriger de cette façon ne prendra que quelques secondes, une bonne raison de le faire !

Pour de plus longues modifications, il est intéressant de disposer des fichiers : il vous faudra pour cela installer *L^AT_EX*, mais aussi *git*. Si cela pose problème, nous sommes évidemment ouverts à des contributeurs envoyant leur changement par mail ou n'importe quel autre moyen.

Le lien donné ci-dessus contient aussi un README contenant de plus amples informations, vous êtes invités à le lire si vous voulez faire avancer ce projet !

Licence Creative Commons

Le contenu de ce document est sous la licence Creative Commons : *Attribution-NonCommercial-ShareAlike 4.0 International (CC BY-NC-SA 4.0)*. Celle-ci vous autorise à l'exploiter pleinement, compte-tenu de trois choses :



1. *Attribution* ; si vous utilisez/modifiez ce document vous devez signaler le(s) nom(s) de(s) auteur(s).
2. *Non Commercial* ; interdiction de tirer un profit commercial de l'œuvre sans autorisation de l'auteur
3. *Share alike* ; partage de l'œuvre, avec obligation de rediffuser selon la même licence ou une licence similaire

Si vous voulez en savoir plus sur cette licence :

<http://creativecommons.org/licenses/by-nc-sa/4.0/>

Merci !

Contents

1 Explain how lift can generated around an airfoil for inviscid incompressible flow.	3
1.1 Explain the origin of the bound vortex which exists around a profile which generates lift. Explain using the Kelvin theorem	3
1.2 What is the start-up vortex, what happens with it when the flow reaches a steady state	3
1.3 Explain the Kutta condition	4
2 Derive an expression for the aerodynamic lift of on airfoil for inviscid incompressible flow (i.e. neglecting viscous effects).	4
2.1 Express conservation of momentum over a closed surface S far away from the wing, neglecting viscous forces	5
2.2 Show that the lift force is linked to the vorticity through the closed surface S . .	6
2.3 Show that for the 2D airfoil the lift force is linked to the circulation around the airfoil, derive the Kutta-Joukowski formula for the lift generated by a 2D profile	6
3 Characteristics of a 2D airfoil:	6
3.1 Define lift and drag, give the principle components of lift and drag force in normal operation and in case of separation	6
3.2 Explain the non-dimensional force coefficients(C_l , C_d , C_m) and which are the similarity parameters influencing these coefficients	7
3.3 Explain:	8
3.4 Compute the Location of the center of pressure CP as a function of the angle of attack alpha	8
3.5 Explain the lift, drag and moment curves as a function of the angle of attack alpha	9
3.6 Explain what is stall and critical angle of attack. Explain different types of stall.	9
3.7 Discuss the polar curve of the airfoil, i.e. lift coefficient as a function of drag coefficient, show the glide ratio on this plot	10
3.8 What is the importance of the glide ratio, discuss the case of a gliding plane (engine off situation)	10
4 Computation of inviscid irrotational flow around a 2D airfoil using conformal mapping - Joukowski profiles	11
4.1 Explain methods based on complex potential function, explain the connection with usual stream function and potential function	11
4.2 Explain how the velocity can be computed from the complex potential function .	12
4.3 Derive the complex potential function for uniform flow, source/sink flow, free vortex	12
4.3.1 Uniform flow	12
4.3.2 Source / Sink	12
4.3.3 Free vortex	12
4.4 Compute flow around Rankine body and around a cylinder	13
4.5 Explain how a the class of Joukowski profiles is obtained by conformal mapping of a circle	13
5 Computation of inviscid irrotational flow around a thin airfoil based on a continuous distribution of vortices	15
5.1 Explain what is a free vortex	15

5.2	Explain what is a continuous distribution of free vortices on a line	15
5.3	Explain principle of the method of free vortex distribution applied thin airfoils, limitations and hypotheses	15
5.4	Establish the integral equation which allows to compute the vortex distribution for a given profile	16
5.5	Show how to solve this equation using a spectral method, i.e. by expressing the vortex distribution as a truncated Fourier series	17
5.6	How is the Kutta-Youkowsky condition imposed (allowing to compute the lift) . .	18
5.7	Starting from the expressions for the Fourier coefficients, compute the circulation and lift coefficient as a function of angle of attack, explain the result	18
5.7.1	Calculation of the total circulation	18
5.7.2	Calculation of the lift coefficient	18
5.8	Starting from the expression for the momentum coefficient at the leading edge $c_m(\text{LE})$, show that it's a linear function of the lift coefficient c_l	19
5.9	Compute the location of the aerodynamic center AC and the momentum coefficient in the aerodynamic center	19
5.10	Compute the location of the center of pressure	19
6	Computation of inviscid irrotational flow around a thin airfoil based on a continuous distribution of vortices	20
7	3D wing theory	21
7.1	Explain mean chord, span, aspect ratio, taper, sweep of wing	21
7.2	Explain downwash effect, downwash angle, effective angle of attack, total and induced drag	21
7.3	Starting from the given expression for the downwash angle, compute the induced drag force and the induced drag coefficient	22
7.4	Explain the lift curve as a function of the angle of attack for a 3D wing, compare with the lift curve for a 2D profile	22
7.5	Give the expression for the total drag coefficient as a function of C_L	22
7.6	Give the expression of the drag force D as a function of the velocity at infinity .	23
8	3D wing theory – Derivation of Prandtl lifting line method. Give the basic ideas and the development of Prandtl's lifting line theory	23
8.1	Velocity induced by a vortex filament	23
8.2	Helmholtz theorems, Biot-Savart law	24
8.3	Circulation around a vortex sheet	24
8.4	Downwash velocity induced by a single horseshoe vortex, why this model for a wing is not working	24
8.5	Downwash velocity induced by a superposition of horseshoe vortices	25
8.6	Derivation of Prandtl's fundamental equation of lifting line theory	25
9	3D wing theory: application of Prandtl lifting line theory for a wing with given circulation. Starting from Prandtl's fundamental equation of lifting line theory and the formula for the induced angle of attack:	26
9.1	Discuss the different terms of the equation	26
9.2	Apply to a wing with a given circulation distribution: find lift and drag coefficients	26
9.3	Apply to a wing with a given shape and unknown circulation distribution defined by a truncated Fourier series and compute the lift C_L and the induced drag C_{Di} coefficients	26

9.4	Apply to a tapered wing	27
9.5	Assume an elliptic distribution for the circulation. Show that the platform of the wing must be an ellipse.	28
10	2D airfoil compressible flow around an airfoil using the small perturbation approach	29
10.1	Derive the compressible potential equation / Derive the equation governing compressible potential equation, what are the assumptions	29
10.2	Assume a thin airfoil at small angle of attack: derive the linearized potential equation. What is the range of validity as a function of the free stream Mach number / Derive the equation in the case of small perturbations. What are the assumptions for this equation to be valid ?	30
10.3	Discuss the type of this equation as a function of free stream Mach number, what are the consequences	32
10.4	Discuss the application to an airfoil in supersonic flow: lift coefficient, influence of the Mach number, Ackeret formula, lift and drag formula	33
10.4.1	Application to a flat plate	34
10.5	What is wave drag ? discuss supersonic flow over double wedge profile	35
10.6	Transonic flow over a profile: what is critical free stream Mach number(+ discussion), what is drag divergence Mach number	36
10.6.1	Critical Mach number	36
10.6.2	Drag divergence Mach number	37
10.7	Compute the lift coefficient for a 2D profile in compressible flow, assuming that the lift coefficient for the same airfoil is known for incompressible flow.	39
10.8	Discuss the graph giving the slope of the lift curve as a function of the free stream Mach number ($M_{infinity}$)	39
11	Transonic flow over an airfoil - critical Mach number and drag divergence Mach number	39
11.1	Give definition of critical free stream Mach number	39
11.2	Explain the effect of the thickness of the profile on the critical Mach number	39
11.3	All questions related to divergence Mach number, shock patterns from sub- to supersonic, C_D versus Mach, buffeting	39
11.4	Explain supercritical wing profiles	40
12	2D thin airfoil airfoil in flow at supersonic free stream Mach number	40
12.1	Derive the pressure coefficient on the surface of the airfoil using the second order wave equation	40
12.2	Compute the lift coefficient using the method of characteristics for the potential system written in the primitive variables u and v (Ackeret's law). Wave drag computation.	40
13	3D wing in compressible flow in subsonic and supersonic flow	40
13.1	Discuss the 3D linearized potential equation for subsonic flow, compare the compressible and incompressible case	40
13.2	Derive Prandtl Glauert rule for a subsonic wing in compressible flow	41
13.3	Discuss the 3D linearized potential equation for supersonic flow, compare the compressible flow with the supersonic flow at freestream Mach number $\sqrt{2}$	41

14 3D wing in compressible transonic flow. Discuss effect of sweep on performance of a 3D wing in compressible flow – Influence on Lift and drag	42
14.1 Lift of swept wings	42
14.2 Lift coefficient as a function of the angle of attack for swept wings	43
14.3 Influence of the sweep angle on the drag	43
14.4 Separation behavior	43
14.5 Area rule	44
14.6 Forward Swept wings	44
15 Delta wings	45
15.1 Discuss the mechanism for lift creation over a delta wing	45
15.2 Discuss the formula of Jones giving the lift coefficient as a function of the angle of attack	45
15.3 What are the advantages and disadvantages of delta wings with respect to:	45
16 High lift devices	46
16.1 Why and when are high lift devices needed	46
16.2 How can the lift be increased: 2 basic principles	46
16.3 Discuss different kinds of trailing edge flaps	46
16.3.1 Plain flap	46
16.3.2 Split flap	46
16.3.3 Slotted flap	47
16.3.4 Fowler flap	47
16.4 Discuss the effect of slats	47
16.5 Discuss boundary layer control	48
17 Tailplanes	48
17.1 Discuss why tail planes are needed in order to have a stable wing configuration .	48
17.2 Discuss canard as an alternative for tail plane	49
18 Viscous and turbulent effects	49
18.1 Discuss skin friction drag for laminar and turbulent flow	49
18.1.1 Laminar flow	49
18.1.2 Turbulent flow	50
18.2 Discuss methods to reduce viscous drag: natural laminar flow and riblets . . .	50
18.2.1 Natural laminar flow and control of laminar flow	50
18.2.2 Reduction of the drag in turbulent flows	51
19 Weak solutions – shocks and contact discontinuities.	
Start form the Euler equations in conservative form:	51
19.1 Determine shock relations starting from the weak formulation	51
19.2 Discuss contact or slip discontinuities	53
19.3 Explain propagation of disturbances in a subsonic and supersonic flow (sound waves). Discuss Mach waves	53
19.3.1 Subcritical and supercritical waves	54
20 Discuss characteristic theory for a first order scalar wave equation	55
20.1 Discuss the theory of characteristics for a first order linear wave equation with wave speed a . Define characteristic curves, what are Riemann invariants. Can discontinuous solutions exist ?	55

20.1.1 a cst	55
20.1.2 a linear	55
20.2 What changes for a nonlinear wave equation, take the case $a(u) = u$	55
20.2.1 a non linear	55
20.3 Discuss shock formation for the previous case	56
20.4 Discuss the link between a characteristic curve and a shock curve	56
21 Discuss characteristic theory for steady supersonic potential flow	56
21.1 What are the assumptions for potential flow	56
21.2 Write the two equations which govern the velocity components u and v	57
21.3 How is the sound speed computed as a function of the velocity components	57
21.4 Write the above system in the canonical form and apply characteristic theory to find the Mach lines and Riemann invariants on the Mach lines	57
21.5 What are simple wave solutions, explain properties of simple waves. Explain why one of the families of characteristic curves are given by straight lines	59
21.6 Discuss simple waves in the hodograph plane.	60
21.7 Apply to flow around a convex bend and to flow around a sharp convex corner. Explain why this is an expansion	60
21.7.1 Prandtl-Meyer expansion	61
22 Oblique shock relations for steady 2D inviscid flow	61
22.1 Define critical state, critical Mach number, what are the key properties of the critical sound speed – compare with total state.	61
22.2 The characteristic (or Critical) Mach number	61
22.3 Derive the relation between normal critical Mach numbers before and behind an oblique shock	62
22.4 Derive the relation between densities before and behind the shock	63
22.5 Discuss the graph θ (flow angle) as a function of β (shock angle) with upstream Mach number as a parameter.	63
22.5.1 Interpretation of the β, θ, M curves	63
23 Oblique shock relations	64
23.1 Derive the shock polar for the velocity components behind the shock, with the upstream velocity as a parameter (shock polar in the hodograph plane)	64
23.2 Using this graph, discuss maximum deviation, weak shock and strong shock solu- tions, normal shock and Mach wave	65
23.3 Consider the flow around a sharp concave corner. Using the above graph, find the downstream Mach number for a given upstream Mach number	65
23.4 Discuss the shock structure appearing for supersonic flow around a cylindrical body	65
23.5 Discuss shock reflection in a supersonic channel	65

1 Explain how lift can be generated around an airfoil for inviscid incompressible flow.

See

Q2

for

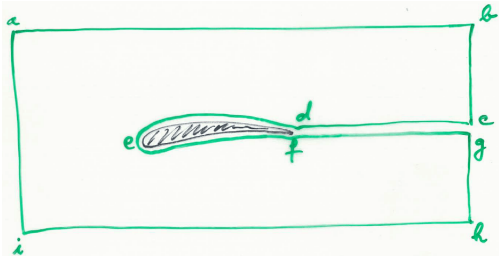


Figure 1

mathematical

explanation.

When looking at an airfoil, we have a pressure that is applied around it. This pressure is non uniform, due to the presence of the airfoil. The integral of pressures over the surface gives a force expressed as the product of the incoming speed and the vorticity vector: the lift.

1.1 Explain the origin of the bound vortex which exists around a profile which generates lift. Explain using the Kelvin theorem

In inviscid case, the Kelvin theorem states that there cannot be vorticity, so no lift. If we take an arbitrary contour around the airfoil we will have no circulation. In inviscid case we can never get a lift \rightarrow D'Alembert paradox. At the trailing edge, if the flow wants to continue on the other corner from below, the velocity must be infinity so that the flow separates. But this is not the case in reality.

To satisfy the Kutta condition (the flow has to leave the airfoil smoothly), there needs to be circulation if we take a contour that contains the airfoil, but for all contour that does not contain the airfoil it is null. Γ varies with the stagnation point position, but only one corresponds to the Kutta condition.

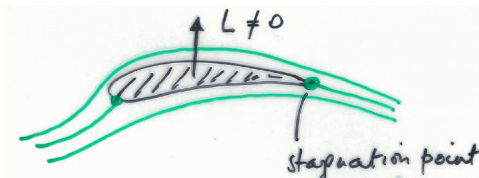


Figure 2

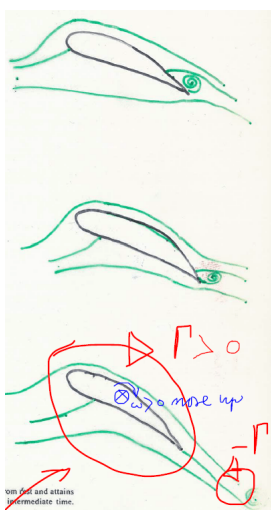


Figure 3

The bound vortex is the vortex around the airfoil. It is compensated by a starting vortex that detaches from the airfoil.

We can show that every contour containing the airfoil has a non 0 circulation. Let's proof that a contour that doesn't contain the airfoil has $\Gamma = 0$:

$$\oint_C \vec{v} d\vec{l} = \oint_{\text{airfoil}} \vec{v} d\vec{l} + \oint_{cd} \vec{v} d\vec{l} + \oint_{fg} \vec{v} d\vec{l} = 0. \quad (1)$$

As the contour elements are exactly opposed to each other, the result is null.

1.2 What is the start-up vortex, what happens with it when the flow reaches a steady state

What happens is that initially we have the first kind of flow, then the formation of the starting vortex due to viscous effects (separation) which is compensated by a **bound vortex** around the airfoil (to respect Kelvin theorem of irrotational flow) that makes $\Gamma \neq 0$. Then the vortex goes away to infinity. Indeed if we take $R = \rho v_\infty \Gamma$, $\Gamma \neq 0$, so we have lift.

1.3 Explain the Kutta condition

The Kutta condition states that the flow can only have a stagnation point at the trailing edge. If this was not the case, the underwing flow would need to accelerate "going backwards" to meet the upperwing flow, see figure 2.

2 Derive an expression for the aerodynamic lift of on airfoil for inviscid incompressible flow (i.e. neglecting viscous effects).

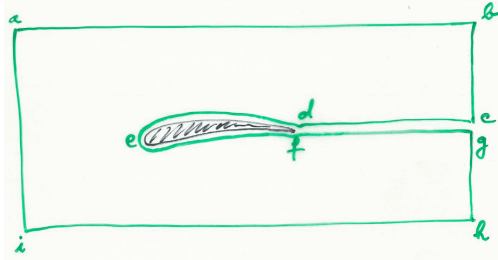


Figure 4

The fundamental integral form of the mass conservation equation is:

$$\frac{d}{dt} \int_V \rho dV + \oint_S \rho \vec{v} d\vec{S} = 0. \quad (2)$$

By applying Gauss theorem $\oint_S \vec{a} \cdot \vec{n} dS = \int_V \nabla \cdot \vec{a} dV$:

$$\int_V \left[\frac{d\rho}{dt} + \nabla \cdot (\rho \vec{v}) \right] dV = 0. \quad (3)$$

True for all volumes:

Continuity equation

$$\frac{d\rho}{dt} + \nabla \cdot (\rho \vec{u}) = 0 \quad (4)$$

General form of the momentum equation is:

$$\rho \ddot{\vec{v}} = \frac{\partial \rho \vec{v}}{\partial t} + \rho (\vec{v} \nabla) \vec{v} = -\nabla p + \nabla \bar{\tau}. \quad (5)$$

Steady state, time derivative goes away. If we consider the x component of the velocity, we can expand the derivative to the whole left term as:

$$\rho (\vec{v} \nabla) v_x = \nabla (\rho \vec{v} v_x) - v_x \nabla (\rho \vec{v}) \quad (6)$$

where the last term is null related to (4) in steady state. Integrating both sides around the volume contained in the closed surface S (abcdefghi on figure) in (6), and applying Gauss theorem, we obtain:

$$\oint_S \vec{v} (\rho \vec{v} \vec{n}) dS = - \oint_S p d\vec{S} + \oint_S \bar{\tau} d\vec{S}. \quad (7)$$

New closed contour $S^* = S - \text{airfoil} - cd - fg$ (previous abhi in fact). (7) becomes:

$$\begin{aligned} & \oint_{S^*} \vec{v} (\rho \vec{v} d\vec{S}) + \oint_{\text{airfoil}} \vec{v} (\rho \vec{v} d\vec{S}) + \oint_{cd+fg} \vec{v} (\rho \vec{v} d\vec{S}) \\ &= - \oint_{S^*} p d\vec{S} - \oint_{\text{airfoil}} p d\vec{S} - \oint_{ed+fg} p d\vec{S} + \oint_{S^*} \bar{\tau} d\vec{S} + \oint_{\text{airfoil}} \bar{\tau} d\vec{S} + \oint_{ed+fg} \bar{\tau} d\vec{S} \end{aligned} \quad (8)$$

Forces applied to a wing:

$$\vec{R} = \oint_{\text{airfoil}} p d\vec{S} - \oint_{\text{airfoil}} \bar{\tau} d\vec{S} \quad (9)$$

$$\oint_{S^*} \vec{v}(\rho \vec{v} d\vec{S}) = - \oint_{S^*} p d\vec{S} + \oint_{S^*} \vec{\tau} d\vec{S} - \vec{R}. \quad (10)$$

Pressure effects induced by the body remains at a long distance from the body. We have to analyse the **non uniform** p along S^* . In order to apply Bernoulli equation $p + \frac{1}{2}\rho v^2 = cst$, let's add the constants p_∞ and v_∞ to (10), as $\oint p_\infty d\vec{S} = p_\infty \oint d\vec{s} = 0$:

$$\vec{R} = - \oint_{S^*} (p - p_\infty) d\vec{S} - \oint_{S^*} (\vec{v} - \vec{v}_\infty) d\vec{m} \quad (11)$$

Let's express $\vec{v} = \vec{v}_\infty + \vec{\delta}_c$ with $\vec{\delta}_c$ a perturbation. Introducing this in Bernoulli equation:

$$p_\infty + \frac{1}{2}\rho \vec{v}_\infty^2 = p + \frac{1}{2}\rho(\vec{v}_\infty + \vec{\delta}_c)^2 = p + \frac{1}{2}\rho(\vec{v}_\infty^2 + 2\vec{v}_\infty \cdot \vec{\delta}_c + \vec{\delta}_c^2) \Rightarrow p - p_\infty = -\rho \vec{v}_\infty \cdot \vec{\delta}_c. \quad (12)$$

If we replace this result in (11), we find:

$$\vec{R} = \oint_{S^*} \rho[(\vec{v}_\infty \cdot \vec{\delta}_c) d\vec{S} - \vec{\delta}_c \cdot (\vec{v}_\infty \cdot d\vec{S})] \quad (13)$$

by using a vector property $\vec{a} \times (\vec{b} \times \vec{c}) = (\vec{a} \cdot \vec{b})\vec{c} - (\vec{a} \cdot \vec{c})\vec{b}$:

$$= \rho \vec{v}_\infty \times \oint_{S^*} \vec{\delta}_c \times d\vec{S} = \rho \vec{v}_\infty \times \left[\oint_{S^*} \vec{v} \times d\vec{S} - \oint_{S^*} \vec{v}_\infty \times d\vec{S} \right] \quad (14)$$

and by applying Stokes theorem $\oint_S \vec{a} \times d\vec{S} = \int_V \nabla \times \vec{a} dV$:

$$= \rho \vec{v}_\infty \times \int (\nabla \times \vec{v}) dV = \rho \vec{v}_\infty \times \int \vec{\omega} dV \quad (15)$$

where $\vec{\omega}$ is the **vorticity vector** of direction $\vec{1}_z$ (pointing in the paper):

$$\vec{\omega} = \begin{vmatrix} \vec{1}_x & \vec{1}_y & \vec{1}_z \\ \partial_x & \partial_y & 0 \\ v_x & v_y & 0 \end{vmatrix} = [\partial_x v_y - \partial_y v_x] \vec{1}_z \quad (16)$$

This shows that the lift force is always perpendicular to the flow!

2.1 Express conservation of momentum over a closed surface S far away from the wing, neglecting viscous forces

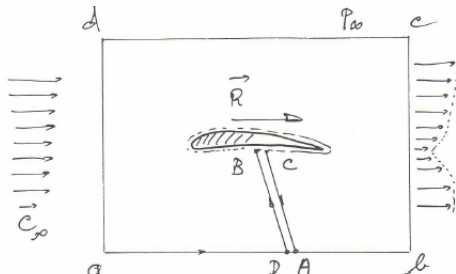


Figure 5

horizontal so that $\vec{R} = R \vec{1}_x$, at the inlet we have \vec{v} and \vec{n} are opposed while at the outlet they are in the same direction:

By considering this (assumption of far field), we can compute the force only by knowing the far field parameters. Indeed, uniform pressure implies null surface integral, so that (10) becomes:

$$\vec{R} = - \oint_{S^*} \vec{v}(\rho \vec{v} d\vec{S}). \quad (17)$$

The velocity term remains, as by experience we know that there is a **wake** making the velocity profile non-uniform. Let's now consider that the velocity is horizontal so that $\vec{R} = R \vec{1}_x$, at the inlet we have \vec{v} and \vec{n} are opposed while at the outlet they are in the same direction:

$$\vec{R} = \int_a^d \vec{v} d\dot{m} - \int_b^e \vec{v} d\dot{m} > 0 \quad (18)$$

showing that there is only **drag** force.

2.2 Show that the lift force is linked to the vorticity through the closed surface S

See above.

2.3 Show that for the 2D airfoil the lift force is linked to the circulation around the airfoil, derive the Kutta-Joukowski formula for the lift generated by a 2D profile

We will now introduce the circulation $\Gamma = -\oint \vec{v} d\vec{l} > 0$ around a body. The convention is to take the anticlockwise direction for $d\vec{l}$ and so for Γ to be > 0 we must have \vec{v} in the clockwise direction. There is a link between the lift force and the circulation. Let's introduce **Stokes theorem**:

$$\oint \vec{a} d\vec{l} = \int_S (\nabla \times \vec{a}) d\vec{S} \quad \Rightarrow -\Gamma = \int_S \vec{\omega} d\vec{S}. \quad (19)$$

We remember that:

$$\begin{aligned} \vec{R} &= \rho \vec{v}_\infty \times \int \vec{\omega} dV = \rho \vec{v}_\infty \times \int l \vec{\omega} dS \quad \Leftrightarrow \frac{\vec{R}}{l} = \rho \vec{v}_\infty \times \int \vec{\omega} dS \\ \frac{\vec{R}}{l} &= \rho \vec{v}_\infty \times \int \vec{\omega} (d\vec{S} \cdot \vec{l}_z) = \rho \vec{v}_\infty \times (-\Gamma) \vec{l}_z = \rho v_\infty \Gamma \vec{l}_y \end{aligned} \quad (20)$$

to finally obtain a very good approximation of the lift:

Kutta formula for lift 2D airfoil

$$|R| = \rho v_\infty \Gamma \quad (21)$$

3 Characteristics of a 2D airfoil:

3.1 Define lift and drag, give the principle components of lift and drag force in normal operation and in case of separation

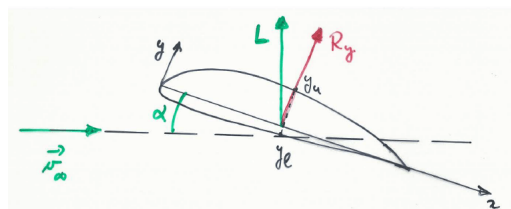


Figure 6

Force applied on the wing:

$$\vec{R} = -\oint p d\vec{S} + \oint \bar{\tau} d\vec{S} \quad (22)$$

with an external normal to the airfoil. The angle of attack is represented on Figure 6.

The pressure term is responsible for lift and the friction term is responsible for drag. Friction forces work tangential to the airfoil and the pressure forces are perpendicular, if there is **no separation** in the flow. The drag created by the stress is called the **skin or friction** drag. Note that in a subsonic inviscid incompressible flow, we have the paradox of d'Alembert because we

have no drag. This shows that the pressure only contributes to lift.

Separation: region above the airfoil where $p - p_\infty \approx 0 \Rightarrow$ high pressure below $p \gg p_\infty$ that slows down the wing. This implies that the applied force is higher than the case without separation and due to the attack angle, the drag force too. This phenomenon is called **pressure drag** (form drag), and here the pressure contributes to drag.

3.2 Explain the non-dimensional force coefficients (C_l , C_d , C_m) and which are the similarity parameters influencing these coefficients

Let's look to the non-dimensional parameters that will influence the lift, the drag and the momentum. We have to define some reference quantities:

$$\begin{aligned} L_{ref} &= C & v_{ref} &= v_\infty & t_{ref} &= L_{ref}/v_{ref} & \rho_{ref} &= \rho_\infty \\ t' &= t/t_{ref} & p_{ref} &= \rho_{ref} \frac{v_{ref}^2}{2} & \text{Mach} &= V_{ref}/a_{ref} & a_{ref} &= \gamma \pi T_{ref} \\ \gamma &= c_p/c_v & Re_{ref} &= \frac{\rho_{ref} v_{ref} L_{ref}}{\mu_{ref}} \end{aligned} \quad (23)$$

where a is the speed of sound. By replacing all these in the mass, momentum and energy equations, we obtain the non-dimensional ones (see Fluid Mechanics II):

$$\begin{aligned} &\bullet \frac{\partial \rho'}{\partial t'} + \nabla (\rho' \vec{v}') = 0 \\ &\bullet \rho' \frac{d\vec{v}'}{dt'} = -\frac{1}{\gamma M_{ref}^2} \nabla p' + \frac{1}{Re_{ref}} \nabla \bar{\tau}' \\ &\bullet \frac{d}{dt'} (\rho' e') + \frac{\gamma(\gamma-1)}{2} M_{ref}^2 \frac{d}{dt'} (\rho' \vec{v}'^2) \\ &= \frac{\gamma}{Pr_{ref} Re_{ref}} \nabla (k' \nabla T') - (\gamma-1) \nabla (p' \vec{v}') + \gamma(\gamma-1) \frac{M_{ref}^2}{Re_{ref}} \nabla (\bar{\tau}' \vec{v}') \end{aligned} \quad (24)$$

We can see that a solution can only be function of 4 parameters: $M, Re, Pr = \frac{c_p \mu}{k}, \gamma$, but we know that the geometry and the angle of attack α have a role by means of the boundary conditions. Then, we assume that the fluid is air ($\gamma = 1.4$) and that we can neglect heat effects (no influence of Pr , incompressible and so low speed flows). The non-dimensional lift, drag and moment are thus function of M, Re , geometry and α . We can define **lift**, **drag** and **moment coefficient** as (we forget about compressibility $\rightarrow M$, and Re effects are low for C_L and C_M):

$$\begin{aligned} C_L(M, Re, geometry, \alpha) &= \frac{L}{\frac{1}{2} \rho_{ref} v_{ref}^2 S} \\ C_D(M, Re, geometry, \alpha) &= \frac{D}{\frac{1}{2} \rho_{ref} v_{ref}^2 S} \\ C_M(M, Re, geometry, \alpha) &= \frac{M}{\frac{1}{2} \rho_{ref} v_{ref}^2 Sc} \end{aligned} \quad (25)$$

where L, D, M are the **dimensional** forces, c the mean chord (S/b) and S a reference surface (3D wing \rightarrow total wing surface, 2D wing $\rightarrow S = c$). We can experimentally show that the lift increases mainly linearly with α and the drag force is caused by friction effects and pressure differences involving with α . This gives the following equations (lower case for 2D):

$$c_l = m(\alpha - \alpha_{L_0}) \quad c_d = c_{d_0} + k c_l^2 \quad (26)$$

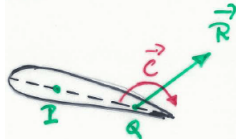
where $m \approx 2\pi$ theoretically and 5.7 practically, k is a constant of order of magnitude 0.01.

3.3 Explain:

center of pressure CP: It's the x value on the chord where the carrier of the force \vec{R} intersects the chord. It's function of the angle of attack. Indeed, if alpha increases, the suction peak will be higher, this induces that the center of pressure move forward (participation of the forward pressure more important).

Note that the center of pressure is not a fixed point. Indeed, it varies with the angle of attack: if $\alpha \nearrow$, the pressure peak on the LE is more important making the x_p move upstream, and the contrary for $\alpha \searrow$. This notion will be completed by the **zero lift angle** α_0 .

equivalent force system in an arbitrary point Q on the chord of the profile:



The force at the pressure center P is equivalent to another force in point Q, but by adding the moment to compensate the one added by moving the force. This moment is:

$$\vec{C}_Q = -\vec{PQ} \times \vec{R}. \quad (27)$$

Figure 7

aerodynamic center AC: Suppose that there is a point Q where the couple C_Q is independent of the angle of attack (because the pressure center changes with alpha). This point is called the aerodynamic center.

The moment at this point is always nose-down and the point is situated upstream to the center of pressure.

the graph of the momentum coefficient c_m at a point Q versus the lift coefficient c_l for Q located at the trailing edge, at the leading edge and at the aerodynamic center of the profile: It is shown experimentally that:

$$c_m(Q) = c_{m0} + k c_l \quad (28)$$

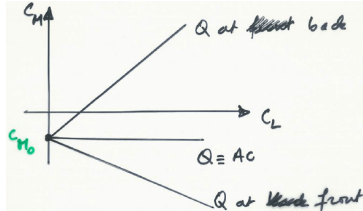


Figure 8

k is a constant that is related to the reference point chosen. If Q is taken on the LE for example, increasing α will produce an increase of the lift and make the center of pressure move upstream. The L increase will compensate the moving x_p such that the moment becomes even more nose-down (more negative following \vec{l}_z) $\Rightarrow k < 0$ for a decrease in (28). The same reasoning applied on the trailing edge gives $k > 0$.

3.4 Compute the Location of the center of pressure CP as a function of the angle of attack alpha

$$\begin{aligned} 1) \quad c_m &= c_{m0} + k c_l & 2) \quad M_{ac} &= (x_{ac} - x_{cp}) N \\ 3) \quad m_{ac} &= M_{AC} = M_0 < 0 & 4) \quad N &= n(\alpha - \alpha_0) \end{aligned} \quad (29)$$

The AC being always upstream the CP the difference in 2) is < 0 . In 4), $n > 0$. By using equation 3,4 and 2, we can compute:

$$M_0 = -(x_{cp} - x_{ac}).n(\alpha - \alpha_0) \Leftrightarrow -\frac{M_0}{n} = (x_{cp} - x_{ac}).(\alpha - \alpha_0) \quad (30)$$

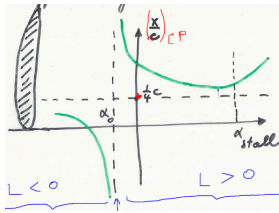


Figure 9

This is the equation of an **hyperbola**. To see it, we only have to compute the limits:

$$\begin{aligned} x_{cp} &= x_{ac} - \frac{M_0}{n} \frac{1}{\alpha - \alpha_0} \\ \lim_{\alpha \rightarrow \pm\infty} x_{cp} &= x_{ac} \quad \lim_{\alpha \rightarrow \alpha_0 > 0} x_{cp} = +\infty \quad \lim_{\alpha \rightarrow \alpha_0 < 0} x_{cp} = -\infty \end{aligned} \quad (31)$$

Let's finally say that commonly, $x_{ac} = cst \approx \frac{1}{4}C$.

3.5 Explain the lift, drag and moment curves as a function of the angle of attack alpha

Starting from what is said in 3.2, experiment showed that lift is increasing linearly with α , and drag goes proportionnaly to c_d^2 . The moment is proportionnal to c_l , we thus expect it to be linear with respect to α .

3.6 Explain what is stall and critical angle of attack. Explain different types of stall.

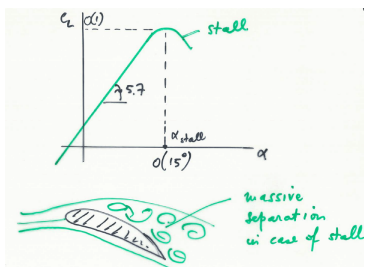
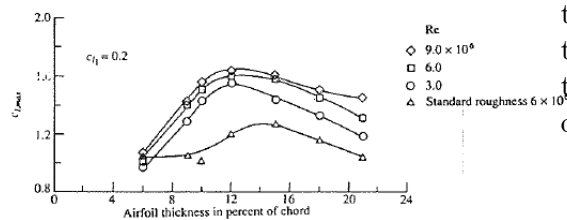
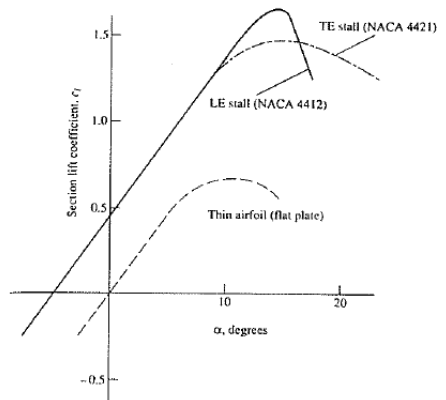


Figure 10

At a certain angle of attack ($\approx 15^\circ$), the lift suddenly drops. This is due to massive separation on the suction side (reverse pressure gradient too high) and happens at the **critical angle of attack**. This phenomenon is called **stall**. In the separated part, the pressure will no longer decrease and will form a pressure plateau.

We have to make the difference between leading-edge stall and trailing-edge stall. For **leading-edge stall**, the massive separation occurs suddenly near the LE resulting in a strong and sudden drop of lift, when at maximum lift. This especially occurs to thin airfoils with cross-sections between 10 and 16% of the chord. For the **trailing-edge stall**, the point of separation gradually goes upstream with increasing angle of attack resulting in a more gradual drop of lift (more thick airfoils). The comparison is done on the right figure. We can also see a third type of stall called **thin airfoil stall** with the example of a flat plat.

In conclusion, the LE must be sufficiently rounded to have a good maximum lift. In fact the profile may nor be too



13

Figure 12

thick nor too thin. The figure on the left shows the influence of the thickness on the lift. We notice that the optimum thickness is situated around 12% of the chord. The maximum lift increases with RE,

indeed higher the Re, higher is the ratio of speed versus viscosity. So we can better oppose to separation. Unlike the Re number, the roughness has great effects on the maximum lift. Finally, let's notice that the camber have also an effect on maximum lift, the best is a camber of 8 up to 10%.

$$L = C_L \frac{1}{2} \rho_{ref} v_{ref}^2 S. \quad (32)$$

The lift force must always at least be equal to the weight of the plane. This implies that for low speed (take-off and landing), the C_L must be large. This is accomplished with large α and slats or flaps. The minimum speed where the lift can still balance the weight (C_L maximum) is called **stall speed** and from (32) we find:

$$v_{stall} = \sqrt{\frac{W}{C_{L_{max}} \frac{1}{2} \rho_{ref} S}} \quad (33)$$

3.7 Discuss the polar curve of the airfoil, i.e. lift coefficient as a function of drag coefficient, show the glide ratio on this plot

The curve that represents C_L in function of C_D is the **polar curve** of the wing. The ratio $\frac{C_L}{C_D}$ is the **glide ratio** or **finesse** and is like an efficiency parameter.

3.8 What is the importance of the glide ratio, discuss the case of a gliding plane (engine off situation)

The best parameter is obtained using the graph by calculating β such that:

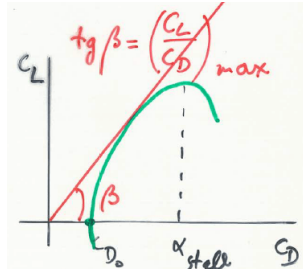


Figure 13

$$\tan \beta = \left(\frac{C_L}{C_D} \right)_{max} \quad (34)$$

This point is important for the quality of the wing because if we plot the thrust, the lift, the drag and the weight of a plane describing a horizontal flight (Figure 14), the thrust is given by:

$$T = \frac{L}{\tan \beta} = \frac{W}{\tan \beta} \quad (35)$$

where we see that when $\tan \beta$ (so the glide ratio) increases, T decreases. Another interpretation can be given when we have no thrust (Figure 15). In this case the gliding ratio has to be adapted to travel the larger distance knowing that:

$$\frac{C_L}{C_D} = \frac{\text{distance travelled}}{\text{height loss}} \quad (36)$$

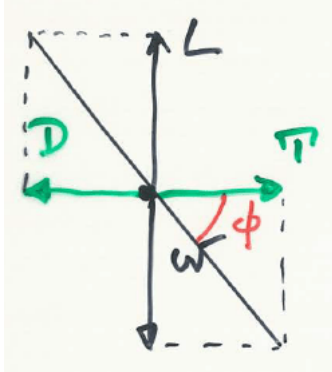


Figure 14

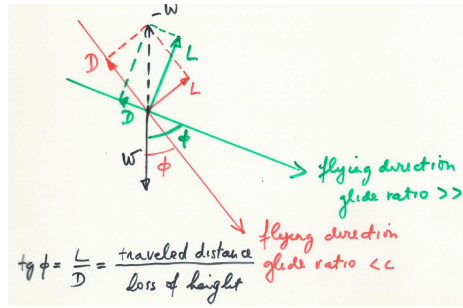


Figure 15

4 Computation of inviscid irrotational flow around a 2D airfoil using conformal mapping - Joukowski profiles

4.1 Explain methods based on complex potential function, explain the connection with usual stream function and potential function

We will begin here with steady, inviscid irrotational flows. This gives for the mass conservation equation:

$$\frac{\partial \rho}{\partial t} + \nabla(\rho \vec{v}) = 0 \quad \Rightarrow \nabla \cdot \vec{v} = 0 = \partial_x u + \partial_y v \quad (37)$$

In the other hand, we have the assumption of irrotational flow:

$$\vec{\omega} = 0 \quad \Rightarrow \partial_x v - \partial_y u = 0. \quad (38)$$

Then we define the **complex potential function** w :

$$w = \phi + I\psi \quad (39)$$

where ϕ is the **potential function** (satisfies $w = 0$ by construction) such that:

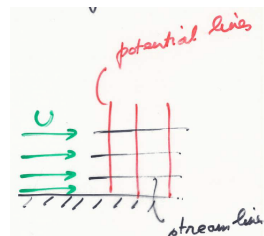
$$\begin{cases} u = \partial_x \phi \\ v = \partial_y \phi \end{cases} \quad \nabla \phi = \vec{v} = \partial_x \phi \vec{i}_x + \partial_y \phi \vec{i}_y \quad (40)$$

We must satisfy the mass conservation equation:

$$\nabla \cdot (\nabla \phi) = 0 \quad \Rightarrow \Delta \phi = 0 \quad (41)$$

coupled with boundary conditions, we can find a solution $\phi(x, y)$. The **stream function** satisfies the mass conservation by construction:

$$\begin{cases} u = \partial_y \psi \\ v = -\partial_x \psi \end{cases} \quad \Rightarrow \partial_x u + \partial_y v = 0 \Leftrightarrow \partial_x(\partial_y \psi) + \partial_y(-\partial_x \psi) = 0 \quad (42)$$



We still have to verify the $\omega = 0$ condition:

$$\partial_x v - \partial_y u = 0 \quad \Rightarrow \frac{\partial^2 \psi}{\partial x^2} + \frac{\partial^2 \psi}{\partial y^2} = 0 \quad \Delta \psi = 0 \quad (43)$$

Figure 16

A streamline and a potential line are perpendicular to each other:

$$\nabla\psi \cdot \nabla\phi = \partial_x\psi\partial_x\phi + \partial_y\psi\partial_y\phi = -vu + uv = 0. \quad (44)$$

Analytical means differentiable. This consist in defining a function $f(z)$ analytical such that:

$$w = f(z) \quad z, \omega \in \mathbb{C} \quad \Rightarrow w = \phi + i\psi \quad \begin{cases} z = x + iy \\ \phi = \phi(x, y) \in \mathbb{R} \\ \psi = \psi(x, y) \in \mathbb{R} \end{cases} \quad (45)$$

If this is differentiable everywhere, $\Delta\phi = \Delta\psi = 0$.

4.2 Explain how the velocity can be computed from the complex potential function

The complex velocity (velocity field):

$$\frac{dw}{dz} = \frac{df}{dz} = A + iB \quad A = \frac{\partial\phi}{\partial x} = -\frac{\partial\psi}{\partial y} = u \quad B = \frac{\partial\psi}{\partial x} = -\frac{\partial\phi}{\partial y} = -v \quad (46)$$

A property of this $f(z)$ is the superposition principle: $w_1 = f_1(z), w_2 = f_2(z)$ so $w_1 + w_2 = f_1(z) + f_2(z)$.

4.3 Derive the complex potential function for uniform flow, source/sink flow, free vortex

4.3.1 Uniform flow

$$w = Uz \quad \frac{dw}{dz} = U = u + iv \quad \Rightarrow u = U; v = 0 \quad (47)$$

4.3.2 Source / Sink

In this case, using the cylindrical coordinates, the complex potential is defined as (Λ being the volumetric flow):

$$\begin{aligned} w &= \frac{\Lambda}{2\pi} \ln z = \frac{\Lambda}{2\pi} \ln(re^{i\theta}) = \frac{\Lambda}{2\pi} (\ln r + i\theta) \\ \Rightarrow \phi &= \frac{\Lambda}{2\pi} \ln r, \psi = \frac{\Lambda}{2\pi} \theta. \end{aligned} \quad (48)$$

We see that complex lines corresponds to $r = cst$ so are circles and streamlines $\theta = cst$ are line of constant angle. $\oint \vec{v} d\vec{l} = 0$ as velocity is everywhere tangent to any circular contour. Let's compute the derivative for the velocity field.

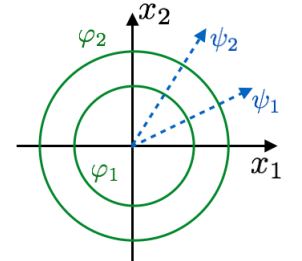


Figure 17

$$\frac{dw}{dz} = \frac{\Lambda}{2\pi z} = \frac{\Lambda(x - iy)}{2\pi(x^2 + y^2)} = \frac{\Lambda}{2\pi r} (\cos\theta - i\sin\theta). \quad (49)$$

We see that the velocity decreases in $1/r$, this is due to the constant mass flow, so if the surface increases with r the velocity has to decrease to keep $\dot{m} = \rho v S$ constant.

4.3.3 Free vortex

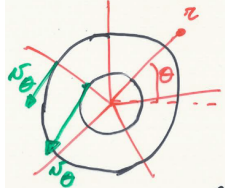


Figure 18

We do the same as the other cases:

$$w = \frac{i\Gamma}{2\pi} \ln z = \frac{i\Gamma}{2\pi} \ln(re^{i\theta}) = \frac{i\Gamma}{2\pi} (\ln r + i\theta) = -\frac{\Gamma}{2\pi} \theta + \frac{i\Gamma}{2\pi} \ln r$$

$$\phi = -\frac{\Gamma}{2\pi} \theta, \psi = \frac{\Gamma}{2\pi} \ln r$$
(50)

We see that this is the inverse case of the previous one, streamlines are circles oriented in negative rotational motion around z-axis (z entering in the sheet) so clockwise. We can compute the velocity field by deriving among z and we find that:

$$u = \frac{\Gamma \sin \theta}{2\pi r} \quad v = -\frac{\Gamma \cos \theta}{2\pi r}$$
(51)

Let's specify that $v_\theta = \frac{1}{r} \frac{\partial \phi}{\partial \theta} = -\frac{\Gamma}{2\pi r}$, and that we have a vortex singularity in the center because $\Gamma = 0.\infty$.

4.4 Compute flow around Rankine body and around a cylinder

Let's make a combination of a uniform flow and a source + sink as shown on the figure. The combination gives:

$$w = Uz + \frac{\Lambda}{2\pi} \ln \frac{z+a}{z-a} = Uz + \frac{\Lambda}{2\pi} \ln \frac{1+a/z}{1-a/z}. \quad (52)$$

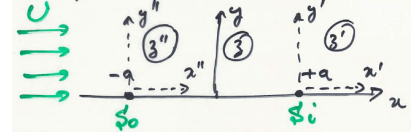


Figure 19

To have the flow around a cylinder we need to compute the limit $a \rightarrow 0$, and will need the Taylor expansion of \ln :

$$\ln \frac{1+\epsilon}{1-\epsilon} \approx 2\epsilon + o(\epsilon^2) \quad \Rightarrow \lim_{a \rightarrow 0} w = \lim_{a \rightarrow 0} \left[Uz + \frac{\Lambda}{2\pi} 2 \frac{a}{z} \right]$$
(53)

by defining $\mu = 2\Lambda a$ we find the **flow around a cylinder**:

$$w = Uz + \frac{\mu}{2\pi z}.$$
(54)

If we replace $z = x + iy$ to find ϕ and ψ we find:

$$\phi = Ux + \frac{\mu}{2\pi} \frac{x}{r^2} \quad \psi = Uy - \frac{\mu}{2\pi} \frac{y}{r^2}.$$
(55)

In this flow a closed streamline exists forming the so called **Rankine body** and which describes a cylinder in the case $a \rightarrow 0$. Indeed it is possible to find an exact solution for $\psi = 0$. This configuration has a symmetry according to x and y-axis when taking the center of the cylinder as origin. This implies that $\vec{F} = -\oint_{cyl} p d\vec{S} = 0$. This is the so called **paradox of d'Alembert** because we expect to find at least a drag force. A lift force can be found on the cylinder by adding a vortex. We conclude by saying that we can rewrite (54) as (R the radius of the cylinder):

$$w = U \left(z + \frac{R^2}{z} \right) \quad \text{with } R^2 = \frac{\mu}{2\pi U}.$$
(56)

4.5 Explain how the class of Joukowski profiles is obtained by conformal mapping of a circle

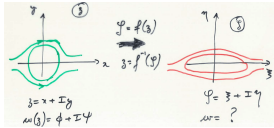


Figure 20

Let's do a mapping, a transformation, to try to find our airfoil based on simple geometries. Let's as first example apply the transformation $Z = z + \frac{R^2}{z}$ to the cylinder of radius R . Let's first remark that the cylinder will become a flat plate:

$$Z = z + \frac{R^2}{z} = Re^{i\theta} \frac{R^2}{Re^{i\theta}} = 2R \cos \theta \quad (57)$$

Indeed, as $\cos \theta \in [-1, 1]$ and the result is real, we have a flat plate between $-2R$ and $2R$ in the x -axis. The flow Z is directly found: $W(Z) = UZ$. The second example will be the application of the same transformation on a cylinder of this time radius $r > R$. In this case the circle becomes an ellipse:

$$Z = re^{i\theta} + \frac{R^2}{r^2} e^{-i\theta} = \left(r + \frac{R^2}{r} \right) \cos \theta + i \left(r - \frac{R^2}{r} \right) \sin \theta. \quad (58)$$

Let's also compute the velocity field using the chain rule:

$$\frac{dW}{dZ} = \frac{dw}{dZ} = \frac{dw}{dz} \frac{dz}{dZ} = \left(1 - \frac{r^2}{z^2} \right) \left(\frac{1}{1 - \frac{R^2}{z^2}} \right). \quad (59)$$

We see that the expression becomes infinite when $z^2 = R^2$. The reason is that the transformation is not analytical in these points so they must not be in the flow.

The examples are summarized in the figures below

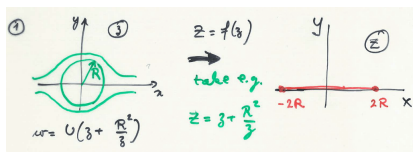


Figure 21

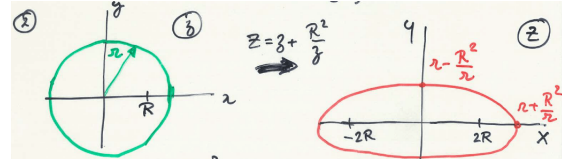


Figure 22

Now suppose that we place no longer the center of the cylinder at the origin, but on the real axis. The mapping of the cylinder now takes the shape of a **symmetrical wing profile**. We see that there are two remarkable points that are H and A corresponding to the points H_1 and A_1 of the black and red circles, our profile is in between them. Now to give camber we only have to move the center of the cylinder on the y -axis. Please refer to figures below.

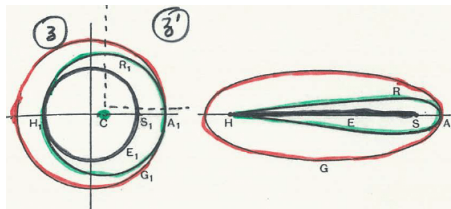


Figure 23

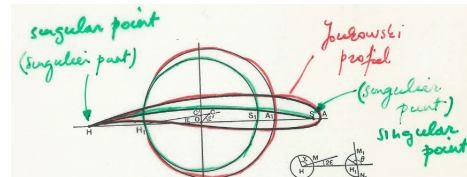


Figure 24

Note that for the green circle in first figure, the complex potential becomes:

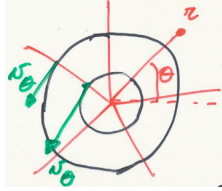
$$w = U \left(z - z_c + \frac{r^2}{z - z_c} \right) \quad (60)$$

As last remark, let's remind that we had singularities in the second example. These points corresponds here to H_1 and S_1 . The mapping of H_1 is always H the trailing edge, the velocity is there infinitely large. This was the discussion we've previously done with the stagnation point that has to move on the trailing edge otherwise $v = \infty$ because of the sharp edge. We can solve this by adding a vortex. This methods gives a limited amount of airfoils.

5 Computation of inviscid irrotational flow around a thin airfoil based on a continuous distribution of vortices

5.1 Explain what is a free vortex

A free vortex is an irrotational vortex where the flow velocity u is inversely proportional to the distance r .



Streamlines are circles oriented in negative rotational motion around z-axis (z entering in the sheet) so clockwise. We can compute the velocity field by deriving among z and we find that:

$$u = \frac{\Gamma \sin \theta}{2\pi r} \quad v = -\frac{\Gamma \cos \theta}{2\pi r} \quad (61)$$

Figure 25

Let's specify that $v_\theta = \frac{1}{r} \frac{\partial \phi}{\partial \theta} = -\frac{\Gamma}{2\pi r}$, and that we have a vortex singularity in the center because $\Gamma = 0.\infty$.

5.2 Explain what is a continuous distribution of free vortices on a line

A way to represent thin airfoils is to use only their camberline and to retrieve the flow using an infinite line of free vortices (or sources). A infinite line of vortices thus represents an infinite thin airfoil.

5.3 Explain principle of the method of free vortex distribution applied thin airfoils, limitations and hypotheses

We will suppose infinitely thin airfoil and small angle of attack, so that the airfoil is represented by the camber line. This means also small camber about 2-3% of the chord and $\alpha < 8\%$. We can try to retrieve the flow by superposition principle by using infinite number of elementary sources or elementary vortices. The potential function for the sources is:

$$\phi = \frac{\Lambda}{2\pi} \ln r \quad d\phi = \frac{d\Lambda}{2\pi} \ln r \quad (62)$$

We then describe the source distribution by the source intensity $\lambda = \frac{d\Lambda}{ds}$ on a part ds of the wing so that the last equation becomes:

$$d\phi = \frac{\lambda}{2\pi} \ln r ds. \quad (63)$$

We will use the second method presented now which is using the vortices:

$$\phi = -\frac{\Gamma}{2\pi} \theta \quad \vec{v} = \nabla \phi = \underbrace{\frac{\partial \phi}{\partial r} \vec{1}_r}_{=v_r=0} + \underbrace{\frac{1}{r} \frac{\partial \phi}{\partial \theta} \vec{1}_\theta}_{=v_\theta} \quad \Rightarrow v_\theta = -\frac{\Gamma}{2\pi r}. \quad (64)$$

In the same way as the other we can define a **vortex intensity** to characterize the vortex distribution on a part ds $\gamma = \frac{d\Gamma}{ds}$, the derivative of ϕ and the elementary velocity are then:

$$d\phi = -\frac{\gamma}{2\pi} \theta ds \quad dv_\theta = -\frac{\gamma ds}{2\pi r}. \quad (65)$$

The aim now is to make that infinitely thin airfoil a streamline. We assume because of superposition that the flow is a uniform flow \vec{U}_∞ , that we have an angle of attack α . Because of the vorticities, we have a velocity perturbation \vec{v} such that the total velocity is:

$$\vec{V}_\infty = \vec{U}_\infty + \vec{v}. \quad (66)$$

5.4 Establish the integral equation which allows to compute the vortex distribution for a given profile

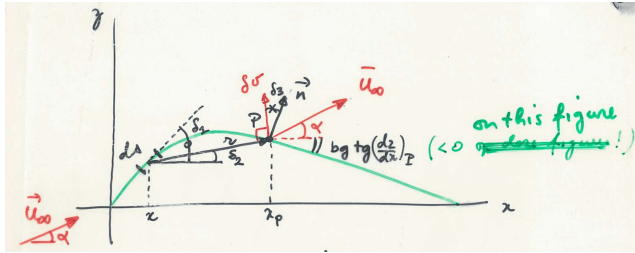


Figure 26

We must now choose γ such that \vec{V} is tangential to the airfoil everywhere (we want the camber line to be a streamline). In other words, $\forall P$ the normal component of the velocity should be null $V_{nP} = U_{\infty nP} + v_{nP} = 0$. Let's determine these components by projection. First, for $U_{\infty nP}$ we can remark the sum of angle α and the camber line slope $\tan \beta = \left(-\frac{dz}{dx}\right)_p \Rightarrow \beta = -\arctan\left(\frac{dz}{dx}\right)_p$, the projection is (camber line: $z = f(x)$):

$$U_{\infty nP} = U_\infty \sin \left[\alpha - \arctan \left(\frac{dz}{dx} \right)_P \right]. \quad (67)$$

Now for v_{np} , we consider an elementary vortex on a point x on the airfoil that creates an elementary perturbation δv_n on point P . This velocity direction is θ in a (r, θ) axis with origin at x , so perpendicular to r on the figure. If the angle with the normal is δ_3 , the projection will be:

$$\delta v_n = -\frac{\gamma(x)ds}{2\pi r} \cos \delta_3. \quad (68)$$

Now we have infinite number of contribution of the infinite vorticities, as γ, r and δ_3 depend on position P , we have to integrate over the whole airfoil:

$$v_n = -\frac{1}{2\pi} \int_0^c \frac{\gamma(x)ds}{r} \cos \delta_3 \quad (69)$$

where c is the chord length. We can express both r and ds in function of x as:

$$r = \frac{x_P - x}{\cos \delta_2} \quad ds = \frac{dx}{\cos \delta_1} \quad (70)$$

which gives

$$v_n = -\frac{1}{2\pi} \int_0^c \frac{\gamma(x)dx}{x_P - x} \frac{\cos \delta_2}{\cos \delta_1} \cos \delta_3. \quad (71)$$

We are able to reconsider the condition (67) by replacing our results:

$$\frac{1}{2\pi} \int_0^c \frac{\gamma(x) dx}{x_P - x} \cos \delta_2 \cos \delta_3 = U_\infty \sin \left[\alpha - \arctan \left(\frac{dz}{dx} \right)_P \right]. \quad (72)$$

This is a relatively complicated equation, we can simplify it by **assuming a small camber** (in practice 2% of the chord), which allows to say that $\delta_1 \approx \delta_2 \approx \delta_3 \approx 0$ and $\arctan \left(\frac{dz}{dx} \right)_P = \left(\frac{dz}{dx} \right)_P$. By considering α small, $\sin \alpha \approx \alpha$:

$$\frac{1}{2\pi} \int_0^c \frac{\gamma(x) dx}{x_P - x} = U_\infty \left[\alpha - \left(\frac{dz}{dx} \right)_P \right]. \quad (73)$$

We will introduce a new variable θ , considering $x = \frac{1}{2}c(1 - \cos \theta)$ and $dx = \frac{1}{2}c \sin \theta d\theta$:

$$\frac{1}{2\pi} \int_0^\pi \frac{\gamma(\theta) \sin \theta d\theta}{\cos \theta - \cos \theta_P} = U_\infty \left[\alpha - \left(\frac{dz}{dx} \right)_P \right]. \quad (74)$$

5.5 Show how to solve this equation using a spectral method, i.e. by expressing the vortex distribution as a truncated Fourier series

Let's express $\gamma(\theta)$ in series:

$$\gamma(\theta) = 2U_\infty \left(A_0 \coth \frac{\theta}{2} + \sum_{n=1}^{\infty} A_n \sin(n\theta) \right). \quad (75)$$

This is in fact a solution of the last equation.

Now we can replace this definition on the previous equation, knowing that $\coth(\theta/2) \sin \theta = 1 + \cos \theta$ and writing $\theta_P = \theta'$, we get:

$$\frac{1}{2\pi} \int_0^\pi \frac{\gamma(\theta) \sin \theta d\theta}{\cos \theta - \cos \theta_P} = \frac{U_\infty}{\pi} \left[\int_0^\pi \frac{A_0(1 + \cos \theta) d\theta}{\cos \theta - \cos \theta'} + \sum_n A_n \int_0^\pi \frac{\sin(n\theta) \sin \theta d\theta}{\cos \theta - \cos \theta'} \right] \quad (76)$$

By using the equality here and the **Glauert integral**:

$$\sin(n\theta) \sin \theta = -\frac{1}{2} [\cos((n+1)\theta) - \cos((n-1)\theta)] \quad \int_0^\pi \frac{\cos(n\theta) d\theta}{\cos \theta - \cos \theta'} = \pi \frac{\sin(n\theta')}{\sin \theta'} \quad (77)$$

The integral becomes:

$$\frac{U_\infty}{\pi} \left[A_0.0 + A_0.\pi - \frac{\pi}{2} \sum_n A_n \frac{\sin((n+1)\theta') - \sin((n-1)\theta')}{\sin \theta'} \right] = U_\infty \left[A_0 - \sum_n A_n \cos(n\theta') \right] \quad (78)$$

where we used the Simpson equation. The (74) becomes:

$$A_0 - \sum_n A_n \cos(n\theta') = \alpha - \left(\frac{dz}{dx} \right)' \quad (79)$$

This equation must be valid $\forall P$ on the airfoil. To find the coefficients A_i , let's integrate first this for $0 \leq \theta' \leq \pi$ in order to compute A_0 :

$$A_0\pi - \sum_n A_n \int_0^\pi \cos(n\theta') d\theta' = \alpha\pi - \int_0^\pi \frac{dz}{dx} d\theta \quad \Rightarrow A_0 = \alpha - \frac{1}{\pi} \int_0^\pi \frac{dz}{dx} d\theta. \quad (80)$$

For the A_n , we multiply the same equation by $\cos(m\theta')$ before integrating (we will drop the '). Let's see that $\int_0^\pi \cos(n\theta) \cos(m\theta) d\theta = 0$ if $m \neq n$ and $= \pi/2$ if $n = m$. We finally get:

$$A_n = \frac{2}{\pi} \int_0^\pi \frac{dz}{dx} \cos(m\theta) d\theta. \quad (81)$$

We can note that for A_n only the camber plays a role, the angle of attack does not appear. Only A_0 is influenced by α . We are now able to compute any vorticity distribution $\gamma(\theta)$, for example for a flat plate $A_n = 0$ and $A_0 = \alpha$.

5.6 How is the Kutta-Youkowsky condition imposed (allowing to compute the lift)

The above respects the Kutta condition that states that there is no vortex allowed on the trailing edge. Indeed, $\gamma(\pi) = 0$ which means no contribution by vortex. We can also state that at the leading edge, the stagnation point is in the pressure side at the front. Indeed, for $\theta = 0$, $\coth \theta = \infty = \gamma(\pi)$ which means that we have a singularity at the TE and that the velocity is infinite due to the turning on the LE.

5.7 Starting from the expressions for the Fourier coefficients, compute the circulation and lift coefficient as a function of angle of attack, explain the result

5.7.1 Calculation of the total circulation

To get Γ we only have to compute the integral over the whole airfoil:

$$\begin{aligned} \Gamma &= \int_0^c \gamma(x) dx = \frac{1}{2} c \int_0^c \gamma(\theta) \sin \theta d\theta \\ &= \frac{1}{2} c \left[2U_\infty \int_0^\pi A_0(1 + \cos \theta) d\theta + 2U_\infty \sum_{n=1}^{\infty} \int_0^\pi A_n \sin(n\theta) \sin \theta d\theta \right] \\ &= U_\infty c \left[A_0 \pi + 2U_\infty + \int_0^\pi \sin^2(\theta) d\theta - \frac{1}{2} \sum_{n=2}^{\infty} \int_0^\pi A_n \cos[(n+1)\theta - \cos(n-1)\theta] d\theta \right] \\ &= U_\infty c [A_0 \pi + A_1 \pi / 2]. \end{aligned} \quad (82)$$

We see that the circulation only depends on two coefficients.

5.7.2 Calculation of the lift coefficient

We can now compute the lift using the kutta formula $L = \rho_\infty U_\infty \Gamma$. We are interested in the c_l and not the lift itself. In 2D we have to divide by the chord so:

$$c_l = \frac{L}{\frac{1}{2} \rho_\infty U_\infty^2 C} = \frac{2\Gamma}{U_\infty c} = \pi(2A_0 + A_1) \quad (83)$$

We can now replace by definition of the coefficients:

$$c_l = 2\pi \left(\alpha - \underbrace{\frac{1}{\pi} \int_0^\pi \frac{dz}{dx} (1 - \cos \theta) d\theta}_{\alpha_0} \right) = 2\pi(\alpha - \alpha_0) \quad (84)$$

where α_0 is the **zero lift angle of attack**. We see that we have a linear relation with respect to α . We have the theoretical model the same for every profile, only α_0 changes with the profile. Remark that the lift is also the integral of the pressure on the lower and upper side:

$$L = \int_0^c (p_l - p_u) dx = \rho_\infty U_\infty \int_0^c \gamma dx \quad \Rightarrow p_l - p_u = \rho_\infty U_\infty \gamma(x). \quad (85)$$

5.8 Starting from the expression for the momentum coefficient at the leading edge $c_m(\text{LE})$, show that it's a linear function of the lift coefficient c_l



Figure 27

The contribution of the elementary parts of the airfoil gives:

$$\begin{aligned} dM_{LE} &= -(\Delta p dx)x \\ \Rightarrow M_{LE} &= - \int_0^c \Delta p x dx = -\rho_\infty U_\infty \int_0^c \gamma x dx \end{aligned} \quad (86)$$

After some manipulations (not detailed):

$$c_{m_{LE}} = \frac{M_{LE}}{\frac{1}{2}\rho_\infty U_\infty^2 c^2} = -\frac{\pi}{4}(2A_0 + 2A_1 - A_2) = -\frac{1}{4}c_l - \frac{\pi}{4}(A_1 - A_2) \quad (87)$$

where we used (83) for the last expression.

5.9 Compute the location of the aerodynamic center AC and the momentum coefficient in the aerodynamic center



Figure 28

The moment on the LE is related to the moment anywhere:

$$M_{LE} = M_{ac} - x_{ac}L \quad \Rightarrow c_{m_{LE}} = c_{m_{ac}} - \frac{x_{ac}}{c}c_l \quad (88)$$

We have:

$$c_{m_{ac}} = \left(\frac{x_{ac}}{c} - \frac{1}{4} \right) c_l - \frac{\pi}{4}(A_1 - A_2). \quad (89)$$

We see that, for this relation to be independent of the angle of attack, we must have $x_{ac} = \frac{c}{4}$ so that:

$$c_{m_{ac}} = \frac{\pi}{4}(A_2 - A_1). \quad (90)$$

Remark that for symmetrical wings $\frac{dz}{dx} = 0 \Rightarrow A_1 = A_2 = 0 \Rightarrow c_{m_{ac}} = 0$.

5.10 Compute the location of the center of pressure

We replace ac by cp in aerodynamic center equation, and since the moment should be null at this point:

$$c_{m_{cp}} = c_{m_{LE}} + \frac{x_{cp}}{c}c_l = 0 \quad \Rightarrow \frac{x_{cp}}{c} = \frac{1}{4} + \frac{\frac{\pi}{4}(A_1 - A_2)}{c_l} = \frac{1}{4} - \frac{c_{m_{ac}}}{c_l}. \quad (91)$$

Some remarks:

- the center of pressure is not fixed and varies with the lift
- at 0 lift, $x_{cp} \rightarrow \infty$ (for symmetric wing $x_{cp} = x_{ac} = c/4$ fixed)
- cp always downstream to ac because $c_{m_{ac}} < 0$.

6 Computation of inviscid irrotational flow around a thin airfoil based on a continuous distribution of vortices

Discuss the influence of a flap located at the trailing edge of the airfoil According to the definition of the zero lift angle in (84), the effect of the shape becomes greater when $\theta \approx 180^\circ$ (trailing edge). By making the zero lift angle more negative we can produce more lift before the critical angle of attack that decreases a bit.

The effect is evaluated by taking a flat plate as camber line with a deflection near the TE, starting at $E\%$ of the chord and slope η . E in function of θ_E is:

$$E = \frac{1}{2}(1 + \cos \theta_E). \quad (92)$$

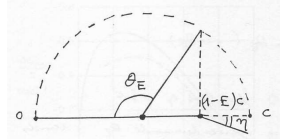


Figure 29

In this case, A_0 and A_n can be rewritten as:

$$\begin{aligned} A_0 &= \alpha - \frac{1}{\pi} \int_0^\pi \frac{dz}{dx} d\theta \approx \alpha - \frac{\eta}{\pi}(\pi - \theta_E) \\ A_n &= \frac{2}{\pi} \int_0^\pi \frac{dz}{dx} \cos(n\theta) d\theta \approx -\frac{2\eta}{\pi} \frac{1}{n} \sin(n\theta_E) \end{aligned} \quad (93)$$

such that the lift coefficient becomes:

$$c_l = \pi(2A_0 + A_1) = \underbrace{2\pi\alpha}_{\text{without flaps}} - \underbrace{-2\eta(\pi - \theta_E + \sin \theta)}_{\Delta c_l > 0 \text{ since } \eta < 0}. \quad (94)$$

This seems to be like $c_l = 2\pi(\alpha - \alpha_0)$ allowing the definition for the zero lift angle:

$$\alpha_0 = \frac{\eta}{\pi}(\pi - \theta_E + \sin \theta) \quad (95)$$

which indicates an increase (decrease since $\eta < 0$) of α_0 since it is null for the flat plate. For the moment at the ac (90)

$$\Delta c_{m_{ac}} = \frac{\eta}{2} \sin \theta_E (1 - \cos \theta_E) \quad (96)$$

which also indicates a decrease in the momentum which is 0 for the symmetric wing.

Determine the effect of the flap on:

the lift curve: from the above, we see that lift goes up with flaps

the zero lift angle of attack: It is increased, see above

the moment at the aerodynamic center: It decreases.

7 3D wing theory

7.1 Explain mean chord, span, aspect ratio, taper, sweep of wing

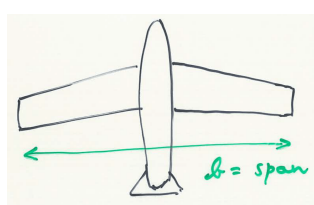


Figure 30

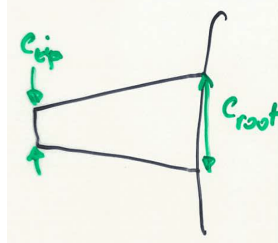


Figure 31

The **span** is the total distance between the tips of the wings, plane body included. It is a straight line.

The **mean chord** is defined by dividing the wing area by the span. This is used to avoid having a chord that varies for calculations.

The **aspect ratio** is the span divided by the mean chord, or the span squared divided by the wing surface. Higher aspect ration means higher lift to drag ratio.

Tapered wings are wing that have a bigger chord near the body. The **taper ratio** is defined by $\frac{c_{tip}}{c_{root}}$

Swept wings are wings that are (at least partially) not \perp to the flow. This is to delay shock wave formation. The sweep is the angle of the leading and/or trailing edge compared to the \perp to the flow.

7.2 Explain downwash effect, downwash angle, effective angle of attack, total and induced drag

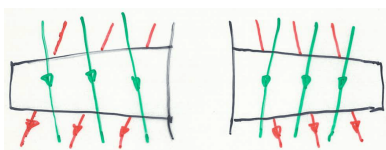


Figure 32

Finite span \Rightarrow the pressure on both side must be equal at the end of the span. This means that the pressure on the upper side must increase when going to the tip, and decrease on the lower side. This creates a pressure gradient between the root and the tip. This gradient will push the streamlines on the upper side towards the fuselage and towards the tip on the lower side.



Figure 33



Figure 34

Looking from downstream, this discontinuity in velocity induces an infinite series of infinitely small vortices, clockwise on the left and anti clockwise on the right wing (Figure 33), resulting in 2 discrete vortices at the tip, the **swung-tip vortices or trailing vortices** (Figure 34).

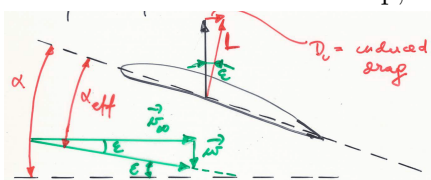


Figure 35

These vortices induce a **downward velocity component**, the **downwash** w . This component superposes on the incoming flow and changes the angle of attack (Figure 35). The angle of change is the **downwash angle**, or induced angle of attack and we compute the **effective angle of attack** $\alpha_{eff} = \alpha - \epsilon$ where ϵ is the induced angle of attack.

The decrease of α means a decrease in lift as the new lift is perpendicular to the new flow, some of it's force produces an **induced drag**.

The **total drag** C_D is computed as being the sum of the profile drag and the induced one. (in reality, we also have to take into account the parasite drags created by the fuselage, antennas,...)

7.3 Starting from the given expression for the downwash angle, compute the induced drag force and the induced drag coefficient

$$\alpha_{eff} = \alpha - \epsilon \quad (97)$$

induced drag:

$$D_i = L \sin \alpha_i \approx L \alpha_i \quad \text{with} \quad \alpha_i = \frac{C_L}{\pi e A R} \quad (98)$$

where e is the **span efficiency factor or Oswald's efficiency factor** $0.85 < e < 1$. We get the Drag coefficient:

$$C_{D_i} = \frac{C_L^2}{\pi e A R}. \quad (99)$$

7.4 Explain the lift curve as a function of the angle of attack for a 3D wing, compare with the lift curve for a 2D profile

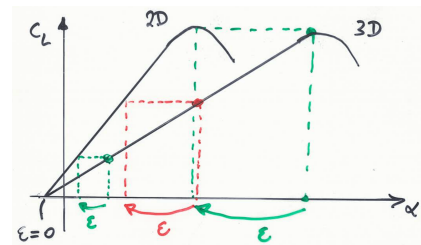


Figure 36

The theoretical lift curve can be obtained based on the 2D wing as Figure 36. We can see that the 3D wing lift for a certain α corresponds to the 2D lift for the effective angle of attack $\alpha - \epsilon$. The induced angle of attack decreases with lift, at α_0 the two curve are on the same point. Algebraically the 2D and 3D curves can be noted:

$$c_l = m(\alpha - \alpha_0), \quad C_L = m(\alpha - \epsilon - \alpha_0) = m^*(\alpha - \alpha_0) \quad (100)$$

where m^* is the slope of the 3D lift. We can isolate this and find that:

$$m^* = m \left(1 - \frac{\epsilon}{\alpha - \alpha_0} \right) = \frac{m}{1 + \frac{m}{\pi e A R}} \quad (101)$$

where we used the definition (98) and (100) for the last result. We see that the slope is independent from α .

7.5 Give the expression for the total drag coefficient as a function of C_L

The total drag is the sum of the profile drag and the induced one:

$$C_D = C_{D_0} + k C_L^2 + C_{D_i} = C_{D_0} + C_L^2 \left(k + \frac{1}{\pi e A R} \right) \quad (102)$$

where k is generally small compared to the other.

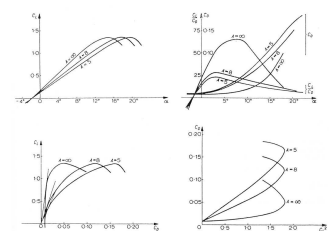


Figure 37

With these formulas we can plot the characteristics in 3D. We can note that the maximum lift does not change so much, but there is a strong decrease in the maximum glide ratio, C_D increases with C_L so α . Finally we note an increase of the stall angle but in practice this is not as large as predicted. This means also that the maximum lift decreases

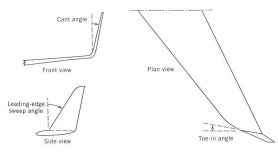


Figure 38

slightly with decreasing AR. No significant difference for the moment.

To avoid the adverse effect which is increasing induced drag. We can use high AR or add winglet on the tip, a kind of end plate that forces a vertical diffusion of the tip vortex, reducing drag. They have to be carefully designed to not increase the viscous drag.

7.6 Give the expression of the drag force D as a function of the velocity at infinity

Let's compute the total drag using the coefficient definition:

$$D = C_D \frac{1}{2} \rho_\infty v_\infty^2 S = C_{D_0} \frac{1}{2} \rho_\infty v_\infty^2 S + \left(k + \frac{1}{\pi e A R} \right) \frac{L^2}{(\frac{1}{2} \rho_\infty v_\infty^2 S)^2} \frac{1}{2} \rho_\infty v_\infty^2 S \\ = k_1 v_\infty^2 + k_2 v_\infty^2. \quad (103)$$

8 3D wing theory – Derivation of Prandtl lifting line method. Give the basic ideas and the development of Prandtl's lifting line theory

8.1 Velocity induced by a vortex filament



Figure 39

The seen free vortex is characterized by circular streamlines around a certain point P. In this point the vorticity is concentrated such that the circulation around the contours that don't contain the point are null. If we consider several planes above each other containing a 2D free vortex, the point P

form a line called **vortex line** or **vortex filament**. The circulation on each point of that line have the same circulation.



Figure 40

This line can be a random line with bending. Now if one places an infinite number of vortex lines besides each other, we get a **vortex sheet**.

The normal component of the velocity is continuous while the tangential one varies as $\Delta v_t = \gamma$ with gamma given by the circulation around a vortex sheet.

Using Bio-Savart at point P:

$$\vec{v} = \frac{\Gamma}{4\pi} \int_{-\infty}^{+\infty} \frac{d\vec{l} \times \vec{r}}{|r|^3}. \quad (104)$$

We have: $d\vec{l} \times \vec{r} = R d\vec{l} \vec{l}_n$, $\vec{v} = v \vec{l}_n$ (see figure). Let's define the length l beginning from the piercing point on the surface until the $d\vec{l}$. We can graphically see that:

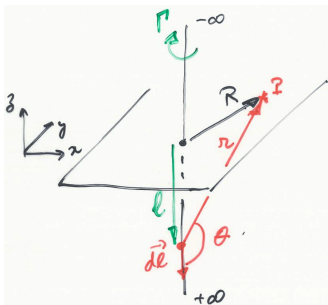


Figure 41

$$l = -R \coth \theta \Rightarrow dl = \frac{R}{\sin^2 \theta} d\theta, \quad r = \frac{R}{\sin \theta} \quad (105)$$

Replacing all this we get:

$$v = \frac{\Gamma}{4\pi} \int_0^\pi \frac{R^2}{\sin^2 \theta} \frac{\sin^3 \theta}{R^3} d\theta \Rightarrow v = \frac{\Gamma}{2\pi R}. \quad (106)$$

This is the velocity distribution of the 2D free vortex.

8.2 Helmholtz theorems, Biot-Savart law

Helmholtz theorems

- Along a vortex line, the circulation must be constant.
- A vortex line cannot finish in the flow but must continue to the edges of the flow or form a closed contour.

This law gives the induced velocity in a certain point P caused by an elementary piece $d\vec{l}$ of the filament:

Law of Biot-Savart

$$d\vec{v} = \frac{\Gamma}{4\pi} \frac{d\vec{l} \times r}{|r|^3} \quad (107)$$

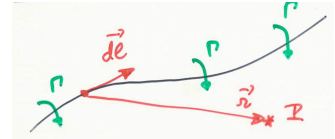


Figure 42

With analogy to electrical wire where we have a current intensity that induces a magnetic field on point P: $d\vec{B} = \frac{\mu I}{4\pi} \frac{d\vec{l} \times r}{|r|^3}$.

8.3 Circulation around a vortex sheet

For the total circulation to be finite, the circulations must be infinitely small, but can vary from one line to the other. The circulation of the vortex sheet is calculated as:

$$\Gamma = \int_a^b d\Gamma = \gamma ds \quad (108)$$

8.4 Downwash velocity induced by a single horseshoe vortex, why this model for a wing is not working

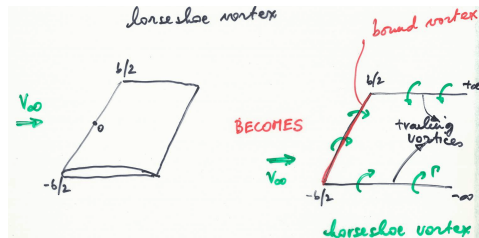


Figure 43

The idea is to represent the 3D wing by means of vortex filaments. On the figure we have the **horseshoe vortex** where the x direction continues to infinity to satisfy the Helmholtz condition and the y direction extends from $-b/2$ to $b/2$ and represents the two wings. This last is the bound vortex and the one in x direction represents the tip vortices. The problem with the representation is that we have a constant circulation while we have seen that the lift decreases when going to the tips.

Let's try to compute the downwash velocity on a point from the bound vortex. The law of Biot-Savart has 3 contributions:

$$\vec{v} = \int_{-\infty}^{-b/2} \dots + \int_{-b/2}^{b/2} \dots + \int_{b/2}^{\infty} \dots \quad (109)$$

The second integral vanishes as dl and r are parallel, the two others were computed at the previous section. Pay attention

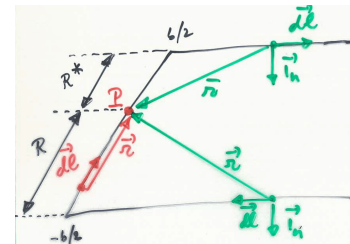


Figure 44

that we have to take half the contribution as the integral is not $-\infty, +\infty$:

$$\vec{v}(y) = \left(\frac{\Gamma}{4\pi R} + \frac{\Gamma}{4\pi R^*} \right) \vec{l}_n \quad (110)$$

We can see that the velocity is infinity at the tips and minimum at the middle. This is clearly not the reality.

8.5 Downwash velocity induced by a superposition of horseshoe vortices

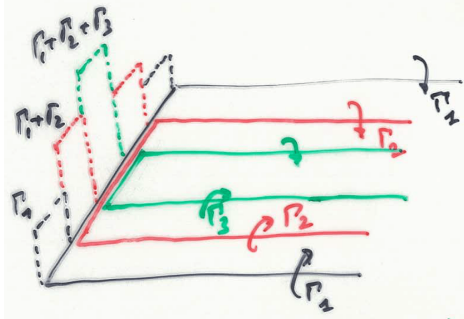


Figure 45

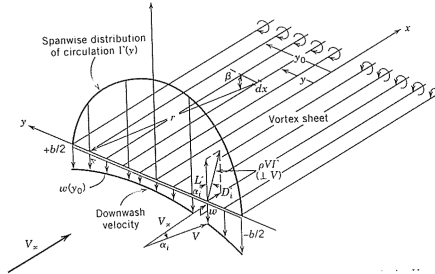


Figure 46

The solution is to superpose the horseshoes with bound vortices with different length (fig:Figure 45). If now we let tend the number of superimposed horseshoe vortices to infinity, we will get a vortex sheet as represented on Figure 46. The continuously varying circulation on the wing is no longer constant and this corresponds better with the reality.

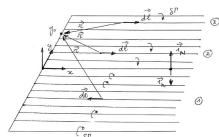


Figure 47

Consider this figure, we will try to compute the downwash velocity by considering a large but finite number of vortices of circulation $d\Gamma$ for each. We have 3 regions to consider with our basic formula:

- $y < 0: d\vec{v}(y_0) = \frac{d\Gamma}{4\pi(y_0-y)} \vec{l}_n$
- $0 < y < y_0: d\vec{v}(y_0) = \frac{d\Gamma}{4\pi(y_0-y)} \vec{l}_N = \frac{-d\Gamma}{4\pi(y_0-y)} \vec{l}_n$
- $y_0 < y: d\vec{v}(y_0) = \frac{d\Gamma}{4\pi(y-y_0)} \vec{l}_n = \frac{-d\Gamma}{4\pi(y-y_0)} \vec{l}_n$

We can see that the three formulas are the same if we take $\Gamma < 0$ for $y > 0$. We can so write the total contribution and its extension to the infinite number of lines:

$$\vec{v} = \left[\sum \frac{d\Gamma}{4\pi(y_0-y)} \right] = \left[\int_{-b/2}^{b/2} \frac{d\Gamma}{4\pi(y_0-y)} \right] \quad (111)$$

8.6 Derivation of Prandtl's fundamental equation of lifting line theory

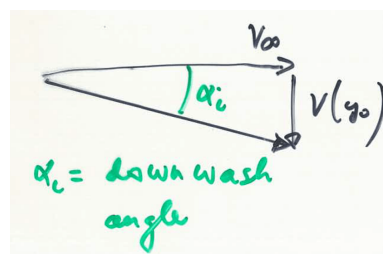


Figure 48

The induced angle of attack is then given by:

$$\tan \alpha_i \approx \alpha_i = \frac{v(y_0)}{v_\infty} = \frac{1}{4\pi v_\infty} \int_{-b/2}^{b/2} \frac{d\Gamma}{y_0 - y}. \quad (112)$$

Now let's denote $\alpha_{eff} = \alpha - \epsilon$. We know that the theory says $c_l = 2\pi(\alpha_{eff}(y_0) - \alpha_0(y_0))$, and using the definition of c_l and the Kutta-Jukowski for $L(y_0)$ we get:

$$c_l = \frac{L(y_0)}{\frac{1}{2}\rho_\infty v_\infty^2 c(y_0)} = \frac{\rho_\infty v_\infty \Gamma(y_0)}{\frac{1}{2}\rho_\infty v_\infty^2 c(y_0)} = \frac{\Gamma(y_0)}{\frac{1}{2}v_\infty^2 c(y_0)} \\ \Rightarrow \alpha_{eff} = \frac{\Gamma(y_0)}{\pi v_\infty c(y_0)} + \alpha_0(y_0) \quad (113)$$

Combining all the result, we can compute the α :

Fundamental equation of Prandtl's lifting line theory

$$\alpha(y_0) = \frac{\Gamma(y_0)}{\pi v_\infty c(y_0)} + \alpha_0(y_0) + \frac{1}{4\pi v_\infty} \int_{-b/2}^{b/2} \frac{d\Gamma}{y_0 - y}. \quad (114)$$

The only unknown in this equation is the circulation: several cases.

9 3D wing theory: application of Prandtl lifting line theory for a wing with given circulation. Starting from Prandtl's fundamental equation of lifting line theory and the formula for the induced angle of attack:

Fundamental equation of Prandtl's lifting line theory

$$\alpha(y_0) = \frac{\Gamma(y_0)}{\pi v_\infty c(y_0)} + \alpha_0(y_0) + \frac{1}{4\pi v_\infty} \int_{-b/2}^{b/2} \frac{d\Gamma}{y_0 - y}. \quad (115)$$

$$\tan \alpha_i \approx \alpha_i = \frac{v(y_0)}{v_\infty} = \frac{1}{4\pi v_\infty} \int_{-b/2}^{b/2} \frac{d\Gamma}{y_0 - y}. \quad (116)$$

9.1 Discuss the different terms of the equation

Γ is the circulation around the vortex sheet, v_∞ the flow speed, $c(y_0)$ the point where we calculate the downwash, y the position of a vortex wire. (see graphs above)

9.2 Apply to a wing with a given circulation distribution: find lift and drag coefficients

Idea is to solve the integral. The discussions below do it for more complicated case, so good luck!

9.3 Apply to a wing with a given shape and unknown circulation distribution defined by a truncated Fourier series and compute the lift C_L and the induced drag C_{Di} coefficients

Local and total lift by:

$$L'(y_0) = \rho_\infty v_\infty \Gamma(y_0) \quad L = \int_{-b/2}^{b/2} L'(y) dy \quad (117)$$

and the local and total induced drag:

$$D'_i(y_0) = \Gamma(y_0)\epsilon(y_0) \quad D_i = \int_{-b/2}^{b/2} D'_i(y) dy \quad (118)$$

We assume a serie:

$$\Gamma = \sum_{n=1}^N A_n \sin(n\theta). \quad (119)$$

Substitution of this in the Prandtl's fundamental equation gives:

$$\alpha(\theta_0) = \frac{1}{\pi v_\infty c(\theta_0)} \sum_n A_n \sin(n\theta_0) + \alpha_0(\theta_0) + \frac{1}{2\pi v_\infty b} \sum_n A_n n \int_\pi^0 \frac{\cos(n\theta)d\theta}{\cos\theta_0 - \cos\theta} \quad (120)$$

→ Glauert integral. We can find a solution by considering N equations for N points distributed along the span.

By integration of the local lift and definition of C_L and C_D :

$$C_L = \frac{1}{\frac{1}{2}v_\infty S} \int_{-b/2}^{b/2} \Gamma(y) dy = \frac{b}{u_\infty S} \sum_n \int_0^\pi A_n \sin(n\theta) \sin\theta d\theta = \frac{\pi b A_1}{2S v_\infty}. \quad (121)$$

$$C_{D_i} = \frac{1}{\frac{1}{2}v_\infty S} \int_{-b/2}^{b/2} \Gamma(y) \alpha_i dy. \quad (122)$$

Using (116), we can express $\alpha_i(\theta_0)$ as:

$$\alpha_i(\theta_0) = \frac{1}{2\pi v_\infty b} \int_\pi^0 \frac{\frac{d\Gamma}{d\theta}}{\cos\theta_0 - \cos\theta} d\theta = \frac{1}{2\sin\theta_0 v_\infty b} \sum_n A_n n \sin(n\theta_0) \quad (123)$$

which gives:

$$C_{D_i} = \frac{1}{2v_\infty^2 S} \int_0^\pi \sum_n \sum_k A_n A_k \sin(n\theta) \sin(k\theta) d\theta = \frac{\pi}{4v_\infty^2 S} \sum_n A_n^2 n \quad (124)$$

and using the lift coefficient:

$$C_{D_i} = \frac{C_L^2}{\pi AR} \left(1 + \sum_{n=2} \left(\frac{A_n}{A_1} \right)^2 \right) \Rightarrow e = \frac{1}{1 + \sum_{n=2} \left(\frac{A_n}{A_1} \right)^2} = \frac{1}{1 + \delta} \quad (125)$$

where δ is the **induced drag factor**, since it is always positive, $e < 1$.

9.4 Apply to a tapered wing



Figure 49



Figure 50

Same 2D profile along the span and no twist. Because of the symmetry, it is obvious that the pair n in the series will have no contribution. Let's go until 7:

$$\Gamma = A_1 \sin\theta + A_3 \sin 3\theta + A_5 \sin 5\theta + A_7 \sin 7\theta. \quad (126)$$

To determine the coefficient we have to apply (120) to 4 points. Let's take half the span because of symmetry: $\theta = \pi/8, \pi/4, 3\pi/8, \pi/2$. Since the 2D profile is constant, α_0 is independent of θ , same for α since there are no twist.

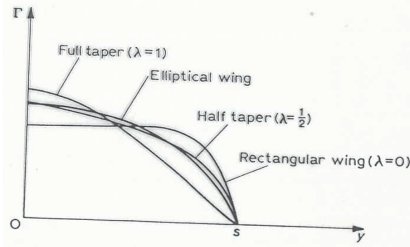


Figure 51

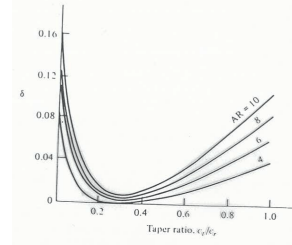


Figure 52

After some calculation one finds a circulation distribution as in Figure 51, where λ is defined such that $c_t = (1 - \lambda)c_r$. $\lambda = 0$ corresponds to a rectangular wing and $\lambda = 1$ is the triangular one. Note that the figure also represents the lift. The lift coefficient no, because it becomes larger at the tips due to $c \searrow$. On Figure 52 is represented the induced drag coefficient δ . We see that it is always possible to find the taper ratio to have the minimum drag. Most of the planes use tapered wings since it is more simple to produce than elliptic wing.

9.5 Assume an elliptic distribution for the circulation. Show that the platform of the wing must be an ellipse.

The elliptic circulation distribution is written:

$$\Gamma(y) = \Gamma_0 \sqrt{1 - \left(\frac{y}{b/2}\right)^2}. \quad (127)$$

where Γ_0 is the circulation in the plane of symmetry. Let's compute the velocity:

$$v(y_0) = \frac{1}{4\pi} \int_{-b/2}^{b/2} \frac{d\Gamma}{y_0 - y} = \frac{\Gamma_0}{2b} = cst \quad \Rightarrow \epsilon = \alpha_i = \frac{v(y_0)}{v_\infty} = \frac{\Gamma_0}{2bv_\infty} = cst. \quad (128)$$

where we used the transformation $y = b/2 \cos \theta$. Induced angle of attack is constant along the span.

$$L'(y) = \rho v_\infty \sqrt{1 - \left(\frac{y}{b/2}\right)^2}. \quad (129)$$

On the other hand we can use (100) to express the lift as:

$$L'(y) = m(\alpha - \alpha_i - \alpha_0) \frac{1}{2} \rho_\infty v_\infty^2 c \quad (130)$$

Combining the equations we get:

$$(\alpha - \alpha_i - \alpha_0)c = \frac{2\Gamma_0}{v_\infty} \sqrt{1 - \left(\frac{y}{b/2}\right)^2}. \quad (131)$$

Note that if the left hand side is constant, the equation is satisfied for an **elliptic platform**. Since α_i is already constant, the whole term is constant only if the geometric angle of attack is constant and the profile does not change along the span. Since $C_{d_i} = C_L \alpha_i$, we can make the same analysis for the drag.

On the other hand, if the platform is non elliptic, since m varies little, the different angles must vary too. This is done by introducing a **twist** in the wing so that α varies. The lift coefficient is obtained by integration of the local lift:

$$\frac{1}{\frac{1}{2}\rho v_\infty^2 S} \int_{-b/2}^{b/2} L'(y) dy = \frac{\Gamma_0 \pi b}{2v_\infty S} = \frac{\Gamma_0 \pi}{2bv_\infty} AR. \quad (132)$$

Combination of this and what we found for α_i in this section we get:

$$\alpha_i = \frac{C_L}{\pi AR} \quad (133)$$

which is what we defined at the beginning of the chapter but for $e = 1$ (span efficiency factor). The induced drag is given by:

$$D'_i(y) = L'(y)\alpha_i \quad \Rightarrow C_{D_i} = C_L \alpha_i = \frac{C_L^2}{\pi AR}. \quad (134)$$

10 2D airfoil compressible flow around an airfoil using the small perturbation approach

10.1 Derive the compressible potential equation / Derive the equation governing compressible potential equation, what are the assumptions

Remind that we have defined a potential function to describe incompressible flows, conservation of mass giving:

$$\vec{v} = \nabla \phi \quad \frac{\partial u}{\partial x} + \frac{\partial v}{\partial y} = 0 = \frac{\partial^2 \phi}{\partial x^2} + \frac{\partial^2 \phi}{\partial y^2}. \quad (135)$$

This can also be used to describe compressible flows, conservation of mass is then:

$$\rho(\phi_{xx} + \phi_{yy}) + \rho_x \phi_x + \rho_y \phi_y = 0 \quad (136)$$

where we introduced the shorthand notation $\frac{\partial a}{\partial x} = a_x$. We assume that the flow is isentropic, this is satisfied by inviscid flows (no shock wave):

$$\frac{\rho}{T^{\frac{1}{\gamma-1}}} = cst \quad \Rightarrow \frac{d\rho}{\rho} = \frac{1}{\gamma-1} \frac{dT}{T} \quad (137)$$

if the flow does not work (turbine), the temperature is constant and the equation becomes:

$$d\rho = -\frac{\rho}{2a^2} d(u^2 + v^2). \quad (138)$$

If we replace the velocities we get:

$$\rho_x = -\frac{\rho}{a^2} (\phi_x \phi_{xx} + \phi_y \phi_{xy}) \quad \rho_y = -\frac{\rho}{a^2} (\phi_x \phi_{xy} + \phi_y \phi_{yy}). \quad (139)$$

That we can substitute in (136):

$$\left(1 - \frac{1}{a^2} \phi_x^2\right) \phi_{xx} + \left(1 - \frac{1}{a^2} \phi_y^2\right) \phi_{yy} - \frac{2}{a^2} \phi_x \phi_y \phi_{xy} = 0. \quad (140)$$

10.2 Assume a thin airfoil at small angle of attack: derive the linearized potential equation. What is the range of validity as a function of the free stream Mach number / Derive the equation in the case of small perturbations. What are the assumptions for this equation to be valid ?

If the far field velocity profile is $u = V_\infty$, we can note the velocity field by means of perturbations: $u = V_\infty + \hat{u}$, $v = \hat{v}$. A perturbation potential function can be defined:

$$\phi = V_\infty x + \hat{\phi} \quad \text{with} \quad \hat{\phi}_x = \hat{u}, \quad \hat{\phi}_y = \hat{v}. \quad (141)$$

By substitution of this in (140):

$$\left[a^2 - (V_\infty + \hat{\phi}_x)^2 \right] \hat{\phi}_{xx} + \left[a^2 - \hat{\phi}_y^2 \right] \hat{\phi}_{yy} - 2(V_\infty + \hat{\phi}_x) \hat{\phi}_y \hat{\phi}_{xy} = 0. \quad (142)$$

Since the total temperature is constant:

$$\frac{a_\infty^2}{\gamma - 1} + \frac{V_\infty^2}{2} = \frac{a^2}{\gamma - 1} + \frac{(V_\infty + \hat{u})^2}{2} \quad (143)$$

If we make the assumption of small perturbation, the quadratic terms cancel and (142) and (143) become:

$$\begin{aligned} \frac{a_\infty^2}{a^2} &= 1 - (\gamma - 1) \frac{\hat{u}}{V_\infty} M_\infty^2 \\ \left[a^2 - V_\infty^2 + 2V_\infty \hat{u} \right] \hat{\phi}_{xx} + a^2 \hat{\phi}_{yy} - 2V_\infty \hat{v} \hat{\phi}_{xy} &= 0 \\ \Rightarrow \left[1 - M_\infty^2 - (\gamma + 1) M_\infty \frac{\hat{u}}{V_\infty} \right] \hat{\phi}_{xx} + \left[1 - (\gamma - 1) M_\infty^2 \frac{\hat{u}}{V_\infty} \right] \hat{\phi}_{yy} - 2M_\infty^2 \frac{\hat{v}}{V_\infty} \hat{\phi}_{xy} &= 0 \end{aligned} \quad (144)$$

where the last expression is obtained by dividing by a_∞^2 and replacing. By considering again the small perturbation ($V_\infty \ll$) equation we get the:

Transonic small perturbation potential equation

$$\left[(1 - M_\infty^2) - (\gamma + 1) M_\infty^2 \frac{\hat{\phi}_x}{V_\infty} \right] \hat{\phi}_{xx} + \hat{\phi}_{yy} = 0. \quad (145)$$

We can see that the \hat{u} appears in $\hat{\phi}_{xx}$ term, this is no longer negligible for **sonic** velocities. For sub- and super-sonic flows however the equation simplifies in:

$$(1 - M_\infty^2) \hat{\phi}_{xx} + \hat{\phi}_{yy} = 0. \quad (146)$$

Note that we retrieve our incompressible equation for $M_\infty \rightarrow 0$. Be aware that this last relation is only valid for small perturbations (small bodies in practice) and sub- or super-sonic flows ($M_\infty > 1.2$, $M_\infty < 0.8$).

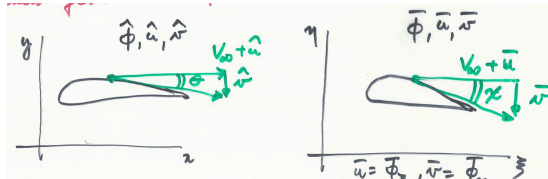
Let's now operate a change of coordinate $(x, y) \rightarrow (\xi, \eta)$, recalling $1 - M_\infty^2 \equiv \beta^2$:

$$\xi = x \quad \eta = \beta y \quad \bar{\phi}(\xi, \eta) = m \cdot \hat{\phi}(x, y) \quad (147)$$

where m is a constant. Let's find the expression of $\bar{\phi}(\xi, \eta)$. The chain rule gives:

$$\begin{aligned}\hat{\phi}_x &= \hat{\phi}_\xi = \frac{1}{m} \bar{\phi}_\xi & \hat{\phi}_y &= \frac{\beta}{m} \bar{\phi}_\eta & \hat{\phi}_{xx} &= \frac{1}{m} \bar{\phi}_{\xi\xi} & \hat{\phi}_{yy} &= \frac{\beta^2}{m} \bar{\phi}_{\eta\eta} \\ &&&& \Rightarrow \bar{\phi}_{xx} + \bar{\phi}_{yy} &= 0\end{aligned}\quad (148)$$

We can see that the compressible flow in (x, y) is reduced to an incompressible flow in the (ξ, η) plane. Pay attention that $\bar{\phi}$ describes the perturbation velocities \bar{u}, \bar{v} . in the (ξ, η) plane.



We can now focus on the shape of the profile in the new axis. Let's analyze the tangent to the profile by defining the angle θ for the profile in (x, y) . Under the assumption of small perturbation (thin airfoil), we can see that:

$$\tan \theta \approx \theta = \frac{\hat{v}}{V_\infty + \hat{u}} \approx \frac{\hat{v}}{V_\infty} = \frac{1}{V_\infty} \hat{\phi}_y \quad \Rightarrow \chi \approx \frac{1}{V_\infty} \bar{\phi}_\eta \quad (149)$$

where the analogy for the new plane is done. Using (148), we get:

$$\theta = \frac{\beta}{m} \chi. \quad (150)$$

Let's investigate two cases:

- If we choose $m = \beta$, $\theta = \chi$, the two profiles are identical. We have for the velocity:

$$\hat{u} = \hat{\phi}_x = \frac{\bar{\phi}_\xi}{\beta} = \frac{\bar{u}}{\beta} \quad (151)$$

and since the pressure coefficient is given by $C_p = -\frac{2\hat{u}}{V_\infty}$:

Prandtl-Glauert rule

$$C_p = \frac{C_{p,inc}}{\beta} = \frac{C_{p,inc}}{\sqrt{1 - M_\infty^2}}. \quad (152)$$

This equation allows us to compute the pressure distribution in compressible flow, beginning from the incompressible one.

Since the lift and moment coefficient are given by the integration of the pressure coefficient along the wing, we have the same result for them (so also the slope of lift curve m). Here is plotted the experimental data and the approximated m by means of the above relation for $\alpha = 0$ and for different airfoil thickness τ . We can see that for the thinner wings, we have a good agreement, until we reach the **critical Mach number** (Mach number at infinity for which Mach number 1 is reached on the profile). This value exceeded, we have shock waves (formula valid only for Mach until 0.8). For thicker wings, we see that the slope m is always underestimated. The critical Mach number is here much lower.

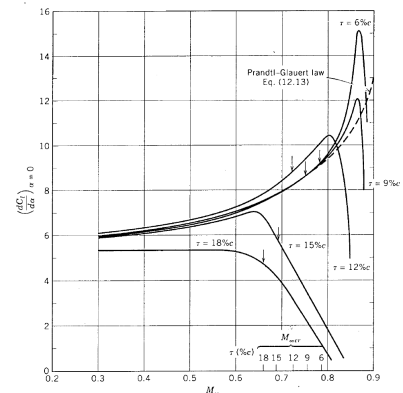
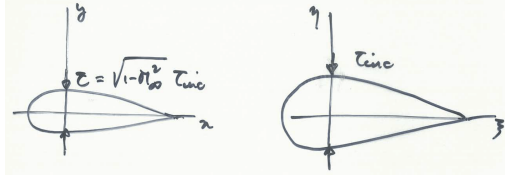


Figure 54

- If we choose $m = 1, \hat{u} = \bar{u}$ so that $C_p = C_{p,inc}$. We see that the pressure coefficient is now the same but the profiles are different following we are in the compressible or incompressible case $\theta = \beta\chi$.



The angle relation must be true along the entire profile, particularly at the maximum thickness:

$$\tau = \beta \tau_{inc}. \quad (153)$$

Remark 1 Figure 55 If we take into account the aspect ratio, we can rewrite the slope m as:

$$m = \frac{m_{inc}}{\beta} \frac{2\pi}{\beta \left(1 + \frac{2}{eAR}\right)} \quad (154)$$

where we used the theoretical 2D slope 2π . Another possibility is to write the lift as:

$$c_l = \frac{2\pi}{\beta} (\alpha - \alpha_{L_0} - \alpha_i) = \frac{2\pi}{\beta + \frac{2}{eAR}} (\alpha - \alpha_{L_0}) \quad (155)$$

We can last note the existence of the DATCOM formula that accounts for the effect of the aspect ratio, sweep angle Λ , Mach number and has also a correction factor for viscous effects $\kappa \approx 0.97$:

$$m = \frac{2\pi AR}{2 + \sqrt{\frac{AR^2 + beta^2}{\kappa^2} \left(1 + \frac{\tan^2 \Lambda}{\beta^2}\right) + 4}}. \quad (156)$$

Remark 2 We can also rearrange the expression of C_p with the approximation of small angles, we had:

$$C_p = \frac{p - p_\infty}{\frac{1}{2} \rho_\infty V_\infty^2} = \frac{\gamma 2 p_\infty}{\gamma \rho_\infty V_\infty^2} \left(\frac{p}{p_\infty} - 1 \right) = \frac{2}{\gamma M_\infty^2} \left(\frac{p}{p_\infty} - 1 \right) \quad \gamma \frac{p_\infty}{\rho_\infty} = \gamma r T = a^2 \quad (157)$$

The isentropic flow and the constant T_c give:

$$\begin{aligned} \frac{p}{p_\infty} &= \left(\frac{T}{T_\infty} \right)^{\frac{\gamma}{\gamma-1}} = \left(\frac{T_t - \frac{1}{2c_p} [(V_\infty + \hat{u})^2 + \hat{v}^2]}{T_\infty} \right)^{\frac{\gamma}{\gamma-1}} \quad T_t = T_\infty + \frac{V_\infty^2}{2c_p} \\ &\Rightarrow \frac{p}{p_\infty} = \left[1 - \frac{\gamma-1}{2} M_\infty^2 \left(\frac{2\hat{u}}{V_\infty} + \frac{\hat{u}^2 + \hat{v}^2}{V_\infty^2} \right) \right]^{\frac{\gamma}{\gamma-1}} = 1 - \frac{\gamma}{2} M_\infty^2 \left(\frac{2\hat{u}}{V_\infty} + \frac{\hat{u}^2 + \hat{v}^2}{V_\infty^2} \right) + \dots \end{aligned} \quad (158)$$

where the last expression comes from the fact that the second term is small so that we have the Taylor development of $1 + \epsilon$ (first order limited). We can neglect the second term in bracket since we have small perturbation square, and we get by (157):

$$\frac{p}{p_\infty} = -\frac{2\hat{u}}{V_\infty} \quad (159)$$

10.3 Discuss the type of this equation as a function of free stream Mach number, what are the consequences

Transonic small perturbation potential equation

$$\left[(1 - M_\infty^2) - (\gamma + 1) M_\infty^2 \frac{\hat{\phi}_x}{V_\infty} \right] \hat{\phi}_{xx} + \hat{\phi}_{yy} = 0. \quad (160)$$

We can see that the \hat{u} appears in $\hat{\phi}_{xx}$ term, this is no longer negligible for **sonic** velocities. For sub- and super-sonic flows however the equation simplifies in:

$$(1 - M_\infty^2) \hat{\phi}_{xx} + \hat{\phi}_{yy} = 0. \quad (161)$$

Note that we retrieve our incompressible equation for $M_\infty \rightarrow 0$. Be aware that this last relation is only valid for small perturbations (small bodies in practice) and sub- or super-sonic flows ($M_\infty > 1.2, M_\infty < 0.8$).

10.4 Discuss the application to an airfoil in supersonic flow: lift coefficient, influence of the Mach number, Ackeret formula, lift and drag formula

The potential equation we used in the framework of potential equation can be rewritten in the case of supersonic flow as:

$$(1 - M_\infty^2) \hat{\phi}_{xx} + \hat{\phi}_{yy} = 0 \quad \Rightarrow \lambda^2 \hat{\phi}_{xx} - \hat{\phi}_{yy} = 0. \quad (162)$$

The linearized potential equation corresponds to the wave equation with $\lambda^2 = M_\infty^2 - 1 > 0$. We can show that the solution of this equation is

$$\hat{\phi}(x, y) = f(x - \lambda y) = \hat{\phi}_1(x - \lambda y) + \hat{\phi}_2(x + \lambda y). \quad (163)$$

Let's define 2 families of characteristic curves:

$$\begin{cases} C^+ : x - \lambda y = cst & \Rightarrow y = \frac{1}{\lambda}x + cst = \frac{1}{\sqrt{M_\infty^2 - 1}}c + cst \\ C^- : x + \lambda y = cst & \Rightarrow y = -\frac{1}{\lambda}x + cst = -\frac{1}{\sqrt{M_\infty^2 - 1}}c + cst \end{cases} \quad (164)$$

In this way, $\hat{\phi}_1$ and $\hat{\phi}_2$ are respectively constant on C^+ and C^- .

The slope is denoted μ_∞^\pm for C^\pm such that:

$$\tan \mu_\infty^\pm = \pm \frac{1}{\sqrt{M_\infty^2 - 1}} \quad \sin \mu_\infty^\pm = \pm \frac{1}{M_\infty}. \quad (165)$$

To find the general solution in P, let's first consider the initial data given on the y-axis:

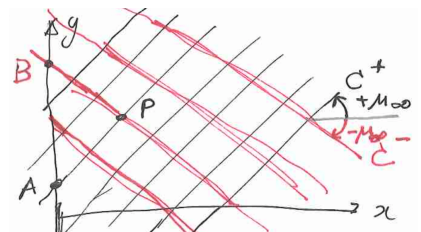


Figure 56

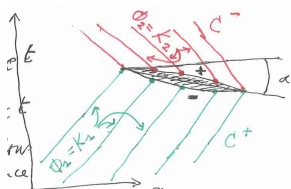
$$\hat{\phi}_1(y) = F(y) \quad \hat{\phi}_2(y) = G(y) \quad (166)$$

Now let's construct C^+ and C^- :

$$C^+ : x - \lambda y = x_A - \lambda y_A \quad C^- : x - \lambda y = x_B + \lambda y_B. \quad (167)$$

Finally, the solution in P is so given by:

$$\hat{\phi}(x_p, y_p) = \hat{\phi}(x_A - \lambda y_A) + \hat{\phi}_2(x_B + \lambda y_B) = F(x_A - \lambda y_A) + G(x_B + \lambda y_B) \quad (168)$$



Now let's define the initial conditions at $x = 0$ for small α for a thin profile:

$$F(y) = K_1 = cst \quad G(y) = K_2 = cst \quad \Rightarrow \hat{\phi} = cst \quad (169)$$

Figure 57

since the incoming flow is uniform. On the pressure side, we have $\hat{\phi}_1(x - \lambda y) = K_1$ which gives in the solution:

$$\hat{\phi}(q) = K_1 + \hat{\phi}_2(q) \quad \rightarrow \hat{\phi}_x = \frac{d\hat{\phi}_2}{dq} = \hat{u}^- \quad \hat{\phi}_y = \frac{d\hat{\phi}_2}{dq}\lambda = \hat{v}^- \quad \Rightarrow \hat{v}_{wall} = \lambda \hat{u}_{wall} \quad (170)$$

If we express the tangent as $\tan \theta_w \approx \theta_w = \frac{\hat{v}_w^-}{\hat{u}^- + V_\infty} \approx \frac{\hat{v}_w^-}{V_\infty}$, We can get by replacing the last results in the previous pressure coefficient equation for small perturbations:

Law of Ackeret

$$C_p^- = -\frac{2\hat{u}_w^-}{V_\infty} = -\frac{2\theta_w^-}{\sqrt{M_\infty^2 - 1}}. \quad (171)$$

The same reasoning can be done for the suction side where we'll get:

$$\hat{\phi}_x = \frac{d\hat{\phi}_1}{dq} = \hat{u}_w^+ \quad \hat{\phi}_x = \frac{d\hat{\phi}_1}{dq}(-\lambda) = \hat{v}_w^+ = -\lambda \hat{u}_w^+ \quad \Rightarrow C_p^+ = \frac{2\theta_w^+}{\sqrt{M_\infty^2 - 1}}. \quad (172)$$

10.4.1 Application to a flat plate

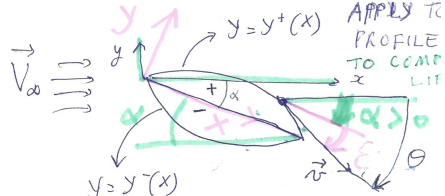


Figure 58

Consider the thin profile define by functions $y^+(x)$ and $y^-(x)$ with angles defines as:

$$\begin{aligned} \epsilon &= \frac{dy}{dx} < 0 & \theta &= \frac{\hat{v}}{\hat{u} + V_\infty} < 0 \\ \Rightarrow \theta &= \epsilon - \alpha = \frac{dy}{dx} - \alpha \end{aligned} \quad (173)$$

as $\alpha > 0$. We can then apply the last formula:

$$C_p^+ = \frac{2\theta_w^+}{\sqrt{M_\infty^2 - 1}} = \frac{2\left(\frac{dy^+}{dx} - \alpha\right)}{\sqrt{M_\infty^2 - 1}} \quad C_p^- = -\frac{2\theta_w^-}{\sqrt{M_\infty^2 - 1}} = \frac{2\left(\alpha - \frac{dy^-}{dx}\right)}{\sqrt{M_\infty^2 - 1}}. \quad (174)$$

We are now interested in computing the normal and tangential force applied on the wing, for a counter-clock contour:

$$C_N = \int_0^1 C_p^- \frac{dx}{c} + \int_1^0 C_p^+ \frac{dx}{c} = \frac{4\alpha}{\sqrt{M_\infty^2 - 1}} \quad (175)$$

where we replace the C_p 's by their definition and we neglect $\frac{dy}{dx}$ terms. For the drag we have the same procedure but by neglecting this time α :

$$\begin{aligned} C_\Gamma &= -\int_0^1 C_p^- \frac{dy}{c} - \int_1^0 C_p^+ \frac{dy}{c} = \frac{2}{\sqrt{M_\infty^2 - 1}} \left[\int_0^1 \left(\frac{dy^-}{dx} \right)^2 \frac{dx}{c} + \int_0^1 \left(\frac{dy^+}{dx} \right)^2 \frac{dx}{c} \right] \\ \Rightarrow C_\Gamma &= \frac{2}{\sqrt{M_\infty^2 - 1}} [I^- + I^+] \end{aligned} \quad (176)$$

To compute the lift and drag coefficient we only have to make the projections, and in case of flat plate $\frac{dy}{dx} = 0 = I^\pm$:

$$C_l = -C_\Gamma \sin \alpha + C_N \cos \alpha \approx -\alpha C_\Gamma + C_N \quad C_d = C_\Gamma + \alpha C_N$$

$$\Rightarrow C_l = \frac{4\alpha}{\sqrt{M_\infty^2 - 1}} \quad C_d = \frac{4\alpha}{\sqrt{M_\infty^2 - 1}}. \quad (177)$$

The drag is the **wave drag**.

10.5 What is wave drag ? discuss supersonic flow over double wedge profile

A wave drag is a drag due to a shock wave. When a shock wave appears, it uses energy, which has to be provided by the aircraft, it is thus seen as a drag.

If we apply the Ackeret law to this profile we have:

$$C_{p1} = \frac{2(\delta - \alpha)}{\sqrt{M_\infty^2 - 1}} \quad C_{p2} = \frac{2(\delta + \alpha)}{\sqrt{M_\infty^2 - 1}}$$

$$C_{p3} = \frac{-2(\delta + \alpha)}{\sqrt{M_\infty^2 - 1}} \quad C_{p4} = \frac{-2(\delta - \alpha)}{\sqrt{M_\infty^2 - 1}} \quad (178)$$

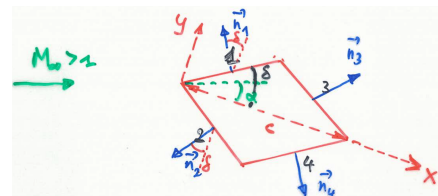


Figure 59

We can compute the lift and drag coefficients by integrating over the surface:

$$\vec{F} = - \oint p d\vec{S} = - \oint (p - p_\infty) d\vec{S} = -\frac{1}{2} \rho_\infty V_\infty^2 \oint C_p d\vec{S}$$

$$\Rightarrow \vec{F}_1 = -\frac{1}{2} \rho_\infty V_\infty^2 C_{p1} \frac{c}{2} \vec{n}_1 \quad (179)$$

If we make the force non dimensional:

$$\vec{C}_1 = \frac{\vec{F}_1}{\frac{1}{2} \rho_\infty V_\infty^2 c} = -\frac{C_{p1}}{2} \vec{n}_1 \quad \Rightarrow \vec{C}_i = -\frac{C_{pi}}{2} \vec{n}_i \quad (180)$$

If we look to the normal and tangent forces we find:

$$C_y = \vec{C}_i \cdot \vec{i}_y = \left(-\frac{C_{p1}}{2} + \frac{C_{p2}}{2} - \frac{C_{p3}}{2} + \frac{C_{p4}}{2} \right) \cos \delta = \frac{4\alpha}{\sqrt{M_\infty^2 - 1}} \cos \delta \approx \frac{4\alpha}{\sqrt{M_\infty^2 - 1}}$$

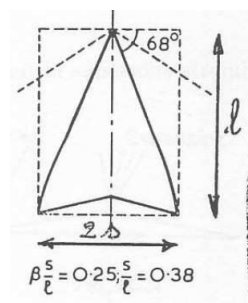
$$C_x = \vec{C}_i \cdot \vec{i}_x = \left(\frac{C_{p1}}{2} + \frac{C_{p2}}{2} - \frac{C_{p3}}{2} - \frac{C_{p4}}{2} \right) \sin \delta = \frac{4\delta}{\sqrt{M_\infty^2 - 1}} \sin \delta \approx \frac{4\delta^2}{\sqrt{M_\infty^2 - 1}} \quad (181)$$

Then we make the same projection as previously:

$$c_l \approx C_y - \alpha C_x = \frac{4\alpha}{\sqrt{M_\infty^2 - 1}} - \frac{4\delta^2 \alpha}{\sqrt{M_\infty^2 - 1}} \approx \frac{4\alpha}{\sqrt{M_\infty^2 - 1}} \quad (182)$$

We find thus the same lift coefficient as the flat plate. Let's see the drag:

$$c_d = C_x + \alpha C_y = \frac{4\delta}{\sqrt{M_\infty^2 - 1}} + \frac{4\alpha}{\sqrt{M_\infty^2 - 1}}, \quad (183)$$



where the first term is **incidence wave drag** (result of lift), the same as the flat plate and the second term the **thickness wave drag** (result of volume) corresponding to the drag of the wedge at 0 degrees and angle of attack. The following empirical formula can be used for both drag on wing and on **complete plane**:

$$C_{Dw} = k_0 \frac{128}{\pi} \frac{V^2}{Sl^4} + k_1 \frac{1}{2\pi} \frac{S}{l^2} \lambda^2 C_L^2 \quad (184)$$

where k_0 and k_1 are constant of order 1 depending on the geometry and l the average length as represented on the figure.

10.6 Transonic flow over a profile: what is critical free stream Mach number(+ discussion), what is drag divergence Mach number

10.6.1 Critical Mach number

The critical Mach Number is the M_∞ when $M = 1$ somewhere on the airfoil. Consider a point A, the drag is given by:

$$C_{p,A} = \frac{2}{\gamma M_\infty^2} \left(\frac{p_A}{p_\infty} - 1 \right) \quad (185)$$

If we combine the fact that the flow is isentropic:

$$\frac{p_A}{p_\infty} = \left(\frac{T_A}{T_\infty} \right)^{\frac{\gamma}{\gamma-1}} = \left(\frac{1 + \frac{\gamma-1}{2} M_\infty^2}{1 + \frac{\gamma-1}{2} M_A^2} \right)^{\frac{\gamma}{\gamma-1}} \Rightarrow C_{p,A} = \frac{2}{\gamma M_\infty^2} \left[\left(\frac{1 + \frac{\gamma-1}{2} M_\infty^2}{1 + \frac{\gamma-1}{2} M_A^2} \right)^{\frac{\gamma}{\gamma-1}} - 1 \right] \quad (186)$$

If now we consider $M_\infty = M_{kr} \rightarrow M_A = 1$, so that the equation becomes:

$$C_{p,A} = \frac{2}{\gamma M_\infty^2} \left[\left(\frac{1 + \frac{\gamma-1}{2} M_\infty^2}{1 + \frac{\gamma-1}{2} M_A^2} \right)^{\frac{\gamma}{\gamma-1}} - 1 \right] \quad C_{p,A} = \frac{C_{p,A,inc}}{\sqrt{1 - M_{kr}^2}}, \quad (187)$$

where the second equation is the Prandtl-Glauert relation. We can plot the two equations on a graph. The intersection of the two graphs gives the critical Mach number. We can see that the minimum lift coefficient at low velocities is more negative than the thin case, characterized by a smaller M_{kr} . The perturbation of the flow is higher. Flying at high subsonic velocities is important \rightarrow thin airfoil. When the angle of attack increases, the lift increases but the higher velocity on the suction part makes the M_{kr} much lower. We want so the wing to be as thin as possible but we are limited by the structural strength and the fuel storage.

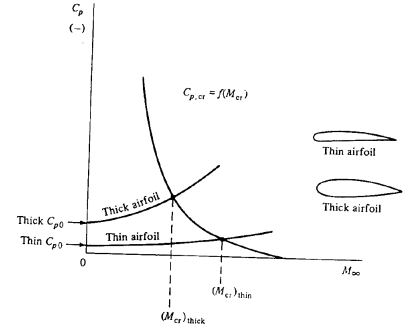


Figure 61

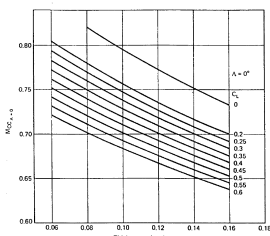


Figure 62

We avoid also large bending of the leading edge to avoid large accelerations. One solution to increase M_{kr} is to place the maximum camber downstream, about 50% of the chord because the velocities on the suction side will be lower. Placing it too downstream will create a too high opposite gradient and cause separation.

Symmetrical wings have a larger M_{kr} , however be careful with combination of sharp LE because of LE separation. In practice we have a quasi-symmetrical profile with camber near LE. Swept wings also increase the M_{kr} .

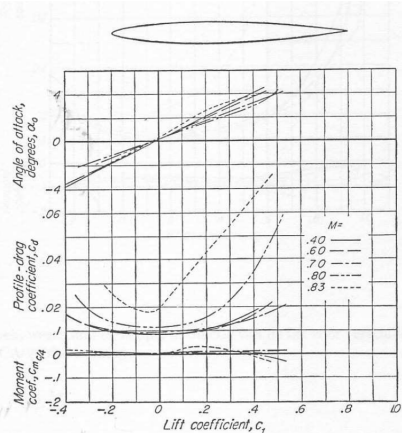


Figure 63

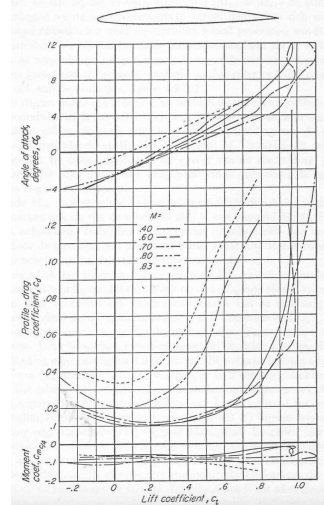


Figure 64

We can observe here above, the plot of α , C_L and C_D for a symmetrical and a non-symmetrical airfoil. We can observe on Figure 63 that the slope of the lift curve goes up to $M = 0.83$ (Prandtl-Glauert). Once above M_{kr} it starts to decrease and the drag suddenly increases.

On Figure 64 we can see similar effects at the difference that around M_{kr} we have a positive increase of the zero lift angle, having a negative effect on longitudinal stability. Note that the decrease of the lift curve starts earlier, M_{kr} is smaller.

10.6.2 Drag divergence Mach number

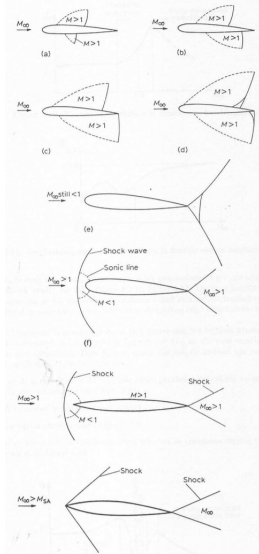


Figure 65

At the critical Mach number $M_\infty = M_{cr}$, the flow reaches $M = 1$ somewhere on the wing. If the velocity at ∞ is increased, M_∞ also (still < 0), a small area where the flow becomes **supersonic** will develop on the **suction side**. For increasing M_∞ this area will grow and at a certain M_∞ a **shock wave** will develop, as a result of which the flow will become **subsonic** again (the supersonic area abruptly terminated). Such area also develops on the **pressure side** at high M_∞ (Figure 65 (a)).

If M_∞ increases further, the supersonic regions further extends and the shock waves move downstream, the one on the pressure side more rapidly (Figure 65 (b) (c)). As soon as the shock waves are strong enough, they can cause separation of the boundary layer, this separation is the **shock stall** and the M_∞ where this happens is called the **drag divergence Mach number**. Indeed, the drag suddenly increases as a result of the separation, this called **transonic drag rise**, shown on Figure 66.

For further increase of $M_\infty < 1$, the shock wave on the pressure side eventually reaches the trailing edge (Figure 65 (d)). In a certain Mach number range, the shock wave manifests the so-called **λ shocks**. Near the profile the shock has two legs, a first oblique one through which the flow is slowed down but remains supersonic, and a second normal one

through which the flow becomes subsonic.

Eventually the shock wave on the suction side can also reach the trailing edge and give birth to the **bifurcated trailing edge shock pattern** (Figure 65 (e)).

For further increase of M_∞ there is no change, till M_∞ exceeds 1. In this case, a so-called **detached bow shock** develops upstream of the leading edge. There is a small subsonic region between this shock and the leading edge. This manifests both for thick, bounded leading edge and thin one (Figure 65 (f) (g)). In the second case, the bow shock changes into 2 oblique shocks at the leading edge for increasing M_∞ (Figure 65 (h)). This happens at the **shock attachment Mach number**, M_{SA} . For further M_∞ , the flow becomes fully supersonic and the drag decreases. In the case of rounded leading edge, the bow shock continues to exist and comes closer to the leading edge.

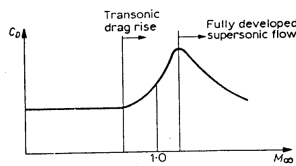


Figure 66

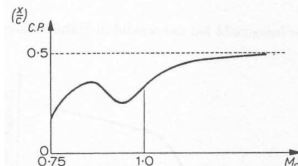


Figure 67

Under transonic conditions the flow is non-stationary, the shock waves moves up and down on the wing. The pilot senses this as **buffeting** (response of the structure to aerodynamic excitation) and vibrations. This can make the plane uncontrollable or cause serious damages. The cause of the excitation is the fluctuating pressure in non-stationary conditions. Normally one flies under the buffeting margin but one can exceed it in case of sudden maneuvers for fighters for example.

The center of pressure is also moving with M_∞ (Figure 67). First, it goes backward as the shock wave going backward on the suction side makes the underpressure greater. Then, it goes forward because the shock wave on the pressure side is moving faster. The latter reaches the trailing edge while the shock wave on the suction side still moves backward, making the center of pressure again move backward, tending to the 50% chord. This makes the control of the plane more difficult.

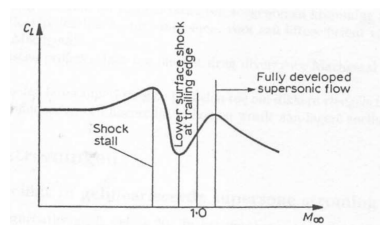


Figure 68

It is this buffeting effect that imposes an upper limit to the velocity of subsonic planes. With the increase of the drag due to separation when shock waves (shock-stall) is associated a decrease of the lift. We can see that the lift temporary increases after the lower shock reaches the trailing edge. This is explained by the smaller separation when in this location. The drag divergence Mach number is 5-10% larger than M_{cr} .

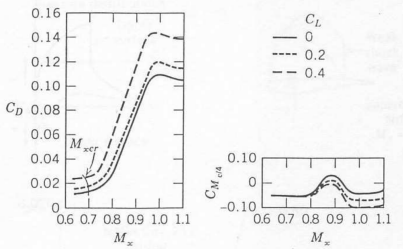


Figure 69

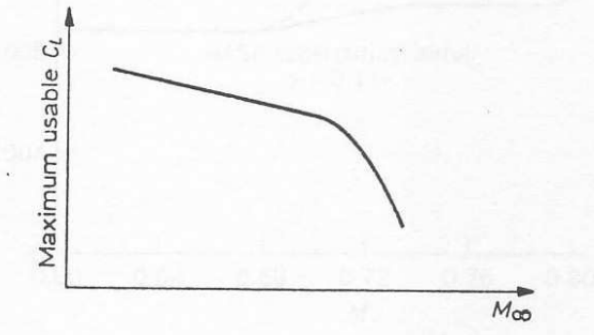


Figure 70

On Figure 69 we can see the influence of increasing lift (increasing α). We can notice that with increasing lift, the drag increases for all Mach numbers, the moment increases in the transonic region and M_{cr} decreases. On Figure 70, we notice that the lift coefficient strongly decreases in the transonic region due to buffering effects.

10.7 Compute the lift coefficient for a 2D profile in compressible flow, assuming that the lift coefficient for the same airfoil is known for incompressible flow.

Using Prandtl-Glauert : $C_p = \frac{C_{p,inc}}{\beta} = \frac{C_{p,inc}}{\sqrt{1-M_\infty^2}}$. Since lift is an integration of pressure: $C_L = \frac{C_{L,inc}}{\beta} = \frac{C_{L,inc}}{\sqrt{1-M_\infty^2}}$

10.8 Discuss the graph giving the slope of the lift curve as a function of the free stream Mach number ($M_{infinity}$)

See Figure 68 and above discussion.

11 Transonic flow over an airfoil - critical Mach number and drag divergence Mach number

11.1 Give definition of critical free stream Mach number

See above

11.2 Explain the effect of the thickness of the profile on the critical Mach number

Thinner airfoil gives higher critical Mach number. This can be explained as following: the M_{kr} is the Mach where $M = 1$ is obtained somewhere on the profile. The flow is accelerated over the profile, if the thickness is bigger, flow accelerates more, which leads to early $M = 1$ compared to a thinner airfoil.

11.3 All questions related to divergence Mach number, shock patterns from sub- to supersonic, C_D versus Mach, buffeting

See above

11.4 Explain supercritical wing profiles

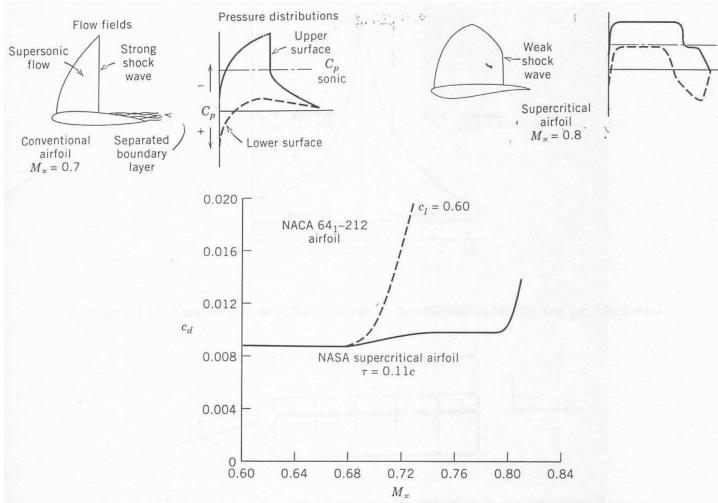


Figure 71

closer to the trailing edge.

The new shape of the suction side has a negative effect on the lift, this is compensated by an increased curvature on the pressure side near the trailing edge. On the figure we can see that the use of critical wings increases the drag divergence Mach number, that can go up to 0.99. These allows the use of thicker wings, allowing more fuel storage at lower speeds.

12 2D thin airfoil airfoil in flow at supersonic free stream Mach number

12.1 Derive the pressure coefficient on the surface of the airfoil using the second order wave equation

This is the same as “Discuss the application to an airfoil in supersonic flow: lift coefficient, influence of the Mach number, Ackeret formula, lift and drag formula”10.4

12.2 Compute the lift coefficient using the method of characteristics for the potential system written in the primitive variables u and v (Ackeret’s law). Wave drag computation.

Same as above, + computing Normal and Tangential forces by integral. Formula’s for lift and wave drag are given in the **Application to a flat plate**.

13 3D wing in compressible flow in subsonic and supersonic flow

13.1 Discuss the 3D linearized potential equation for subsonic flow, compare the compressible and incompressible case

The previous potential equation can be extended into 3D into the same conditions like:

For subsonic wings, it is thus desired to have the largest drag divergence Mach number possible. This can be achieved by using high critical Mach number wings, or increase the difference $M_{div} - M_{cr}$. The second solution led to the supercritical wings. These have a rather flat suction side to limit the acceleration of the flow, keeping the supersonic speeds lower than other profiles and limit the strength of the shock that creates less drag. The comparison between the two type of wings is done on Figure 71. We can see that the M_{cr} is higher and the weaker shock wave

$$\beta^2 \hat{\phi}_{xx} + \hat{\phi}_{yy} + \hat{\phi}_{zz} = 0. \quad (188)$$

Then we apply the transformation of (x, y, z) to (X, y, z) with $X = \frac{x}{\beta}$ so that the previous equation becomes:

$$\hat{\phi}_{XX} + \hat{\phi}_{yy} + \hat{\phi}_{zz} = 0. \quad (189)$$

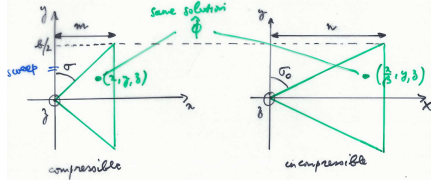


Figure 72

$$\frac{\tan \sigma_0}{\sigma} = \frac{n}{m} = \frac{1}{\beta} \quad \frac{AR_0}{AR} = \frac{b_0^S}{b^2 S} = \frac{c}{c_0} = \beta. \quad (190)$$

The slope of the wing in the z-direction is the same in the two axis:

$$\tan \theta \approx \theta = \frac{\hat{w}}{\hat{u} + V_\infty} \approx \frac{\hat{w}}{V_\infty}. \quad (191)$$

13.2 Derive Prandtl Glauert rule for a subsonic wing in compressible flow

Using the same ideas as the 2D wing, the pressure coefficient for small perturbations is known:

$$C_p = -\frac{2\hat{\phi}_x}{V_\infty} = -\frac{1}{\beta} \frac{2\hat{\phi}_X}{V_\infty} = \frac{C_{p0}}{\beta}. \quad (192)$$

We obtain the same equation as in 2D, whereas now the profiles are not identical! For the lift on a section ($y = \text{cst}$), we can compute the integral:

$$L' = \frac{1}{2} \rho_\infty V_\infty^2 \int_{LE}^{TE} (c_{pl} - c_{pu}) dx = \frac{1}{2} \rho_\infty V_\infty^2 \int_{LE}^{TE} \frac{c_{pl,inc} - c_{pu,inc}}{\beta} \beta dX = L'_0 \quad (193)$$

They are the same, whereas the lift coefficients respect $c'_l = \frac{c'_{l0}}{\beta}$. This is also valid for the lift curve slope.

13.3 Discuss the 3D linearized potential equation for supersonic flow, compare the compressible flow with the supersonic flow at freestream Mach number $\sqrt{2}$

In this case the potential equation becomes:

$$\lambda^2 \hat{\phi}_{xx} + \hat{\phi}_{yy} + \hat{\phi}_{zz} = 0. \quad (194)$$

If we apply the analogous transformation we have:

$$X = \frac{x}{\lambda} \Rightarrow \hat{\phi}_{XX} + \hat{\phi}_{yy} + \hat{\phi}_{zz} = 0. \quad (195)$$

This equation does not correspond anymore to the equation of an incompressible flow since $\lambda = \sqrt{M_\infty^2 - 1}$ and to have $\lambda = 1$ we need $M_\infty = \sqrt{2}$, thus the new flow is a $M_\infty = \sqrt{2}$. The previously found relations with β are valid for λ .

14 3D wing in compressible transonic flow. Discuss effect of sweep on performance of a 3D wing in compressible flow – Influence on Lift and drag

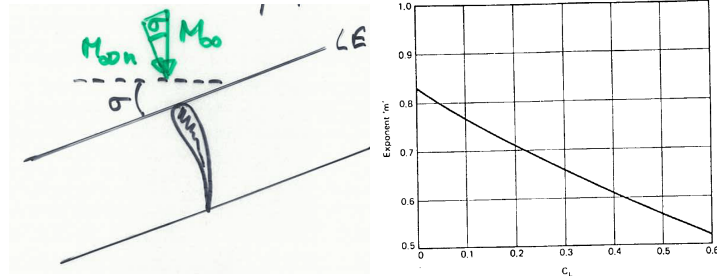


Figure 73

Figure 74

This is a technique used in order to increase the critical mach number. Indeed, the flow seen by the 2D wing is the one perpendicular to the wing:

$$V_{\infty n} = V_{\infty} \cos \sigma \quad \Rightarrow M_{kr}^{\sigma=0} = \frac{M_{kr}^{\sigma=0}}{\cos^m \sigma} \quad (196)$$

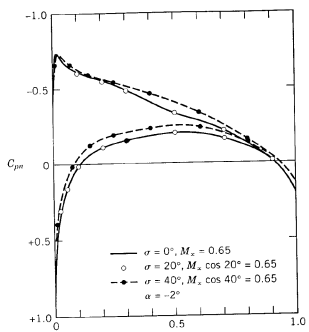
where we can see that the M_{∞} will be higher and where m varying parameter in function of the C_L , it decreases with lift (Figure 74). If the sweep angle is large enough, the flow seen by the LE can become subsonic and allow rounded shapes which is advantageous for subsonic speeds. The drag divergence mach number also increases:

$$M_{div} = M_{kr}[1.02 + 0.08(1 - \cos \sigma)]. \quad (197)$$

14.1 Lift of swept wings

Remind the definition of C_p :

$$C_{pn} = \frac{p - p_{\infty}}{\frac{1}{2}\rho_{\infty}V_{\infty}^2} \quad L_n = \frac{1}{2}\rho_{\infty}V_{\infty n}^2 \int_{LE}^{TE} (C_{pln} - C_{pun}) dx \quad (198)$$



where we see that if $M_{\infty n} = M_{\infty}^*$ (M_{∞}^* in this case is the one we have without sweep), the pressure distribution and thus the lift remains constant. This means that for a same approaching speed V_{∞}^* without and with sweep we will decrease the lift (we have to fly at higher speed). The lift coefficient also decreases for $V_{\infty n} = V_{\infty}^*$:

$$c_l^* = \frac{L^*}{\frac{1}{2}\rho_{\infty}V_{\infty}^*} > c_l = \frac{L^*}{\frac{1}{2}\rho_{\infty}V_{\infty}} \quad (199)$$

where * designate the same value in non swept wing. We see that the lift coefficient decreases.

Pay attention that this is the case when we are in subsonic flight. Indeed, the sweep increases the lift for supersonic as the shock stall is postponed ($M_{\infty n}$ seen smaller). In practice, to have significant influence of sweep σ must be high (at least 30° - 40°).

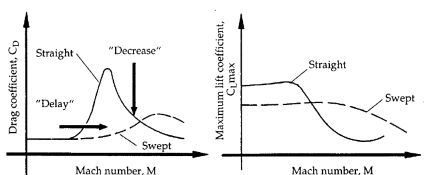


Figure 76

14.2 Lift coefficient as a function of the angle of attack for swept wings

As we have seen, the lift and the lift coefficient decreases when sweep wings. This implies that the slope of the lift curve is also smaller. Remark that we have the same AR in the figure, in practice the AR of swept wing is smaller than the one without (2 to 4 - sweep, 6 to 10 - subsonic), but the lift slope is even smaller.

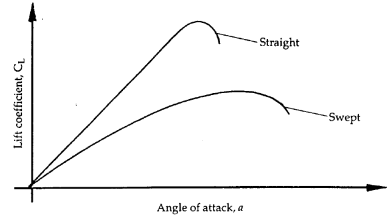


Figure 77

There are structural advantages as it allows to have thinner airfoils (better for high speed), and the M_{kr} increases. To increase the structural strength we use **taper** (chord decreases from root to tip). This smaller AR induces more drag, demanding more take-off and landing distance. The reduced slope of lift requires high α when landing and take-off (Concorde drooped nose), but there is no pronounced stall limit.

14.3 Influence of the sweep angle on the drag

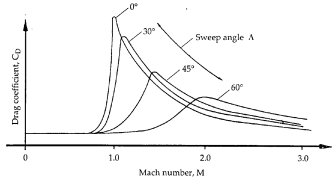


Figure 78

One observes the increase of M_{div} , the decrease of the maximum drag coefficient (must have large angles to have significant effects). At sufficiently high Mach numbers, M_n will reach the supersonic limit and produce the same effect as seen previously. In that case, the drag with no swept wing is smaller at this stage.

14.4 Separation behavior

First, remind that the pressure on the suction side decreases moving from the root to the tip, perpendicularly to the flow, inducing a flow. In practice, we try to have the separation at TE the nearest to the root not to disturb the ailerons (or else loose of control). The problem is that as we are already beyond the peak of underpressure at the root, to the tip we reach the underpressure, thus the boundary layer is pushed to the tip, resulting in a flow of low velocity and low energy. This will separate easily.

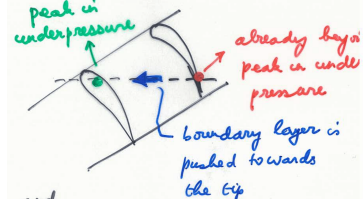


Figure 79

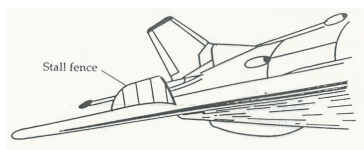


Figure 80

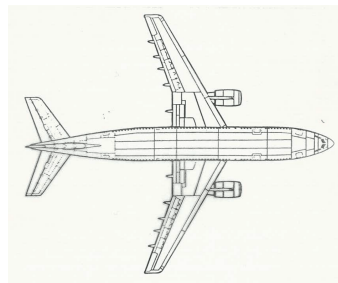


Figure 81

Solutions to limit this are:

- **washout:** we make the geometry in order to reduce α when going to the tip and increase the speed.

- **separation at root:** we force it to happen there for example by sharp LE
- **use of slots and slats** (see further)
- **stall fences:** it is a device placed on the wing in order to brake the flow going from root to tip (Figure 80).

14.5 Area rule

Theorem of Hayes

Within the limits of small perturbations, different planes with the same evolution of the area of their cross section will have the same wave drag at transonic Mach numbers (at zero lift).

Whitcomb

In order to limit the wave drag for transonic flows, the variation of the area of the cross-section of a plane should be as smooth as possible, without abrupt changes.

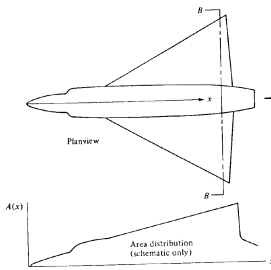


Figure 82

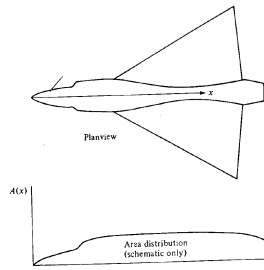


Figure 83

This means that the cross section of the fuselage must be reduced near the tail in order to have that smooth variation. On this figure see the decrease and the late of the peak in drag around $M=1$ with area rule.

14.6 Forward Swept wings

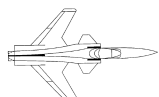


Figure 84

The **Forward Swept Wing (FSW)** has the same effect of the aft swept wing (ASW), but has advantages because the separation principle we have seen is reversed such that the separation occurs on the root \rightarrow higher lift. At maximum lift, the FSW has an elliptic lift distribution along the wing, leading to less induced drag than the ASW which has a peak at the tip. This leads to a better efficiency of ailerons and flaps.

But there is a structural instability. Indeed, the load is always accompanied with a bending of the wing. In straight case, there is no rotation of the profile. For the ASW the profile will move downward implying a decrease of the angle of attack (lift) and compensating the bending. In FSW the profile move upward, increasing α and the lift, causing more bending and so on \rightarrow unstable. This can be avoided by sufficient structural strength.

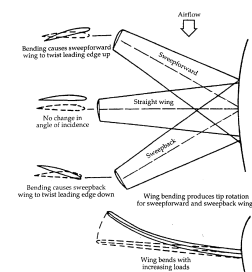


Figure 85

15 Delta wings

15.1 Discuss the mechanism for lift creation over a delta wing

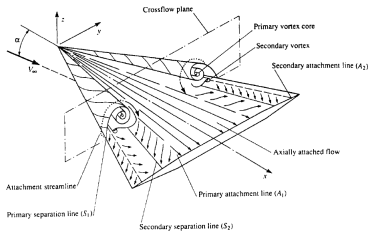


Figure 86

The idea of delta wings is to control the separation. By using a sharp LE one obtains a fixed separation line on LE. This is a considerably swept wing but has less problems with tip stall. This is due to the vorticities at the LE on the upper side that avoid the boundary layer to reach the tips. The separation area being limited, that produces an underpressure on the upper side and contributes to lift.

The slope of the lift curve is small, we can reach high $\alpha \approx 35^\circ$.

At still higher α the vorticities will lose their structure (**vortex burst**) and the underpressure will disappear, lift goes down. The large wings produce large lift and flaps are not needed. Tail plane are not necessary and the large chord at the root allows thick wings, keeping t/c low, increasing structural strength, allowing fuel storage and engines integration (reduction of drag). To have good subsonic conditions, $b/l \approx 0.25$ or not smaller than 2.

Remark 1 This description only applies for subsonic LE. If it is supersonic there is no separation at the LE, there is a shock wave on the wing causing boundary layer separation.

Remark 2 The lift creating process is different here. Joukowski theorem tells that it is based on vortex sheet, which is quasi horizontal for traditional wings. For delta wings the vortex sheet is rolled up. For wings with very low AR, c_l in function of α is given by the **formula of Jones**:

$$c_l = \pi\alpha \frac{db}{dx} \quad (200)$$

under the assumption that the wing lies perfectly in the Mach cone and where $\frac{db}{dx} = cst$ for delta wings.

Remark 3 The vorticities cause the transition to turbulent flow. If one wants laminar flow boundary layer control is needed.

15.2 Discuss the formula of Jones giving the lift coefficient as a function of the angle of attack

$$c_l = \pi\alpha \frac{db}{dx} \quad (201)$$

assuming that the wing lies perfectly in the Mach cone and where $\frac{db}{dx}$ is the variation of the semi span in the direction of the flow, which is constant for a delta wing \Rightarrow the lift coefficient has a constant slope with respect to α .

15.3 What are the advantages and disadvantages of delta wings with respect to:

Stability: Delta wings give high manoeuvrability, which is often seen as competitive to stability for rolling. Delta wings are however stable in pitch (by geometry).

Lift performance: Due to high surface, lift is generally very high (no need for flaps or other high lift devices).

Stall and high angle of attack flight: As discussed above, the stall will operate at much higher angle of attack (up to $\alpha \approx 35^\circ$), and high angle of attack gives high lift.

16 High lift devices

16.1 Why and when are high lift devices needed

The main objective of lift is to counterbalance the weight:

$$W = L = C_L \frac{1}{2} \rho_\infty V_\infty^2 S. \quad (202)$$

In particular at take-off and landing, one wants to have the higher possible lift at the lowest possible speed. 2 solutions: increase S or C_L . The two solutions increase the drag.

16.2 How can the lift be increased: 2 basic principles

$$W = L = C_L \frac{1}{2} \rho_\infty V_\infty^2 S. \quad (203)$$

Suppose now that $V_\infty \ll$, there are 2 options to increase lift: increasing C_L or increasing S . The problem is that the 2 solutions increase the drag, the first need an increased camber, and for the second $D = C_D \frac{1}{2} \rho_\infty V_\infty^2 S$. The best solution is to increase C_L only for $V_\infty \ll$ and this can be done by changing the geometry or by controlling the boundary layer (attached flow).

16.3 Discuss different kinds of trailing edge flaps

16.3.1 Plain flap

The principle of flaps is to increase the camber. This is the most simple, the trailing edge shifts downward, increasing C_L . The characteristics are:

- Because of separation appearing earlier $\alpha_{stall} \searrow$, this is better for the view of the pilot.
- $C_L(\max)$ is up to 50% higher, reached for high deflection $\approx 80^\circ$.
- The drag increases much more than the lift $C_L/C_D \nearrow$, this is good for landing as it helps to decelerate.
- Center of pressure at the trailing edge $\rightarrow \Delta C_m < 0$ (nose down).

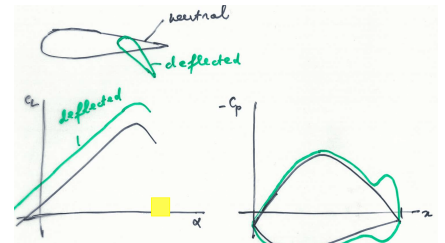


Figure 87

16.3.2 Split flap

- Separation appears later than the previous case, $\alpha_{stall} \searrow$ less.
- Larger wake because of the split \rightarrow more drag, not good for take off.
- $C_L(\max) \nearrow$ up to 60% and nose down less than previous case.



Figure 88

16.3.3 Slotted flap



Figure 89

In this case α_{stall} increases compared to plain because of the slot allowing the control of separation and the increase of C_D is smaller than the plain flap. $C_L(\max) \approx 65\%$.

16.3.4 Fowler flap

This is the most used type of flap, combination of the slotted flap and a backward motion:

- $C_L \nearrow$ further compared to slotted.
- $\alpha_{stall} \searrow$ compared to slotted because of $\frac{t}{c} \searrow$.
- $\Delta C_D \searrow$ because boundary layer control + $\frac{t}{c} \searrow$.
- $\Delta C_m \gg$ because flap going backward. In practice, the fowler flap contains many slots.

The figures below shows a good summary.

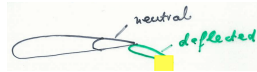


Figure 90

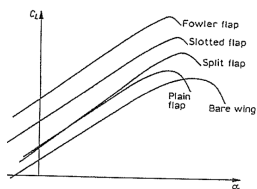


Figure 91

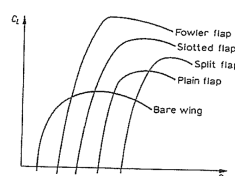


Figure 92

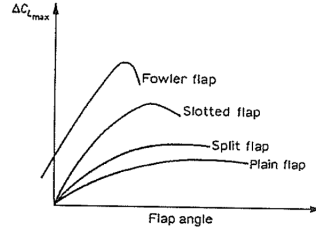


Figure 93

Remarks

- $\frac{dC_m}{dC_L} \approx cst$, this implies that k in $C_m = C_{m0} + kC_L$ does not change and that the **aerodynamic center** doesn't change.
- The flaps are placed near the fuselage, this decreases the efficiency, changes the lift distribution on the wing that have effect on D_i and the pressure center closer to the fuselage can have effects on the stability.
- Other types of flaps: Zap flap (split + fowler), C_L is higher than the split but the drag is higher than fowler.

16.4 Discuss the effect of slats

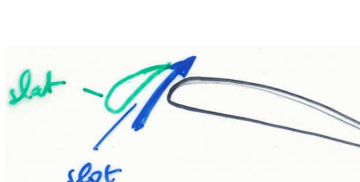


Figure 94

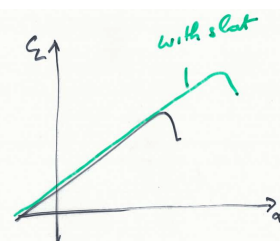


Figure 95

The slats are separated from the airfoil by a slot. This allows to energize the boundary layer by a flow through the slot. This has no effect for small α , it allows to increase α_{stall} going

from 15° to 25° , increasing $C_L(\max)$ up to 60%. The disadvantage is that for low speeds the drag decreases (less detached boundary), this is bad for landing. And for higher speeds the flow disturbance increases the drag. **Controllable slats** are necessary.

The second disadvantage is that to have the lift increase effect we need to go to very high α , not good for the sight of the pilot.

16.5 Discuss boundary layer control

Boundary layer blowing We saw previously that it was possible to energize the boundary layer by injecting high speed air through slots. This makes increase α_{stall} and the high velocity increases the circulation, thus $L \forall \alpha$.

Boundary layer suction This consists in sucking away the low velocity air by means of porous wings or suction holes.

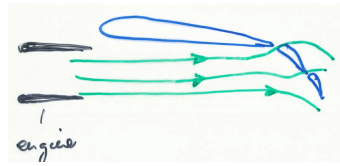


Figure 96

Remark For vertical or short take off and landing, the engine jet is used. The air coming from the engine is redirected to energize the boundary layer. VTOL: jet engine is deflected vertically for vertical take off, where the thrust must be equal to the weight, while it is about 30% for horizontal take off.

17 Tailplanes

17.1 Discuss why tail planes are needed in order to have a stable wing configuration

Consider α small so that the lift is assumed perpendicular to the chord, applied on the AC and the weight is applied on the center of gravity. The moment in the center of gravity is:

$$C_m = C_{M_0} + C_L(h - h_0) \Rightarrow \frac{dC_m}{dC_L} = h - h_0 > 0. \quad (204)$$

And since $dC_L/d\alpha = m$:

$$\frac{dC_m}{d\alpha} = m(h - h_0) > 0 \quad (205)$$

and the wing is **statically unstable** because the increase in α causes an increase in C_m and so even more nose up. We see that in fact the wing alone is stable only if the center of gravity is upstream of the aerodynamic center. **Tail planes** are used to increase stability, one has now:

$$\frac{dC_m}{d\alpha} = m(h - h_0) - \frac{C_{L_T}}{d\alpha} \gamma \quad (206)$$

where $\gamma = \frac{l S_T}{c S}$ as $C_{L_T} = \frac{L_T}{0.5 \rho_\infty V_\infty^2 S_T}$. One can reach stability for sufficiently high γ , by increasing l or S_T .

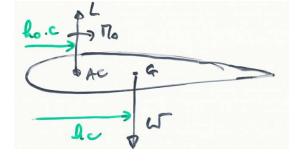


Figure 97

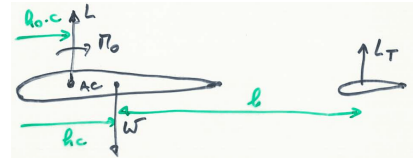


Figure 98

17.2 Discuss canard as an alternative for tail plane

One can use canards, which are similar to tail planes but situated near the nose. One can see that this could lead to the same analysis than above for planes with centre of gravity upstream compared to the aerodynamic centre.

18 Viscous and turbulent effects

18.1 Discuss skin friction drag for laminar and turbulent flow

Drag is caused by first the pressure distribution (form drag) and also by the viscous stresses (skin friction drag). At small α the skin friction represents 80-90% of the total drag and at stall conditions it is the form drag.

The form drag is also consequence of the viscous effects, the boundary layer due to viscous effect influences the pressure distribution. The viscous flow can be interpreted as the inviscid flow around an effective profile corrected with its boundary layer. In general this effective wing changes with α , has a smaller camber than the real wing so that the lift curve has a smaller slope than the inviscid with C_L smaller up to 10% for $Re = 10^6$.

18.1.1 Laminar flow

Consider a flat plate at $\alpha = 0$ and incompressible flow, the skin friction is:

$$C_f = \frac{1}{0.5\rho_\infty V_\infty^2 c} \int_0^c \tau_w dx = \frac{1.328}{\sqrt{Re_c}} \quad Re_c = \frac{V_\infty c}{\nu} \quad (207)$$

The boundary layer thickness δ is given by:

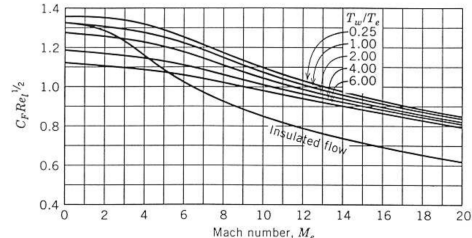
$$\delta(x) = \frac{5x}{\sqrt{Re_x}} \quad (208)$$

If the flow is compressible, the Mach number will play a role and the Prandtl number will appear as we have to take into account the energy equation for Navier-Stokes:

$$Pr = \frac{\mu C_p}{\kappa} \quad (209)$$

In incompressible flow the temperature of the flow remained more or less constant, this is not the case here, the boundary conditions on the plate (temperature) will influence the results. The skin friction and the boundary thickness become:

$$C_f = \frac{1.328}{\sqrt{Re_c}} F \left(M_\infty, Pr, \frac{T_w}{T_\infty} \right) \quad \delta = \frac{5x}{\sqrt{Re_x}} G \left(M_\infty, Pr, \frac{T_w}{T_\infty} \right) \quad (210)$$



The functions F and G are found numerically. Here are plotted for several temperature and Mach numbers the skin friction over an adiabatic flat plate. One notice that the friction decreases with temperature of the wall and with Mach number.

Below is plotted the effect of the temperature on the velocity field and the temperature distribution in the boundary layer. One can see that the increase of T_w decreases $\frac{du}{dy}$ and so the friction $\tau_w = \mu(\frac{du}{dy})$. We

also see that δ increases. On the right figure, we see that the δ increases with increasing Mach number for constant Re number. Increasing Re number decreases the friction.

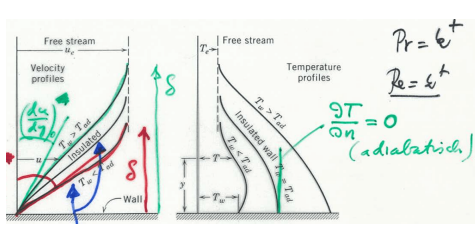


Figure 100

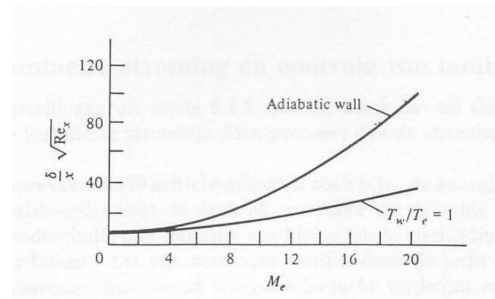


Figure 101

18.1.2 Turbulent flow

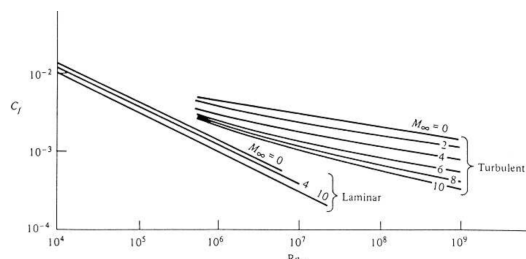


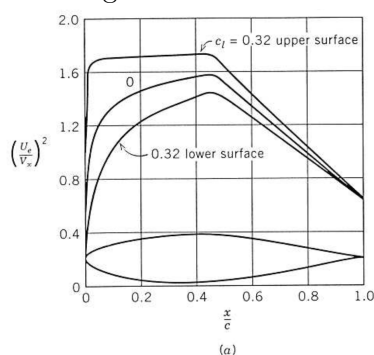
Figure 102

18.2 Discuss methods to reduce viscous drag: natural laminar flow and riblets

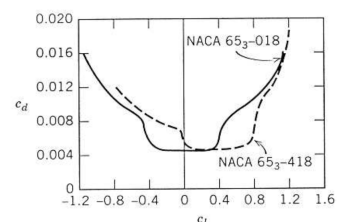
18.2.1 Natural laminar flow and control of laminar flow

As the friction in laminar flow is lower than in turbulent, one tries to keep the flow like that as possible. We have to place an active control in critical areas like the leading edge. When the air accelerates, the pressure decreases and there is a positive pressure gradient pushing from backward and leading to small separation. When the flow reattaches, it becomes turbulent. This is avoided by sucking away the air in the boundary layer (slots or porous wing) as a result of what the low energy air disappears. For laminar flows, one tries to use **adapted wing profiles** and not active control. The wing profile has to be as smooth as possible and the lower pressure point as far downstream from the LE as possible. With this aim, the NACA 6 series has been developed.

For example the NACA 65-218 has a point of min pressure at 0.5 chord downstream of the LE, the design lift coefficient 0.2 and thickness of 18%.



On (a) is represented the pressure distribution over NACA 65-018 for design lift coefficient 0 and $c_l = 0.32$. In both cases there is an undesirable pressure gradient at 50% chord. On (b) one sees that the drag is small for $-0.3 < c_l < 0.3 \rightarrow$ laminar.



18.2.2 Reduction of the drag in turbulent flows

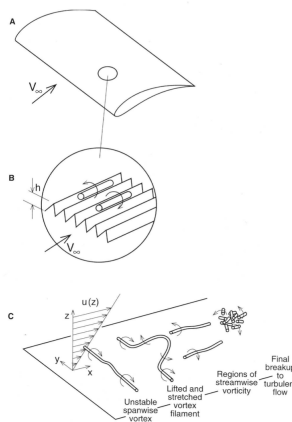


Figure 104

An advantage of turbulent flow is that it resists better to separation, so it is preferred in reverse gradient areas. To reduce the drag, we introduce **riblets** in the flow direction. This is illustrated on (c), the velocity distribution in the boundary layer induces spanwise vortices in the y direction, which is unstable. Because of its instability, it is deformed and lifted away from the wall. Because of this it breaks down and induces vortices in the flow direction which disintegrate and result in turbulent flow. Riblets have a stabilizing effect, they delay the transition to turbulent and make the flow in the viscous layer less chaotic when turbulent, so reducing drag.

The maximum drag reduction for profile 13R is 7-8% obtained for $s^+ \approx 15$ and 33 reduction of $\approx 2\%$.

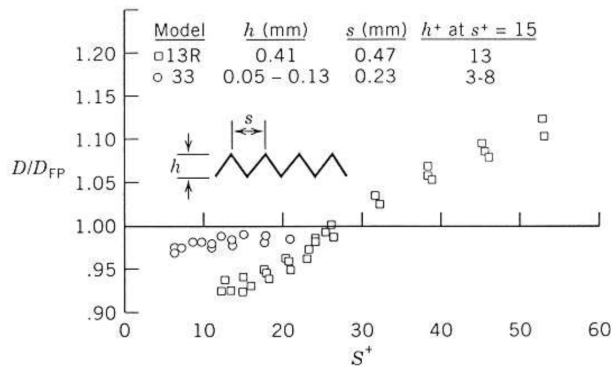


Figure 105

19 Weak solutions – shocks and contact discontinuities. Start from the Euler equations in conservative form:

19.1 Determine shock relations starting from the weak formulation

Flow equations also allow non-continuous solutions → **weak**. We limit the study to stationary weak solutions for which the discontinuity does not change in time. We restrict ourselves to non viscous 2D flows, respecting Euler equations (mass, momentum, energy) which allows discontinuities. Let's remind the Euler hyperbolic equation and the scalar convection equation:

$$\frac{\partial u}{\partial t} + a \frac{\partial u}{\partial x} = 0 \quad u = f(x - at) = f(q) \quad (212)$$

The derivatives give:

$$\frac{\partial u}{\partial t} = \frac{\partial f}{\partial q} \frac{\partial q}{\partial t} = \frac{\partial f}{\partial q}(-a) \quad \frac{\partial u}{\partial x} = \frac{\partial f}{\partial q} \frac{\partial q}{\partial x} = \frac{\partial f}{\partial q}(1) \quad (213)$$

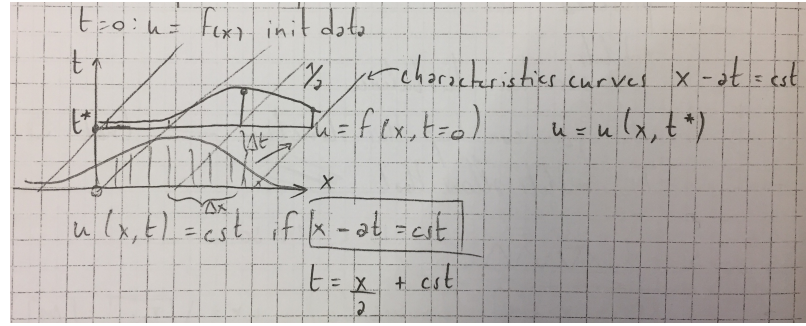


Figure 106

Initial wave is shifted on the right. Euler equation in 2D comes from the 1D momentum equation:

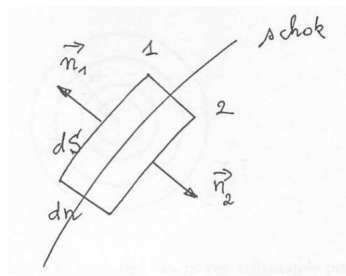
$$\frac{\partial u}{\partial t} + u \frac{\partial u}{\partial x} = \frac{1}{\rho} \mu \frac{\partial u^2}{\partial x^2} + \frac{1}{\rho} \cancel{\frac{\partial p}{\partial x}} \quad (214)$$

If the Re number tends to infinity, the right side is cancelled and we switch from N-S equations to Euler equation:

$$u = \begin{pmatrix} \rho \\ \rho u \\ \rho v \\ \rho E \end{pmatrix} \quad F = \begin{pmatrix} \frac{\partial u}{\partial t} + \frac{\partial F}{\partial x} + \frac{\partial G}{\partial y} = 0 \\ \rho u^2 + p \\ \rho uv \\ \rho u H \end{pmatrix} \quad u = \begin{pmatrix} \rho v \\ \rho uv \\ \rho v^2 + p \\ \rho v H \end{pmatrix} \quad (215)$$

where u is the vector of **conservative variables**, F and G are the **flux vectors**, E the total energy and H the total enthalpy. More compact:

$$\frac{\partial u}{\partial t} + \nabla \bar{F} = 0 \quad \bar{F} = (F, G). \quad (216)$$



When stationary, $\nabla \bar{F} = 0$. A shock is a discontinuity and derivatives are not defined. They have to satisfy the integral to be a weak solution:

$$\int_V \nabla \bar{F} dV = 0 \Rightarrow \oint_S \bar{F} \vec{n} dS = 0 \quad (217)$$

We can split it into the 4 faces of the surface by considering it infinitely thin (so 2 faces vanish):

Figure 107

$$\int_{S_1} \bar{F} \vec{n}_1 dS + \int_{S_2} \bar{F} \vec{n}_2 dS = 0 = [\bar{F} \vec{n}]_1^2 \quad (218)$$

where the last equality comes from $\vec{n} = \vec{n}_2 = \vec{n}_1$ and the control volume infinitely small. If above condition is satisfied, the discontinuity is a solution of the non-viscous equations:

$$\bar{F} \vec{n} = F n_x + G n_y = \begin{pmatrix} \rho(\vec{u} \vec{n}) \\ \rho u(\vec{u} \vec{n} + p n_x) \\ \rho v(\vec{u} \vec{n} + p n_y) \\ \rho H(\vec{u} \vec{n}) \end{pmatrix} \quad (219)$$

The first condition to satisfy, coming from mass conservation, is then:

$$\rho_1 u_{n_1} = \rho_2 u_{n_2} \quad (220)$$

The one coming from impulse conservation is:

$$[\rho \vec{u}(\vec{u} \vec{n}) + p \vec{n}]_1^2 \Rightarrow p_1 + \rho_1 u_{n_1}^2 = p_2 + \rho_2 u_{n_2}^2 \quad (221)$$

where we added a scalar product with \vec{n} . If we make now the scalar product with the tangential component \vec{t} we find:

$$\rho_1 u_{n_1} u_{t_1} = \rho_2 u_{n_2} u_{t_2} \Rightarrow u_{t_1} = u_{t_2} \quad (222)$$

where we used the mass conservation. **The velocity is conserved along the shock in both sides.** The last equation in the same way gives:

$$H_1 = H_2 \quad (223)$$

conservation of entropy across the shock like on a streamline.

19.2 Discuss contact or slip discontinuities

If we consider a discontinuous streamline, $\dot{m} = \vec{u} \vec{n} = 0$ and implies by momentum condition:

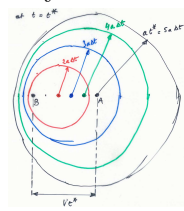
$$p_1 \vec{u} = p_2 \vec{u} \Rightarrow p_1 = p_2 \quad (224)$$

$u n = 0$ is the definition of the **shear layer**. The density is not conserved with the shock, thus by the perfect gas theory, the temperature too.

Contact (or slip) discontinuities are surfaces that separate zones of different density and temperature. Pressure is however in equilibrium for the two sides, and there is no mass exchange. Tangential velocities are often very different, giving the name 'slip' discontinuities. The difference with shock is that shock conserve speed and not pressure.

19.3 Explain propagation of disturbances in a subsonic and supersonic flow (sound waves). Discuss Mach waves

Consider a static source emitting infinitely small perturbations in a standstill fluid. These propagates in all direction with the **speed of sound**. If the source stands still, the perturbations stay within always larger concentric circles.



Suppose now that the source moves to the left with $V_\infty < a$. After a certain time t^* , the source will move from A to B. But in that interval the first perturbation circle has enlarged from at^* and with center A. If we devide the time interval into 5, we will have a situation like on the figure. We can see that the perturbations are both downstream and upstream of the source.

Figure 108

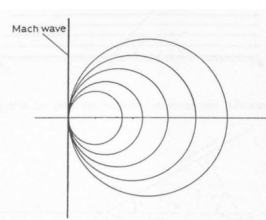


Figure 109

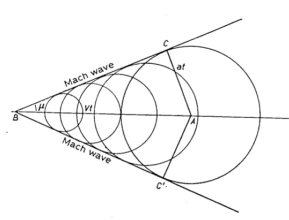
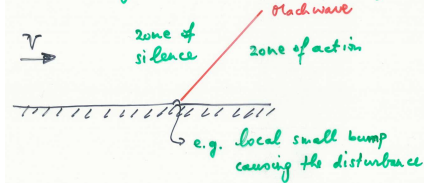


Figure 110

Consider now the case $V_\infty = a$ and the case $V_\infty > a$ represented above. There is now no perturbation upstream the perturbation. In particular, in the first case the perturbation are situated in the half plane downstream the source and the second within a cone of opening 2μ called the **Mach cone**. From the figure, we can directly deduce:

$$\sin \mu = \frac{a}{V_\infty} = \frac{1}{M_\infty}. \quad (225)$$

The area within the cone is the **area of action** and outside the **area of silence**. The lines separating both are the **Mach waves**.



Now consider the reversed case where the source (an infinitesimal irregularity) is standing still and the fluid is moving. Here also we get the same results. Within the assumption of small perturbations, the following equation (elliptic) is valid for supersonic flows:

Figure 111

$$\lambda^2 \hat{\phi}_{xx} - \hat{\phi}_{yy} = 0 \quad \lambda^2 = M_\infty^2 - 1 \quad (226)$$

for subsonic, the signs are reversed. The general solution of this equation was: $\hat{\phi} = f(x - \lambda y) + g(x + \lambda y)$. But $\frac{1}{\lambda} = \tan \mu$ and thus:

$$\hat{\phi} = f(y - x \tan \mu) + g(y + x \tan \mu) \quad (227)$$

the solution is constant along straight lines of slope $\pm \mu$ which corresponds to the Mach waves. Mach waves are thus characteristics of the **hyperbolic** equation:

$$\hat{\phi}_{xx} = \tan^2 \mu \hat{\phi}_{yy} \quad (228)$$

19.3.1 Subcritical and supercritical waves

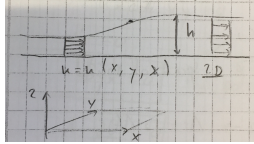


Figure 112

Consider a wave of height h after one time, the equations are:

$$\begin{aligned} \frac{\partial}{\partial x}(uh) + \frac{\partial}{\partial y}(vh) &= 0 \\ \text{x-mom: } \frac{\partial}{\partial x}(u^2 + gh) + \frac{\partial}{\partial y}(uv) &= 0 \\ \text{y-mom: } \frac{\partial}{\partial x}(uv) + \frac{\partial}{\partial y}(v^2 + gh) &= 0 \end{aligned} \quad (229)$$

where \sqrt{gh} is the speed of waves on water. A relation between Mach and Froude number can be made since $a = \sqrt{\gamma p / \rho}$:

$$M = \sqrt{\frac{u^2 + v^2}{\frac{\gamma p}{\rho}}} \quad Fr = \sqrt{\frac{u^2 + v^2}{gh}} \quad (230)$$

If $Fr > 1$: supercritical = supersonic, if $Fr < 1$: subcritical = subsonic.

20 Discuss characteristic theory for a first order scalar wave equation

20.1 Discuss the theory of characteristics for a first order linear wave equation with wave speed a . Define characteristic curves, what are Riemann invariants. Can discontinuous solutions exist ?

We will discuss different cases:

20.1.1 a cst

The prototype equation is the linear scalar wave equation:

$$\frac{\partial u}{\partial x} + a \frac{\partial u}{\partial y} = 0 \quad (231)$$

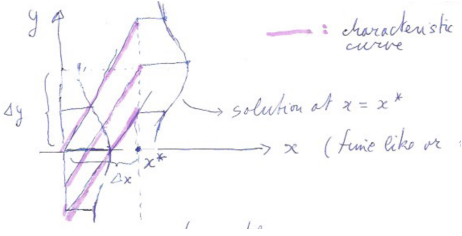


Figure 113

where x is the "time-like" coordinate, y the "space-like" one, a is the convection speed and the initial condition is $u(x, 0) = f(y)$. The solution of this is a wave:

$$u(x, y) = f(y - ax) = f(q(x, y)) \quad (232)$$

If $y - ax = cst$ then $u = cst$, which corresponds to $\frac{dy}{dx}$ characteristic curves. Consider on the figure that left is inlet and right is outlet, then the wave moves to right

with speed $\frac{\Delta y}{\Delta x} = a$.

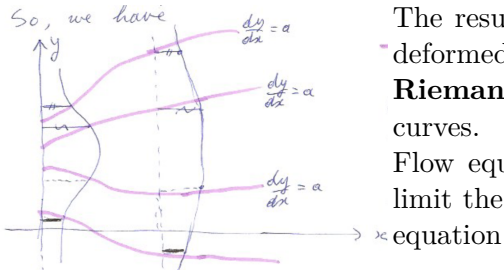
20.1.2 a linear

If a is not a constant but respects $a = a(x, y)$ the results are similar.

Proof. Since the coordinate y is expressed like $y = ax + cst$, u only depends on x . So if $\frac{du}{dx} = 0$ this means that $u = cst$. Let's compute:

$$\frac{du(y(x), x)}{dx} = \frac{\partial u}{\partial y} \frac{dy}{dx} + \frac{\partial u}{\partial x} = \frac{\partial u}{\partial x} - a \frac{\partial u}{\partial y} = 0 \quad (233)$$

which is satisfied since we retrieve the wave equation and u is a solution. \square



The result is shown here, the only change is that the wave is deformed since the propagation speed is not constant.

Riemann invariant are constant along the characteristic curves.

Flow equations allow non-continuous solutions \rightarrow weak. We limit the study to stationary weak solutions, satisfying Euler's

20.2 What changes for a nonlinear wave equation, take the case $a(u) = u$

20.2.1 a non linear

In the case a is expressed as $a(u, x, y)$ nothing changes, $\frac{dy}{dx} = a(u, x, y)$ are the characteristics and $u = cst$ along them. The proof is same as before, $y = y(x)$ on the characteristics and $\frac{du}{dx} = 0$. The only change is a depending on 3 variables.

Consider

$$a = u \quad \frac{\partial u}{\partial x} + u \frac{\partial u}{\partial y} = 0 \quad (234)$$

The solution $u = cst$ on characteristic curves $\frac{dy}{dx} = u$. This means that characteristics are straight lines since $u = cst$ along them and is the slope. They only differs from the initial data $u = f(y)$ at $x = 0$. There are 2 cases to consider since the wave can be converging or diverging as shown on below figures.

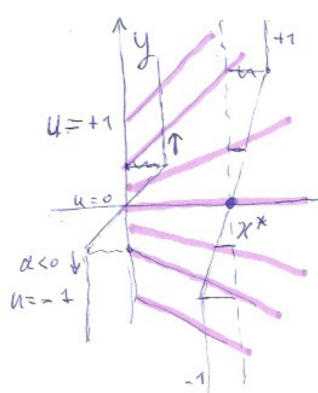


Figure 115

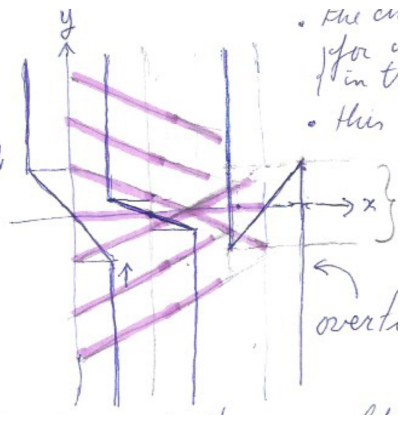


Figure 116

The first one corresponds to an expansion wave, the characteristics are diverging. The wave is smoothed during its expansion on x-axis. In the second case, the characteristics are converging and we call it compression wave. This leads to wave steepening. At the characteristics intersection we have an **overturning wave** as shown, this is a tripled value solution.

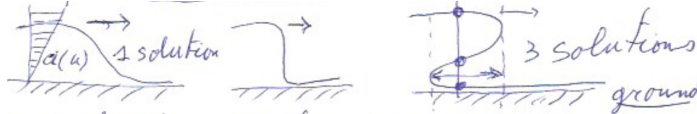


Figure 117

This is due to the fact that the wave moves slower near the ground (ex: wave at the beach). But with Euler equations this is not permitted since the solution has to be unique and thus can be interpreted as a shock wave.

20.3 Discuss shock formation for the previous case

Done above

20.4 Discuss the link between a characteristic curve and a shock curve

See above: overturning wave, unique solution for Euler \rightarrow shock wave

21 Discuss characteristic theory for steady supersonic potential flow

21.1 What are the assumptions for potential flow

Irrational velocity field, steady flow, isentropic flow.

21.2 Write the two equations which govern the velocity components u and v .

$$\begin{cases} \left(1 - \frac{u^2}{a^2}\right) u_x - \frac{uv}{a^2}(u_y + v_x) + \left(1 \frac{v^2}{a^2}\right) v_y = 0 \\ v_x - u_y = 0 \end{cases} \quad (235)$$

This can be put in matrix form as follows:

$$\frac{\partial}{\partial x} \begin{pmatrix} u \\ v \end{pmatrix} + \begin{pmatrix} \frac{-2uv/a^2}{1-u^2/a^2} & \frac{1-v^2/a^2}{1-u^2/a^2} \\ -1 & 0 \end{pmatrix} \frac{\partial}{\partial y} \begin{pmatrix} u \\ v \end{pmatrix} \quad (236)$$

21.3 How is the sound speed computed as a function of the velocity components

TODO

21.4 Write the above system in the canonical form and apply characteristic theory to find the Mach lines and Riemann invariants on the Mach lines

$$\frac{\partial}{\partial x} \begin{pmatrix} u \\ v \end{pmatrix} + \begin{pmatrix} \frac{-2uv/a^2}{1-u^2/a^2} & \frac{1-v^2/a^2}{1-u^2/a^2} \\ -1 & 0 \end{pmatrix} \frac{\partial}{\partial y} \begin{pmatrix} u \\ v \end{pmatrix} \quad (237)$$

Now we do like in previous section, compute the eigenvalues:

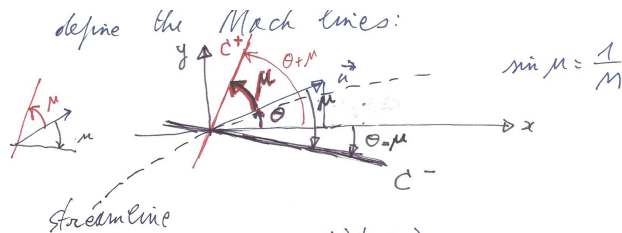
$$\begin{aligned} \lambda^2 \left(1 - \frac{u^2}{a^2}\right) + \frac{2uv}{a^2} \lambda + \left(1 - \frac{v^2}{a^2}\right) &= 0 \\ \Delta = -1 + \frac{u^2 + v^2}{a^2} \Rightarrow \lambda^\pm &= \frac{-uv \pm a^2 \sqrt{M^2 - 1}}{a^2 - u^2} \in \mathcal{R} \end{aligned} \quad (238)$$

where $\lambda^\pm \in \mathcal{R}$ since $M > 1$. We can find after computations that:

$$\lambda^\pm = \tan(\theta \pm \mu) \quad (239)$$

where θ is the flow angle and μ the Mach angle with: $\sin \mu = \frac{1}{M}$, $\tan \theta = \frac{u}{v}$ and $\tan \mu = \frac{1}{\sqrt{M^2 - 1}}$. The curves are thus:

$$C^+ : \left(\frac{dy}{dx} \right)^+ = \tan(\theta + \mu) \quad C^- : \left(\frac{dy}{dx} \right)^- = \tan(\theta - \mu) \quad (240)$$



Now as the eigenvalues are real, we can diagonalize by finding the left eigenvectors and computing $W = LU$, where $L = (l^+ \ l^-)^t$ such that for "+":

$$\frac{\partial W^+}{\partial x} + D \frac{\partial W^+}{\partial y} = 0 \quad (241)$$

We get a decoupled system of equation. To find L, the same method as previously is used, a trick is to choose $\sigma = a^2 - u^2$ and to compute μ using the system of equation $LA = DL$. We get:

$$l^+ = (a^2 - u^2) - uv + \sqrt{M^2 - 1} \quad (242)$$

The equation can be rewritten as a derivative along the streamline:

$$\frac{dW^+}{ds^+} = 0 \Rightarrow l^+ \frac{dU}{ds^+} = 0 = (a^2 - u^2) \frac{du}{ds^+} + (-uv + a^2 \sqrt{M^2 - 1}) \frac{dv}{ds^+} \quad (243)$$

Now we can use a transformation $(u, v) \rightarrow (M, \theta)$:

$$u = aM \cos \theta \quad v = aM \sin \theta \quad a_t = a^2 \left(1 + \frac{\gamma - 1}{2} M^2 \right) \quad (244)$$

where the last equation comes from the total enthalpy, $a = \sqrt{\gamma RT} = \sqrt{\frac{\gamma p}{\rho}}$ and $\frac{c_p}{c_p - c_v} = \frac{\gamma}{\gamma - 1}$:

$$\begin{aligned} H = cst &= h + \frac{u^2 + v^2}{2} \Leftrightarrow \frac{\gamma}{\gamma R} c_p T + \frac{u^2 + v^2}{2} = c_p T \frac{\gamma R}{\gamma R} \\ &\Leftrightarrow \frac{a^2 c_p}{\gamma R} + \frac{u^2 + v^2}{2} = \frac{a_t^2 c_p}{\gamma R} \Leftrightarrow a^2 \left(1 + M \frac{\gamma - 1}{2} \right) = a_t^2 \end{aligned} \quad (245)$$

Then when we solve for M, θ , we get:

$$\frac{\sqrt{M^2 - 1}}{M \left(1 + \frac{\gamma - 1}{2} M^2 \right)} \frac{dM}{ds^+} - \frac{d\theta}{ds^+} = 0 \quad (246)$$

And if we integrate this and define the **Prandtl-Meyer function** $\nu(M)$, we have for the Riemann invariants:

$$C^+ : -\nu(M) = \theta = cst = K^+(M, \theta) \quad C^- : \nu(M) = \theta = cst = K^-(M, \theta) \quad (247)$$

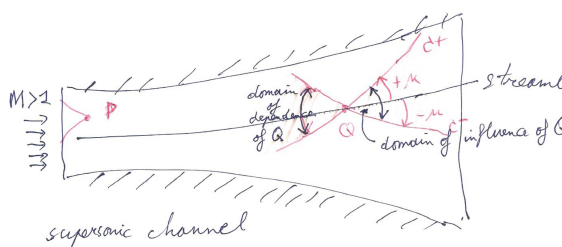


Figure 118

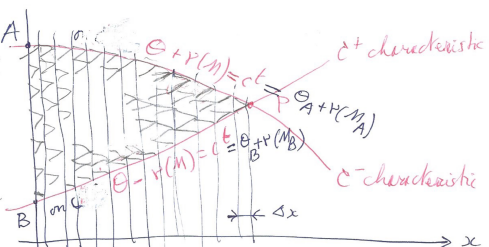


Figure 119

The situation is represented above, remark that the points P and Q depends on all the points upstream them outside the cone. Since the characteristics slope depends on the local M and θ , for the **method of characteristics** one has to compute all the solutions on C^\pm upstream P to compute the solution in P.

21.5 What are simple wave solutions, explain properties of simple waves. Explain why one of the families of characteristic curves are given by straight lines

A simple wave solution is a solution for which the Riemann invariant is constant on the whole space (x, y) and not only on the characteristics. There exist two types since we have 2 families of characteristics.

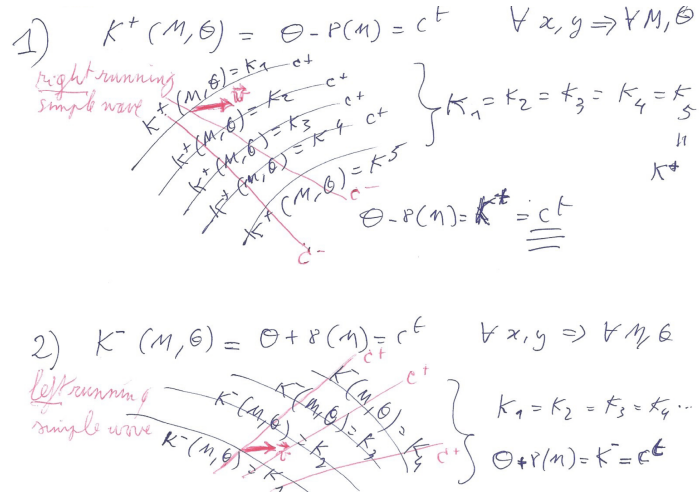


Figure 120

It is easy to see that the slope of C^- and C^+ in respectively case 1 and 2 is constant, for example for case 2:

$$C^+ : \theta - \nu(M) = Cst_1 \quad \text{but } \theta + \nu(M)Cst_2 \quad \Rightarrow (\theta, nu) = cst \quad (248)$$

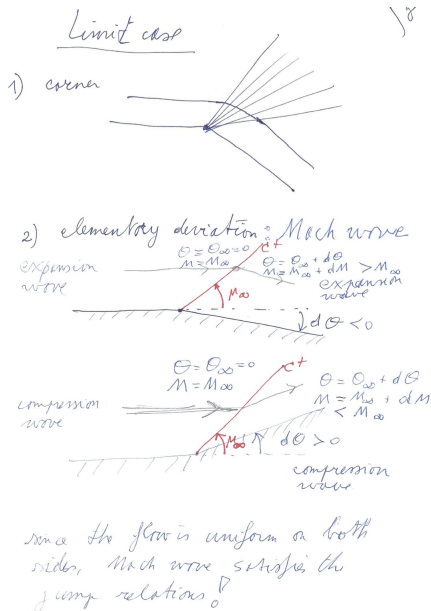


Figure 121

There exist a limit downstream velocity:

$$h = c_p T_t = c_p T + \frac{u^2 + v^2}{2} = cst \quad (249)$$

We can see that a max velocity can be obtained if $T = 0$: $V_{lim}^2 = c_p T_t$ and the corresponding Mach number is $M_{lim} = \frac{V_{lim}}{\sqrt{\gamma RT}} = \infty$ ($a_{lim} = 0$). In that case the Mach angle is

$$\mu = \arcsin\left(\frac{1}{\infty}\right) = 0 \quad (250)$$

This means that the **Mach line collapse with the streamline**. In fact, we will have an inviscid separation downstream and there will be a **vacuum** where no molecule can be. This is shown on Figure 122.

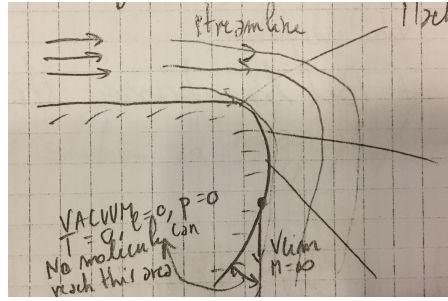


Figure 122

21.6 Discuss simple waves in the hodograph plane.

As shown in Figure 122 they look like a fan, with a limit for the limit case described above.

21.7 Apply to flow around a convex bend and to flow around a sharp convex corner. Explain why this is an expansion

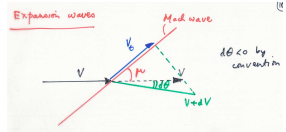


Figure 123

Consider in the figure the convention $d\theta < 0$. The infinitely small $d\theta$ induces an infinitely small perturbation noted $V + dV$. Since the Mach wave is also a solution of the flow equations, V_t before and after the Mach wave is the same. We have:

$$V_t = V \cos \mu = (V + dV) \cos(\mu - d\theta) \quad \Leftrightarrow 1 + \frac{dV}{V} = \frac{\cos \mu}{\cos(\mu - d\theta)} \quad (251)$$

Using the fact that $d\theta$ is very small we get:

$$1 + \frac{dV}{V} \approx \frac{\cos \mu}{\cos \mu + d\theta \sin \mu} = \frac{1}{1 + d\theta \tan \mu} \approx 1 - d\theta \tan \mu \quad \Rightarrow d\theta = -\sqrt{M^2 - 1} \frac{dV}{V} \quad (252)$$

Let's now try to rewrite the dV/V as a function of M . We know from the definition of M that:

$$M = \frac{V}{a} \quad \Rightarrow \frac{dM}{M} = \frac{dV}{V} - \frac{da}{a} \quad (253)$$

In addition we have the total temperature constant across the shock and its derivative gives:

$$\begin{aligned} \gamma R T_t = a^2 \left(1 + \frac{\gamma-1}{2} M^2\right) = cst &\Leftrightarrow 2ada \left(1 + \frac{\gamma-1}{2} M^2\right) + a^2(\gamma-1)MdM = 0 \\ \Rightarrow \frac{da}{a} &= -\frac{\gamma-1}{2} \frac{MdM}{1+\frac{\gamma-1}{2}M^2} \end{aligned} \quad (254)$$

We can now replace these values in (252) and get:

$$d\theta = -\frac{\sqrt{M^2 - 1}}{1 + \frac{\gamma-1}{2} M^2} \frac{dM}{M} \quad (255)$$

and after integration:

Prandtl-Meyer function

$$\theta = -\nu(M) + K^- \quad \nu(M) = \sqrt{\frac{\gamma+1}{\gamma-1}} \arctan \sqrt{\frac{\gamma-1}{\gamma+1}(M^2 - 1)} - \arctan \sqrt{M^2 - 1} \quad (256)$$

Additionally, consider a decrease of θ between a point 1 and 2, the integration will give:

$$\theta_2 - \theta_1 = \delta\theta = -\nu(M_2) + \nu(M_1) \quad (257)$$

Since $\delta\theta < 0$, same for right hand side, meaning $\nu(M_2) > \nu(M_1)$ and since ν is monotonously increasing with M , $M_2 > M_1 \Rightarrow$ expansion. If the properties in 1 are known, we can find the $\nu(M_2)$ and thus the M_2 .

21.7.1 Prandtl-Meyer expansion

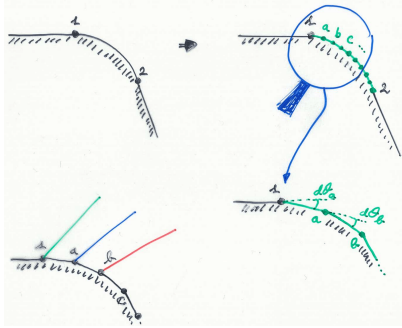


Figure 124

Now we can consider a bend. This can be subdivided into infinitely small bendings with each involving a change of angle and a Mach wave. The Mach wave will keep growing with the angle changes, inducing the Mach wave to decrease continuously, thus the Mach waves never cross each other. When the flow goes through a Mach wave, this induces an infinitely small change of angle, and this done infinitely will end up to a finite change of angle. Remark that the flow in a beginning corner and ending corner is the same. Again, with this reasoning we can conclude that at a straight corner there are infinite Mach waves in a single point.

The variation of M is dictated by the C^- curve. The Mach wave is perpendicular to the tangent at the curve at this point. Such flow is called Prandtl-Meyer expansion.

22 Oblique shock relations for steady 2D inviscid flow

22.1 Define critical state, critical Mach number, what are the key properties of the critical sound speed – compare with total state.

The critical state is defined as bringing a state $P\{\rho, T, u, p, a\}$ to sonic speed using an isentropic transformation $\frac{p}{\rho^\gamma} = \frac{p^*}{\rho^{*\gamma}}$. The critical sound speed is constant over a streamline.

The total(stagnation) state brings P to stand still using an isentropic transformation. $H = c_p T_t = c_p T + \frac{\|u\|^2}{2}$

22.2 The characteristic (or Critical) Mach number

It is defined as:

$$M^* = \frac{q}{a^*} \quad a^* = \sqrt{\gamma R T^*} \quad (258)$$

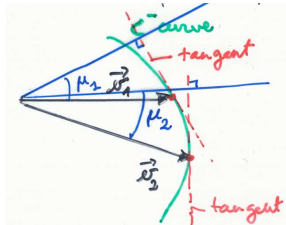


Figure 125

where q is the module of the velocity, a^* and T^* the speed of sound and the static temperature at $M = 1$. Remind that $T = T_t - \frac{v^2}{2c_p}$, if we use:

$$\begin{aligned} T_t = T \left(1 + \frac{\gamma - 1}{2} M^2 \right) &\Rightarrow \left(\frac{M^*}{M} \right)^2 = \frac{T^*}{T} \cdot \left(\frac{T_t}{T} \right) = \frac{\frac{\gamma+1}{2}}{1 + \frac{\gamma-1}{2} M^2} \\ &\Rightarrow M^{*2} = \frac{\frac{\gamma+1}{2} M^2}{1 + \frac{\gamma-1}{2} M^2} \end{aligned} \quad (259)$$

This implicitly assumes that the total temperature is conserved across the shock, but this is indeed the case. We directly deduce that:

$$M < 1 \Leftrightarrow M^* < 1 \quad M \geq 1 \Leftrightarrow M^* \geq 1 \quad (260)$$

Similarly we can define the characteristic normal Mach number:

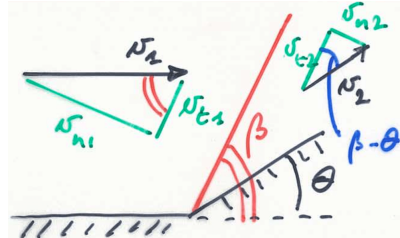
$$M_n^* = \frac{u_n}{a^{**}} \quad a^{**} = \sqrt{\gamma R T^{**}} \quad (261)$$

where a^{**} and T^{**} are the speed of sound and static temperature when the normal Mach number = 1. We can express a relation for the temperatures in normal variables from the definition of total temperature:

$$\begin{aligned} T_t = T + \frac{\vec{v}^2}{2c_p} \Leftrightarrow T_t - \frac{v_t^2}{2c_p} = T + \frac{v_n^2}{2c_p} &\Leftrightarrow \bar{T}_t = T \left(1 + \frac{\gamma - 1}{2} M_n^2 \right) \\ \Rightarrow T^{**} = \frac{\bar{T}_t}{\frac{\gamma+1}{2}} &\Rightarrow M_n^{*2} = \frac{\frac{\gamma+1}{2} M_n^2}{1 + \frac{\gamma-1}{2} M_n^2} \end{aligned} \quad (262)$$

We find exactly the same relations as previously and (260) is valid for normal variables.

22.3 Derive the relation between normal critical Mach numbers before and behind an oblique shock



Consider a compression with deflection angle θ leading to the shock wave angle β . The governing equations are:

$$\begin{aligned} \rho_1 v_{n1} &= \rho_2 v_{n2} & p_1 + \rho_1 v_{n1}^2 &= p_2 + \rho_2 v_{n2}^2 \\ v_{t1} &= v_{t2} & H_1 &= H_2 \end{aligned} \quad (263)$$

If we devide the equation with pressure by ρv_n :

$$R \left(\frac{T_1}{v_{n1}} - \frac{T_2}{v_{n2}} \right) = v_{n2} - v_{n1} \quad (264)$$

If we use the constant total temperature across the shock, we find:

$$\begin{aligned} \bar{T}_t = T_1 \frac{v_{n1}^2}{2c_p} = T_2 \frac{v_{n2}^2}{2c_p} &\Rightarrow R \left(\frac{T_1}{v_{n1}} - \frac{T_2}{v_{n2}} \right) - \frac{R}{2c_p} (v_{n1} - v_{n2}) = v_{n2} - v_{n1} \\ \Rightarrow v_{1n} v_{2n} &= \frac{2\gamma}{\gamma+1} R \bar{T}_t = (a^{**})^2 \end{aligned} \quad (265)$$

From this developpement we finally get an important relation for the Mach numbers before and after the shock:

$$M_{1n}^* M_{2n}^* = 1 \quad (266)$$

We are now able to compute M_2 knowing M_1 . First compute $M_{1n} = M_1 \sin \beta$, then M_1^* using (259), we get M_2^* from our last relation and we go backward: $M_2 = \frac{M_{2n}^2}{\sin(\beta - \theta)}$.

Remark In theory there are two possible cases:

$$\begin{aligned} M_{n1} > 1 \Rightarrow M_{n1}^* > 1 \Rightarrow M_{n2}^* < 1 \Rightarrow M_{n2} < 1 \\ M_{n1} < 1 \Rightarrow M_{n1}^* < 1 \Rightarrow M_{n2}^* > 1 \Rightarrow M_{n2} > 1 \end{aligned} \quad (267)$$

The second one corresponds to an expansion wave and is physically not possible because it leads to an decrease of entropy as we will see later.

22.4 Derive the relation between densities before and behind the shock

From the mass conservation equation we directly get:

$$\frac{\rho_2}{\rho_1} = \frac{v_{n1}}{v_{n2}} \left(\frac{v_{n1}}{v_{n1}} \right) = \frac{v_{n1}^2}{a^{**2}} = M_{n1}^{*2} \quad (268)$$

and we conclude that the density over the shock increases.

22.5 Discuss the graph θ (flow angle) as a function of β (shock angle) with upstream Mach number as a parameter.

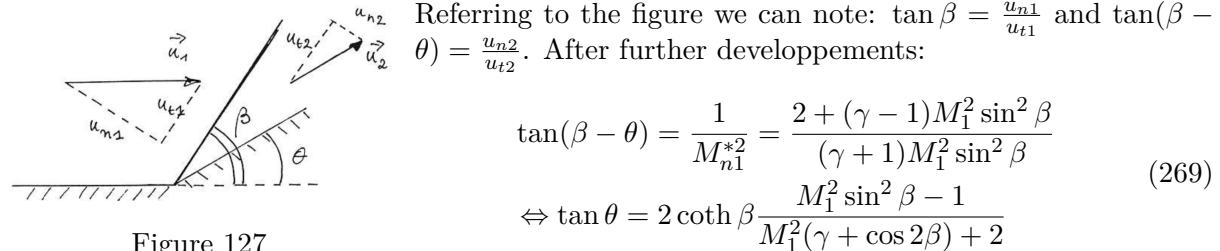


Figure 127

We find thus a relation between θ, β and M_1 and this can be plot on the (θ, β) plane.

22.5.1 Interpretation of the β, θ, M curves

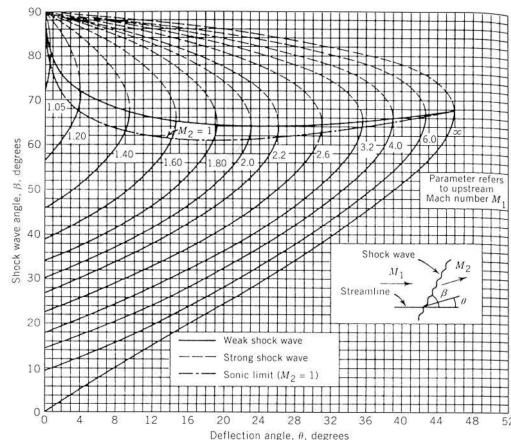


Figure 128

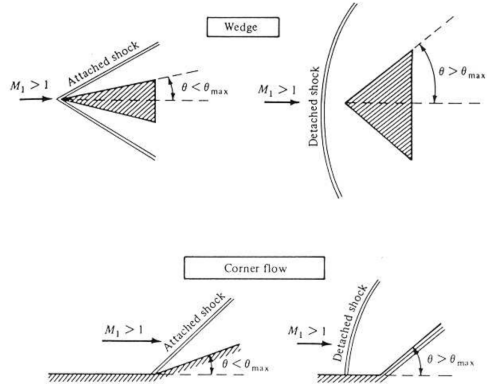


Figure 129

For a given M, θ , there are two possible β . The highest is the **strong shock** and the lower is the **weak shock**. This is due to the increasing pressure gradient between regions 2 and 1 when β increases. The solution depends on the downstream pressure condition, if we have a low pressure, weak shock is more likely appearing and the contrary when a high pressure is

imposed. In this course we always take the weak shock!

Now take for example $M = 2$ and $\theta = 30^\circ$, there is no solution on the graph. In this case there is no straight oblique shock but a **detached bow shock**, it occurs upstream the corner and is bent. Note that for higher M_1 the θ_{max} increases and after 46° there is no attached solution.

Now look at $\theta = 0^\circ$, one of the solution is $\beta = 90^\circ$ whatever M_1 and the other solution is dependent on M_1 . The first case corresponds to a **normal shock**. The other one corresponds to $\beta = \mu$ and thus the **Mach wave**, as previously seen this is the infinitely weak solution.

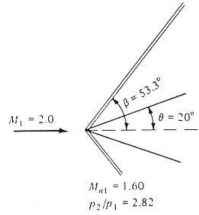


Figure 130

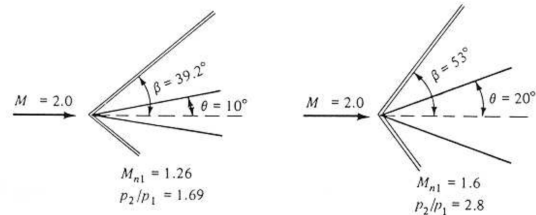


Figure 131

If we increase the Mach number keeping the deflection constant, we have β decreasing, but this means that pressure ratio is increasing. The shock is stronger. When the velocity is kept constant and the deflection increases, β increases and this also means that the pressure ratio increases and thus the wave gets stronger. This has an application for supersonic planes that try to get the weakest shock. As the temperature rising is higher for stronger shock, this is to avoid.

23 Oblique shock relations

23.1 Derive the shock polar for the velocity components behind the shock, with the upstream velocity as a parameter (shock polar in the hodograph plane)

The so-called hodograph plane is the (u, v) plane. It can be constructed as follow:

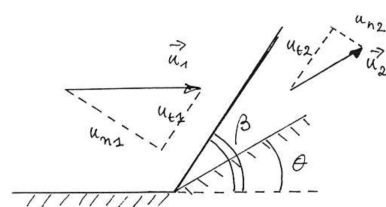


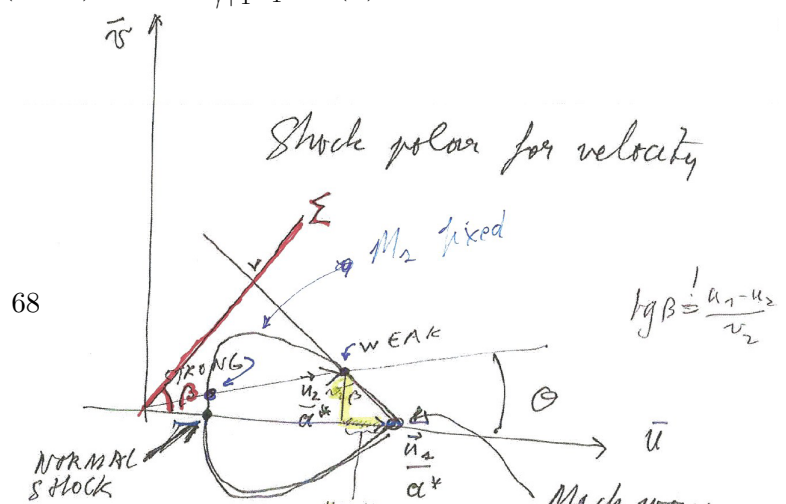
Figure 132

Consider the compression as shown in figure 132 for a finite angle change θ . Assume that velocity \vec{u}_1 before the angle change is known and of x-direction (flow only in x); the velocity \vec{u}_2 can be calculated using the relations seen in previous questions. It makes an angle theta (since the flow is deflected from an angle theta).

To compute \vec{u}_2 starting from $u_{1n}u_{2n} = a^{*2} - \frac{\gamma-1}{\gamma+1}u_t^2$, let's pass in cartesian axes where $\vec{u}_2 = u_{2x}\hat{i} + v_{2y}\hat{j}$, $u_2 = \|\vec{u}_2\| \cos(\theta)$, $v_2 = \|\vec{u}_2\| \sin(\theta)$, one gets $u_1 \sin(\beta) | \vec{u}_2 \sin(\beta - \theta) = a^{*2} - \frac{\gamma-1}{\gamma+1}u_1^2 \cos^2(\beta)$.

Using $\tan^2(\beta) = \frac{u_1 - v_2}{u_2}$, after some calculation:

$$v_2^2 = (u_1 - u_2)^2 \frac{a^{*2} - u_1 u_2}{a^{*2} + \frac{2}{\gamma+1}u_1^2 - u_1 u_2} \quad (270)$$



or, with $\vec{u}_1 = \frac{\vec{u}_1}{M_1^*}$, $\vec{u}_2 = \frac{\vec{u}_2}{a^*}$ and $\vec{v}_2 = \frac{\vec{v}_2}{a^*}$:

$$\vec{v}_2^2 = (\vec{u}_1 - \vec{u}_2)^2 \frac{1 - \vec{u}_1 \cdot \vec{u}_2}{1 + \frac{2}{\gamma+1} \vec{u}_1 \cdot \vec{u}_2} \quad (271)$$

These two can be drawn in the hodograph, where we can see that we have two solutions for the strong and weak shock, and where β is the angle from the vertical passing at the end of \vec{v}_2 and the line connecting the two speed vectors. By drawing the positions of the end of \vec{v}_2 for various θ , we obtain the shock polar for M_1 fixed. Note that the axis are often give divided by a^* .

23.2 Using this graph, discuss maximum deviation, weak shock and strong shock solutions, normal shock and Mach wave

The maximum deviation can easily be seen on the graph by taking the tangent to the shock polar from the origin (θ_{max}). The weak and strong shock where discussed before, the Mach wave is for an infinitively weak shock, hence when the two velocities are identical. The normal shock is the strong version of the Mach wave, one can see that we have an angle β of 90° .

23.3 Consider the flow around a sharp concave corner. Using the above graph, find the downstream Mach number for a given upstream Mach number

One can just draw the circle around the origin passing through the end of \vec{u}_2 , the radius is M_2 .

23.4 Discuss the shock structure appearing for supersonic flow around a cylindrical body

Nothing found in the slides or notes about this, so personal interpretation.

As the cylinder can be seen as a variable angle wall starting from 90° to 0° in compression, then going the other way around in expansion, one would expect a detached shock in front of the cylinder (curved shock) that reattaches going near to the radius of the cylinder and follows its curvature. The same would happen on the expansion side, with the shock detaching after an angle of just above 50° (53 was said to be a limit value for most cases).

23.5 Discuss shock reflection in a supersonic channel

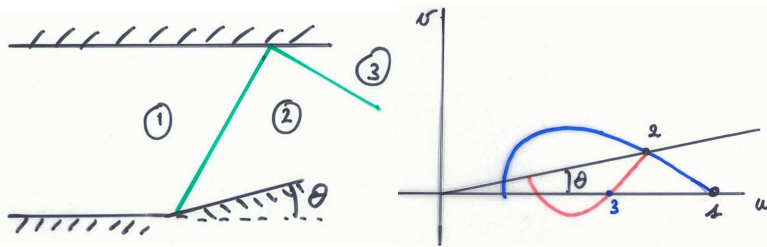


Figure 134

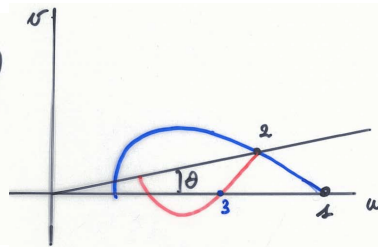


Figure 135

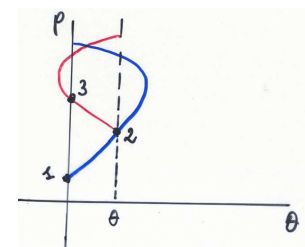


Figure 136

The situation is represented on the first figure, the flow is first deviated by the first shock then the flow must be horizontal near the upper wall, this is possible by a second shock wave appearing at the intersection between the first shock and the upper wall (reflection shock). If this shock touches the lower wall a new shock will appear deviating the flow and so on. The velocities and the pressures can be retrieved as shown on the figures.

Sometimes the angle is too big and there is no crossing from the polar curve, a normal shock appears (Mach reflexion), which connects with the lower wall shock via a bowed shock, with a slip line across which only pressures are conserved. This type of bowed shocks also appear when having a crossing of shocks

Figure 137.

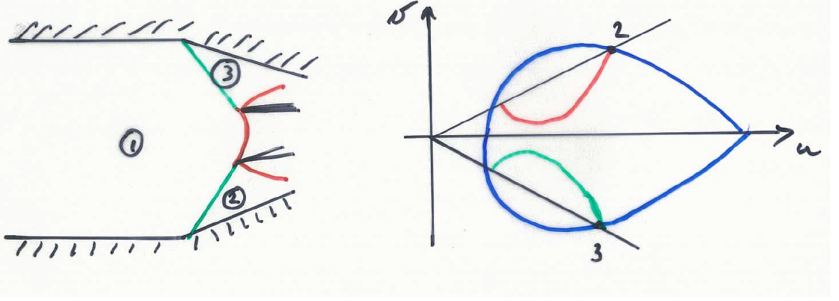


Figure 137